SAARLAND UNIVERSITY

Department of Neuroanatomy,
Institute for Anatomy and Cell Biology,
Faculty of Medicine, Saarland University,
Homburg / Saar, Germany.

MOLECULAR AND FUNCTIONAL CHARACTERIZATION OF RIBEYE - MUNC119 INTERACTION IN THE PHOTORECEPTOR RIBBON SYNAPSE

A thesis submitted to the Faculty of Medicine in fulfilment of the requirements for the degree of

Doctor of Philosophy (Ph.D.)

KANNAN ALPADI

Germany 2008

Declaration

I hereby declare that the Ph.D. thesis entitled "Molecular and functional characterization of RIBEYE-Munc119 interaction in the photoreceptor ribbon synapse" is a presentation of my original research work. Where other sources of information have been used, they have been acknowledged. No portion of work contained in this thesis has been submitted in support of any application for any other degree or qualification.

Homburg,
20.10.2008

Kannan Alpadi

Supervisor:

Co-supervisor:

Acknowledgement

I have a great pleasure in acknowledging the contributors to this thesis. I wish to express my sincere gratitude to all of you.

I would like to express my deep and sincere gratitude to my supervisor Prof. Frank Schmitz, who introduced me to the exciting research in “Ribbon synapse”. His intellectual rigorous approach has been an example to me. I always remember his everlasting enthusiasm, enlivening discussion and timeless support.

I would like to express my sincere thanks to Prof. Dieter Bruns and Prof. Jens Rettig for creating a pleasant and inspiring environment in the “synapse club” seminar.

I am deeply thankful to all of my colleagues Dr. Karin Schwarz, Dr. Jutta Schmitz-Krämer, Venkat Giri Magupalli, Josif Mirceski, Jagadish Kumar, and Sivaraman for creating a happiest and friendliest atmosphere in the laboratory.

I like to thank my colleagues and collaborators, who are shared the authorship with my three publications; Stefanie Käppel, Dr. Louise Köblitz, Prof. Gail M. Seigel and Prof. Ching-Hwa Sung.

I would like to thank Sylvia Brundaler for being helpful all the time regarding scientific and personal work irrespective of working hours. I always feel welcome when I come to work in the morning when she says good morning with happy smile.

Many thanks to Gerlinde Kühnreich, Franziska Markwart, Anne Rupp, Tamara Paul and Jennifer Neumann for their excellent technical assistance.

I would like to thank Prof. Gerald Thiel for donating the plasmid pEBG.

I would like to express my gratitude to Prof.P.Gunasekaran who inspired me the most, scientifically and away from science. His constant support for my academic career is gratefully acknowledged.

My warm thanks to Prof. R. M. Pitchappan for his constant support for my academic career.

I would like to thank my friends Nagaraj and Jonah, for the happiest moments in Germany.

I would like to thank Balachandar and Raspudin for their valuable comment on my thesis.

Especially, I would like to give my special thanks to my wife Dr.Lavanya whose patience and love enabled me to complete my PhD degree.

I cannot end this acknowledgement without thanking my family. I am deeply indebted to my parents, brothers and sister for constant encouragement and love all the time.

The financial support from “SFB” and University of Saarland is gratefully acknowledged.

Dedicated to my wife & my family

Summary

Ribbon synapses constitute a distinct type of chemical synapses present in certain types of neurons such as rod and cone photoreceptors, retinal bipolar cells, hair cells and pinealocytes. Ribbon synapses differ from conventional synapses morphologically and physiologically. Morphologically, ribbon synapses are characterized by the presence of large electron-dense presynaptic specializations in the active zone called synaptic ribbons. Physiologically, ribbon synapses are characterized by tonic neurotransmitter release. It was proposed that synaptic ribbons speed synaptic vesicle trafficking. But how the synaptic ribbon orchestrates ultra-fast synaptic transmission in ribbon synapses is still largely unknown. Prof. Dr. Frank Schmitz identified the protein RIBEYE, as a major component of synaptic ribbons.

RIBEYE consists of a unique aminoterminal A-domain and a carboxyterminal B-domain which is identical to the protein CtBP2. RIBEYE(B)-domain consists of a NADH-binding subdomain (NBD) and substrate-binding subdomain (SBD). We demonstrated that RIBEYE is a scaffolding protein with ideal properties to explain the assembly of synaptic ribbons as well as its ultrastructural dynamics via a modular assembly mechanism. From the identification and characterization of novel interaction partners of RIBEYE, we expected to obtain important informations to better understand how RIBEYE and synaptic ribbons work at the molecular level in the synapse. In the present study, I identified Munc119 as a RIBEYE-interacting protein at photoreceptor ribbon synapses using five independent approaches. Munc119 (also designated as RG4) is a mammalian ortholog of the *Caenorhabditis elegans* protein unc119. Munc119 consists of an aminoterminal Proline-Rich Domain (PRD), and a carboxyterminal Prenyl-Binding Protein δ (PrBP/δ) homology domain. Munc119/RG4 is related to the prenyl-binding protein PrBP/δ and expressed at high levels in photoreceptor ribbon synapses. Munc119 is essential for vision and synaptic transmission in photoreceptor ribbon synapses by unknown molecular mechanisms.

Using RIBEYE(B)-domain as bait, we obtained three independent positive clones of Munc119 from the retinal YTH cDNA library as potential interaction partners of RIBEYE. I showed that the PrBP/δ-homology domain of Munc119 is responsible for the interaction with NADH-binding domain of RIBEYE. I corroborated the Munc119-RIBEYE interaction using various independent approaches. In bacterial GST pull-down assays, Munc119 directly interacts with RIBEYE(B)-domain. The specificity of interaction in this assay was consistently shown by SDS-PAGE and western blot analyses. Next I performed Munc119 and RIBEYE co-transfection in COS-7 cells and showed that the two proteins specifically interacted in a mixture of many proteins. In order to prove the Munc119-RIBEYE interaction

in vivo, I performed co-immunoprecipitation experiments using R28 cells and bovine retina. R28 is an E1A-immortalized retinal precursor cells line. These cells are immature and non-fully differentiated precursor cells that express both neuronal and glial cell markers. R28 cells endogenously express Munc119 and RIBEYE in a TritonX-100 soluble fraction. RIBEYE immune serum co-immunoprecipitated endogenous Munc119 from R28 cells. Furthermore, RIBEYE immune serum co-immunoprecipitated Munc119 from bovine retinal extracts. Similarly, Munc119 immune serum co-immunoprecipitated RIBEYE from bovine retinal extracts. Since RIBEYE is exclusively present at the synaptic ribbons in the mature retina, the co-immunoprecipitation experiments suggested that Munc119 may be a component of synaptic ribbons.

Previous YTH analyses demonstrated that the NADH-binding subdomain (NBD) of RIBEYE(B) is mediating the interaction. The RIBEYE(B)-domain binds to NADH with high affinity via the NADH-binding subdomain. Therefore, I generated further point mutants of the NADH-binding subdomain of RIBEYE to map the docking site of Munc119 on the NADH-binding domain. RIBEYE(B)G730 is an essential component of the NADH-binding motif and the RIBEYE(B) point mutant RIBEYE(B)G730A does not bind significant levels of NADH. In contrast to the NADH-binding deficiency, RIBEYE(B)G730A still interacted with Munc119 in YTH analyses indicating that NADH binding is not important for binding of Munc119 to RIBEYE(B)-domain. Increasing concentration of both NADH and NAD^+ did not significantly influence the binding of Munc119 to the RIBEYE(B) in GST pull-down assays. All of the point mutants of NADH-binding subdomain still interacted with Munc119 except for RIBEYE(B)E844Q. This finding suggested that Glutamate E844 is crucial for the interaction with Munc119. Glutamate E844 is located close to the NADH-binding cleft of the RIBEYE. The NADH binding activity of RIBEYE(B)-domain was assayed by FRET and radioactive $C^{14}NAD^+$ binding analyses. As judged by NADH dependent FRET experiments and $C^{14}NAD^+$ binding analyses, this mutant RIBEYE(B)E844Q still bound NADH. Based on these data, we assume that the Munc119 binding region of RIBEYE is located topographically close to the NADH-binding cleft of RIBEYE(B).

In addition to its capability to bind NADH, the RIBEYE(B)-domain can also homo-dimerize. The homo-dimerization loop present in the NADH-binding subdomain is essential for the dimerization of RIBEYE(B). RIBEYE(B)ΔHDL (delta homo-dimerization loop) is a mutant which is not able to form RIBEYE(B)-RIBEYE(B) dimers. The RIBEYE(B)ΔHDL mutant still interacted with Munc119 pointing that Munc119-RIBEYE interaction is independent from homo-dimerization of RIBEYE(B).

The co-immunoprecipitation experiments from bovine retina suggested the presence of Munc119 on synaptic ribbons. Immunolabelling of bovine retina clearly showed the presence of Munc119 in the presynaptic terminals at the ribbon sites as well as close to the synaptic ribbon. Interestingly, the purified synaptic ribbons isolated from bovine retina specifically recruited Munc119 in synaptic ribbon pull-down assays. Since Munc119 is virtually absent from purified synaptic ribbon, but appears to be a synaptic ribbon-associated component that can easily dissociate from synaptic ribbons. The factors that regulate the association and dissociation of Munc119 with synaptic ribbons *in-vivo*, to be elucidated by further analyses.

The synaptic defects observed in Munc119-transgenic mice and Munc119-deficient patient stress the role of Munc119 for vision and synaptic processing in the visual system. The fact that the PrBP/δ homology domain which is crucial for Munc119 function shown to be the interaction domain with RIBEYE in my study. This finding particularly emphasizes the physiological importance of the RIBEYE-Munc119 interaction for synaptic transmission at the photoreceptor ribbon synapse.

Zusammenfassung

Ribbonsynapsen sind spezialisierte chemische Synapsen, die sich in bestimmten Nervenzellen, wie z.B. Photorezeptoren und Bipolarzellen der Netzhaut, Haarzellen des Innenohrs sowie Pinealozyten finden. Ribbonsynapsen unterscheiden sich morphologisch und physiologisch von konventionellen chemischen Synapsen. Morphologisch sind Ribbonsynapsen durch die Anwesenheit von großen elektronendichten, präsynaptischen Strukturspezialisierungen charakterisiert, die man als Synaptic Ribbons bezeichnet. Synaptic Ribbons sind in der aktiven Zone der Ribbonsynapse verankert und mit großen Mengen von synaptischen Vesikeln assoziiert. Von ihren physiologischen Eigenschaften sind Ribbonsynapsen tonisch aktive Synapsen, die eine große Bandbreite von Stimulusintensitäten präzise und dynamisch weiterleiten können. Die große Menge von synaptischen Vesikeln, die am Synaptic Ribbon gebunden sind, lassen vermuten, dass die Synaptic Ribbons zentrales Strukturelement sind, das die Exozytose und Endozytose von synaptischen Vesikeln in dieser tonisch aktiven Synapse beschleunigt. Aber wie genau die Synaptic Ribbons auf molekularer Ebene arbeiten und zu den bemerkenswerten physiologischen Eigenschaften der Ribbonsynapse beitragen, ist noch unbekannt. Die Arbeitsgruppe von Prof. Dr. Frank Schmitz identifizierte das Protein RIBEYE, das die Hauptkomponente der Synaptic Ribbons bildet.

RIBEYE besteht aus einer aminoterminalen A-Domäne und einer carboxyterminalen B-Domäne, die identisch mit dem Protein CtBP2 ist. Die B-Domäne von RIBEYE wird weiter untergliedert in eine NADH-bindenden Subdomäne (NBD) sowie eine Substrat-bindenden Subdomäne (SBD). Die B-Domäne bindet NADH mit hoher Affinität. Wir haben gezeigt, dass RIBEYE ein Strukturprotein ist, das ideale Eigenschaften besitzt, um die Synaptic Ribbons aufzubauen und um die ultrastrukturelle physiologische Plastizität, die diese Strukturen aufweisen, zu erklären. Die Identifikation und Charakterisierung von neuen Interaktionspartnern von RIBEYE sollte weitere wichtige Informationen liefern, um zu verstehen, wie RIBEYE und die Synaptic Ribbons in der Synapse auf molekularer Ebene arbeiten. In vorliegender Dissertationsarbeit identifizierte ich Munc119 als Interaktionspartner von RIBEYE. Munc119 besteht aus einer aminoterminalen Prolin-reichen Domäne (PRD), sowie einer carboxyterminalen Prenylbindungsprotein δ (PrBP/δ)-Homologiedomäne. Munc119 wird in hohem Masse in den Photorezeptor-Ribbonsynapsen exprimiert. Funktionsstörungen im Munc119 führen zu Störungen für den synaptischen Signalübertragungsprozess und im Sehprozess, die sowohl beim Menschen als auch bei einem entsprechenden Mausmodell zur Erblindung führen.

Unter Verwendung des Hefe-Zwei-Hybrid-Systems haben wir mit RIBEYE(B) als Köderprotein drei unabhängige cDNA Klone von Munc119 aus einer retinalen YTH cDNA-Bibliothek "gefischt". Ich habe gezeigt, das die PrBP/δ-Homologiedomäne von Munc119 für die Interaktion mit der NADH-bindenden Subdomäne von RIBEYE verantwortlich ist. Die RIBEYE-Munc119-Interaktion konnte ich mit fünf verschiedenen unabhängigen Methoden bestätigen. Dazu gehörten neben dem YTH-System Fusionsprotein-Pulldown-Analysen, die eine spezifische Interaktion zwischen RIBEYE(B) und Munc119 sowohl in SDS-PAGE-als auch in Western-Blot-Untersuchungen zeigten. Auch in transfizierten COS-Zellen konnte ich eine spezifische Interaktion zwischen Munc119 und RIBEYE nachweisen. Um auch die physiologische Bedeutung dieser Interaktion näher zu untersuchen, habe ich an retinalen R28 Progenitorzellen und an der bovinen Retina Co-Immunpräzipitationsuntersuchungen durchgeführt. R28 Zellen sind E1A immortalisierte, nicht terminal differenzierte retinale Vorläuferzellen, die sowohl neuronale als auch gliale Markerproteine exprimieren. Diese retinalen Vorläuferzellen exprimieren Munc119 und RIBEYE in einer Triton X-100 löslichen Fraktion. In diesen Co-Immunpräzipitationsuntersuchungen konnte ebenfalls die Interaktion zwischen RIBEYE und Munc119 bestätigt werden. Der Befund, dass diese Komplexe auch in-situ vorliegen betont die physiologische Relevanz der gefundenen Protein-Protein-Interaktion.

Die durchgeführten YTH-Untersuchungen zeigten, dass die NADH-bindende Subdomäne von RIBEYE(B) für die Interaktion mit Munc119 verantwortlich ist. Deshalb habe ich Punktmutanten der B-Domäne von RIBEYE generiert, um diese Punktmutanten für die genaue Kartierung der Interaktionsstelle von Munc119 an RIBEYE(B) einzusetzen. RIBEYE(B)G730 ist eine essentielle Komponente der NADH-Bindungsstelle und ein in dieser Aminosäure punktmutiertes RIBEYE (RIBEYE(B)G730A) bindet kein NADH mehr. Trotz dieser NADH-Bindungsdefizienz kann diese Punktmutante weiter Munc119 binden, was darauf hindeutet, dass die NADH-Bindung und die Munc119-Bindung an RIBEYE unabhängige Ereignisse sind. Diese Arbeitshypothese konnte in Protein-Pulldown-Analysen weiter bestätigt werden, in denen ich gezeigt habe, dass die Interaktion zwischen RIBEYE(B)-MBP und Munc119-GST nicht durch Zugabe von physiologischen Mengen von NAD^+ und NADH beeinflusst wurde. Dennoch befindet sich die Munc119-Bindungsstelle in enger räumlicher Nachbarschaft zur NADH-Bindungsstelle, wie die Analyse verschiedener Punktmutanten der NADH-Bindungsdomäne zeigte. So ist beispielsweise die RIBEYE Punktmutante RIBEYE(B)E844Q nicht mehr in der Lage, Munc119 zu binden, obwohl dieses punktmutierte Protein weiterhin NADH bindet und korrekt gefaltet ist. Dies konnte durch

radioaktive Bindungsexperimente und durch FRET-Untersuchungen gezeigt werden. Die Aminosäure RIBEYE(B)E844 liegt in unmittelbarer Nachbarschaft zur NADH-Bindungsstelle. RIBEYE(B) besitzt die Eigenschaft zu homo-dimerisieren. Unter Verwendung einer Homo-dimerisierungs-defizienten Mutante von RIBEYE (RIBEYE(B)ΔHDL) konnte ich weiterhin zeigen, dass die Dimerisierung von RIBEYE keine essentielle Voraussetzung für die Interaktion zwischen RIBEYE und Munc119 ist.

Die Co-Immunpräzipitationsexperimente legten nahe, dass Munc119 eine Komponente der Synaptic Ribbons ist. Auch Immunmarkierungen zeigten, dass Munc119 stark in den präsynaptischen Terminalen exprimiert wird und dort mit RIBEYE und den Synaptic Ribbons ko-lokalisiert. Interessanterweise besitzen aus der Retina gereinigte Synaptic Ribbons, die stringente Waschschritte bei der Reinigung aus der Retina durchlaufen, wenig Munc119. Die gereinigten Synaptic Ribbons können aber spezifisch Munc119-Fusionsprotein binden. Dies weist darauf hin, dass Munc119 eine periphere Synaptic Ribbon-assoziierte Komponente ist, die relativ leicht von den Synaptic Ribbons abdissoziieren kann. Die Faktoren, die Assoziation/Dissoziation von Munc119 mit den Synaptic Ribbons regulieren, gilt es durch zukünftige Untersuchungen zu identifizieren.

Die synaptischen Defekte, die in Munc119-transgenen Mäusen und in Munc119-defizienten Patienten beobachtet wurden, betonen die große Bedeutung von Munc119 für den Sehprozess und für synaptische Prozessierung in der Photorezeptorsynapse. Die Tatsache, dass die PrBP/δ-Domäne von Munc119, die entscheidend für die Funktion von Munc119 ist, auch die Interaktion mit RIBEYE vermittelt, betont weiter die physiologische Bedeutung der RIBEYE-Munc119 Interaktion in der Photorezeptorsynapse.

List of publications

1. RIBEYE recruits Munc119, a mammalian ortholog of the *C. elegans* protein unc119, to synaptic ribbons of photoreceptor ribbon synapses. Kannan Alpadi, Venkat Giri Magupalli, Stefanie Käppel, Louise Köblitz, Karin Schwarz, Gail M.Seigel, Ching-Hwa Sung and Frank Schmitz. Journal of Biological Chemistry, **283**, 26461-7 (2008).

2. Multiple Ribeye-Ribeye interactions create a dynamic scaffold for the formation of synaptic ribbon. Venkat Giri Magupalli, Karin Schwarz, Kannan Alpadi, Sivaraman Natarajan, Gail M.Seigel and Frank Schmitz. Journal of Neuroscience, **28**, 7954-7967 (2008).

3. The Retinitis Pigmentosa disease protein TULP1 is a component of synaptic ribbons, and interacts with RIBEYE. Venkat Giri Magupalli, Louise Köblitz, Kannan Alpadi, C.H. Sung and Frank Schmitz (*Manuscript in preparation*).

CONTENTS

CHAPTER 1

INTRODUCTION

Vision is a highly complex task that involves several steps of parallel information processing in various areas of the central nervous system. The eye, a remarkable photo-sensor, can detect a single photon and transmit its signal to the higher brain centre. Complex processing of classes of retinal neurons (photoreceptors, bipolar cells, horizontal cells, amacrine cells and ganglion cells) are the cellular substrates for visual signal processing. Conventional neurons encode information by changes in the rate of action potentials; this limits the amount of information transfer. However, sensory neurons such as photoreceptors in the retina and hair cells in the cochlea transmit light and sound signals, over a dynamic range of several orders of magnitude in intensity by graded changes in transmitter release. Graded synaptic output requires the release of several hundreds to several thousands of synaptic vesicles per second (for review, see Parsons and Sterling, 2003; Sterling and Matthews, 2005). To accomplish this high level of performance, the sensory neurons of the eye and cochlea maintain large pools of fast releasable synaptic vesicles and are equipped with a special type of chemical synapse, the ribbon synapse (for review, see Parsons and Sterling, 2003; Sterling and Matthews, 2005).

1. 1. Structure and function of the retina

The eye is a fluid-filled sphere enclosed by three layers of tissue. The outer layer is the sclera and this opaque layer is transformed into the cornea, a specialized transparent tissue that permits light rays to enter the eye. The middle layer of tissue includes three distinct but continuous structures: the iris, the ciliary body, and the choroid. The innermost layer of the eye, the retina, contains neurons that are sensitive to light and are capable of transmitting visual signals to higher brain centre via optic nerve. Despite its peripheral location, the retina or neural portion of the eye is actually part of the central nervous system (for review, see Purves *et al*., 2001)

Although it has the same types of functional elements and neurotransmitters found in other parts of the central nervous system, the retina comprises only a few classes of neurons, and these are arranged in a manner that has been less difficult to unravel than the circuits in other areas of the brain. There are five main types of neurons in the retina: photoreceptors, bipolar cells, ganglion cells, horizontal cells, and amacrine cells. The cell bodies and processes of these neurons are stacked in five alternating layers, with the cell bodies located in the inner nuclear, outer nuclear, and ganglion cell layers, and the processes and synaptic contacts located in the inner plexiform and outer plexiform layers. A direct three-neuron chain

photoreceptor cell to bipolar cell to ganglion cell is the major route of information flow from photoreceptors to the optic nerve (for review, see Purves *et al*., 2001)

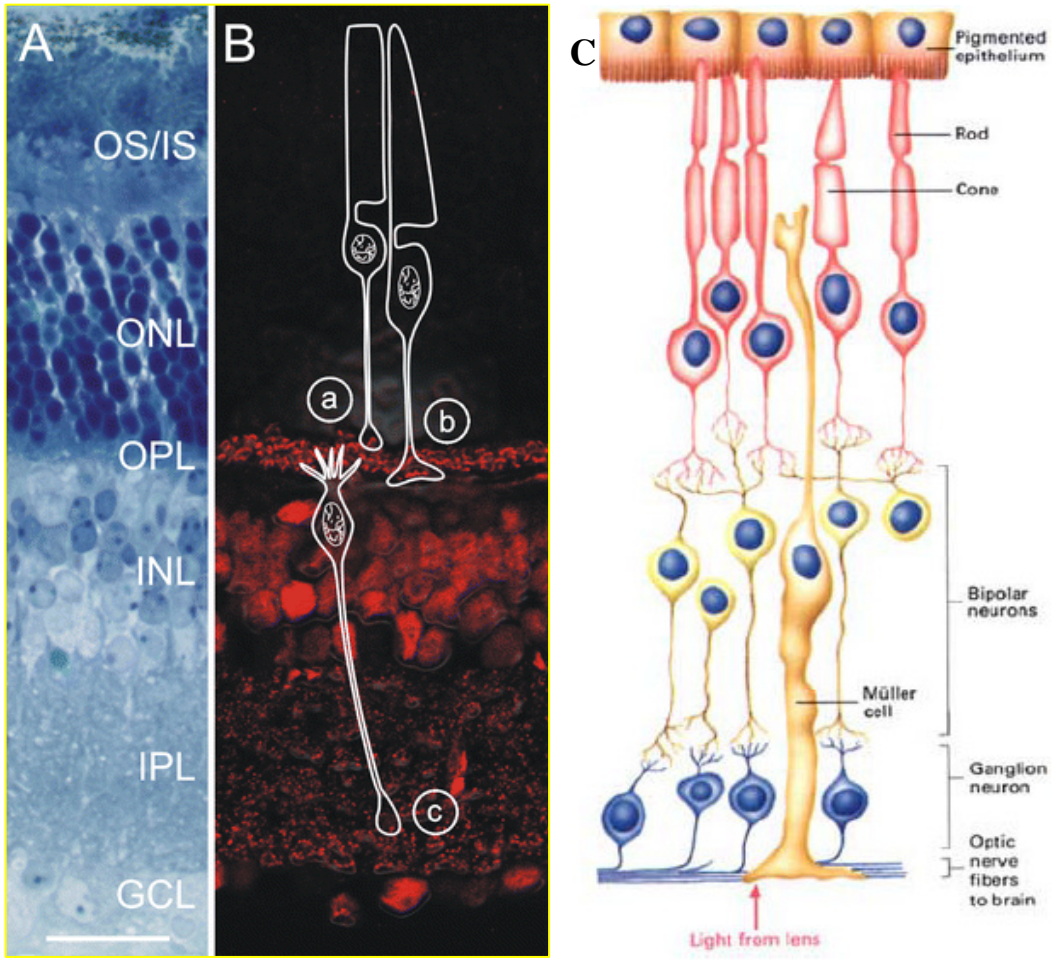

Figure.1.**Ribbon synapses of the mammalian retina**
A. Toluidine blue-stained vertical cryostat section of a mammalian retina showing the various retinal layers (*OS/IS* outer and inner segments of the rod and cone photoreceptors, *ONL* outer nuclear layer containing the somata of the photoreceptors, *OPL* outer plexiform layer or first synaptic region, *INL* inner nuclear layer containing the somata of the second order neurons, i.e. horizontal, bipolar and amacrine cells, *IPL* inner plexiform layer or second synaptic region, *GCL* ganglion cell layer containing the somata of the ganglion cells and of displaced amacrine cells). **B.** Confocal laser scanning micrograph of a vertical cryostat section through mouse retina stained with an antibody against CtBP2/RIBEYE, which labels the ribbon synapses in the two synaptic layers of the retina (cell somata in the INL and the GCL are also CtBP2-immunoreactive). The rod (cell *a*) and cone (cell *b*) photoreceptors make ribbon synaptic contacts onto postsynaptic bipolar cells in the OPL. The bipolar cells (cell *c*), in turn, transmit the signals at their ribbon synapses onto amacrine and ganglion cells in the IPL. *Bar* 20 µm (A, B) (adapted from tom Dieck *et al*., 2006) C. Diagrammatic representation of retina (Purves *et al*., 2001)

There are two types of light-sensitive elements in the retina: rods and cones. Both types of photoreceptors have an outer segment that is composed of membranous disks that contain photo-pigment and lies adjacent to the pigment epithelial layer and an inner segment that contains the cell nucleus and gives rise to synaptic terminals that contact bipolar and horizontal cells. Absorption of light by the photo-pigment in the outer segment of the photoreceptors initiates a cascade of events that changes the membrane potential of the

receptor, and therefore the amount of neurotransmitter released by the photoreceptor synapses on to the cells they contact. The synapses between photoreceptor terminals and bipolar cells (and horizontal cells) occur in the outer plexiform layer. More specifically, the cell bodies of photoreceptors make up the outer nuclear layer, whereas the cell bodies of bipolar cells lie in the inner nuclear layer. The axonal processes of bipolar cells make synaptic contacts in turn on the dendritic processes of ganglion cells in the inner plexiform layer. The much larger axons of the ganglion cells form the optic nerve and carry the information about retinal stimulation to lateral geniculate nucleus of thalamus (for review, see Purves *et al*., 2001). The other two types of neurons in the retina, horizontal cells and amacrine cells, have their cell bodies in the inner nuclear layer and are primarily responsible for lateral interactions within the retina. These lateral interactions between receptors, horizontal cells, and bipolar cells in the outer plexiform layer are mostly responsible for the visual system's sensitivity to luminance contrast over a wide range of light intensities (for review, see Purves *et al*., 2001).

1.2. Ribbon synapses of the retina

Ribbon synapses of the vertebrate retina are unique chemical synapses characterized by pre-synaptic specializations, the synaptic ribbons. Synaptic ribbons are sheet-like organelles with a lamellar organization (Dowling, 1987; Sterling, 1998). The photoreceptor ribbon is a plate like, ~ 30nm thick structure, which extends perpendicular to the plasma membrane. The ribbon juts ~200nm into the cytoplasm, varies in length from 200-1000nm (Photoreceptor ribbons are longer than bipolar cells ribbon). The ribbon anchors along its base to an electron-dense structure (arciform density) that in turn anchors to the pre-synaptic membrane.

Physiologically ribbon synapses are characterized by a high rate of tonic neurotransmitter release mediated by continuous synaptic vesicle exocytosis (Dowling, 1987; Sterling, 1998). It is generally thought that ribbon synapses are specialized for rapid supply of synaptic vesicles for release and that this is achieved by fast delivery of synaptic vesicles to the active zone on the ribbon, analogous to a conveyor belt (for review, see Sterling and Matthews, 2005; tom Dieck *et al*.,2006). The ribbon's surface is studded with small particles (~5nm diameter) to which synaptic vesicles tether via fine filaments (~5nm thick and ~40nm long). Usually there are several filaments per vesicle (Usukura *et al*., 1987). Vesicles tethered along the base of the ribbon directly contact the presynaptic membrane and thus are considered 'docked'. Detailed studies of the distribution of various presynaptic proteins in ribbon synapses demonstrated that they generally contain the same proteins as conventional

synapses (for review, see Sterling and Matthews, 2005). Only minor differences were observed, such as the use of syntaxin 3 instead of syntaxin 1 for fusion and of L-type Ca^{2+} channels instead of N-, P/Q-, or R-type channels for Ca^{2+} influx. Furthermore, rabphilin and synapsins are absent from ribbon synapses in some but not all species (for review, see Sterling and Mathews, 2005)

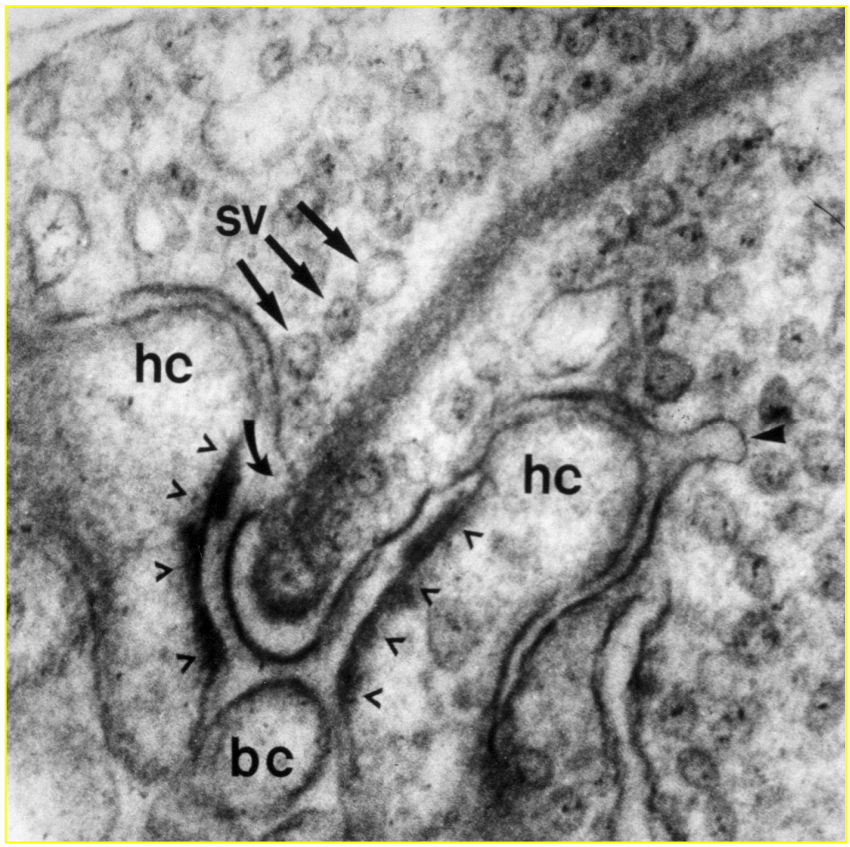

Figure.2. Electron Micrograph of synaptic ribbon
Abbreviations: sr, Synaptic Ribbon; sv, Synaptic Vesicle; bc, postsynaptic dendrites of bipolar cell; hc, postsynaptic dendrites of horizontal cells; black arrows-synaptic vesicle; bold arrow head –endocytosis ; arrow head -post synaptic density (Schmitz, 1996)

1.3. The synaptic vesicle cycle at ribbon synapses

Exocytosis at the bipolar ribbon synapse has been observed directly. The synaptic vesicles labelled by the dye FM1-43 are seen to pause at the membrane and then, upon opening of $Ca2^{+}$ channels, all the dye released promptly within milliseconds. We can observe this process by total internal reflection microscopy (Zenisek *et al*., 2000). The de-staining is consistent with full fusion (Zenisek *et al*., 2002). The bipolar cell active zone can release neurotransmitter continuously for hundreds of milliseconds during strong stimulation. This release exhibits two kinetically distinct components: a small fast pool (20% of the total vesicle pool) is released in 1 ms, and a large sustained pool (80%) is released over several hundred milliseconds (for review, see Sterling and Matthews, 2005). The fast pool matches

the number of vesicles docked at the base of the ribbon, and the sustained pool matches the number of vesicles tethered to the ribbon in higher rows, more distant from the plasma membrane (for review, see Sterling and Matthews, 2005). The neat correspondence between the pool of tethered vesicles and the pool for sustained release in both rods and bipolar cells suggests that the ribbon might serve as a platform where vesicles can be primed to allow sustained release (for review, see Sterling and Matthews, 2005).

The large amount of exocytosis during sustained vesicle exocytosis requires equally high-capacity endocytosis to retrieve the added membrane. In cone photoreceptors, fused membrane is directly recycled into small synaptic vesicles, without intermediate pooling into endosomes (Rea *et al*., 2004). The recycled vesicles are mobile and, diffusing as fast as similarly sized microspheres and rapidly replenish the releasable pool (Rea *et al*., 2004). Surprisingly, bipolar cells rely on a different mechanism for rapid retrieval, in which membrane is endocytosed in large bites that only later give rise to recycled synaptic vesicles (Paillart *et al*., 2003). Unlike cones, where newly recycled vesicles rapidly appear in the pool tethered to ribbons, recycled vesicles make up only 10% of the vesicles on bipolar cell ribbons, even after 10 min of activity (Rea *et al*., 2004). Thus, the bipolar cell relies on its large reserve of synaptic vesicles to replenish the releasable pool, whereas cone photoreceptors evidently have no large reserve pool and rely instead on rapid recycling. In this regard, the cone ribbon synapse resembles the conventional amacrine cell synapse, where extensive labelling of recycled synaptic vesicles was observed, without significant labelling in larger endosomes (Paillart *et al*., 2003).

1. 4. RIBEYE- a major component of synaptic ribbons

1.4.1. The molecular structure of RIBEYE

The major component of synaptic ribbons from retina was identified as RIBEYE (Schmitz *et al*., 2000). RIBEYE is composed of unique N-terminal `A` domain specific for ribbons, mediates assembly of RIBEYE into large structures, and a `B` domain identical with CtBP2, a transcriptional repressor that in turn is related to 2-hydroxyacid dehydrogenases. RIBEYE(B)-domain binds to NADH/NAD^+ with high affinity (Schmitz *et al*., 2000). The A-domain contains 563 aa residues and B-domain contains 425 aa residues. The A-domain is not significantly homologous to any of the currently described proteins and it contains abundance of serine and proline residues (Schmitz *et al*., 2000). The B-domain is identical to CtBP2, a nuclear protein and together with CtBP1 constitutes a family of transcriptional co-repressors except to the first 20 amino terminal amino acids. CtBP1 was originally identified as a

C terminal binding protein for the adenovirus E1A protein (Schaeper *et al*, 1995), and CtBP2 was subsequently identified as close structural and functional homolog of CtBP1. (Katsanis *et al*., 1998). The RIBEYE(A)-domain is not present in D. melanogastor, *C. elegens* and other lower vertebrates and invertebrates. This is supporting the notion that RIBEYE and retinal synaptic ribbons are an evolutionary innovation of vertebrates (Schmitz *et al*., 2000).

The teleosts fish, *Fugu* and zebra fish have two *ribeye* genes, *ribeye a* and *ribeye b.* Depletion of RIBEYE in zebra fish (by the use of morpholino antisense oligonucleotides) has been shown to result in shorter synaptic ribbons (Wan *et al*., 2005). Fish deficient in *ribeye a* lacks an optokinetic response. It has shorter synaptic ribbons in photoreceptors and fewer synaptic ribbons in bipolar cells (Wan *et al*., 2005).

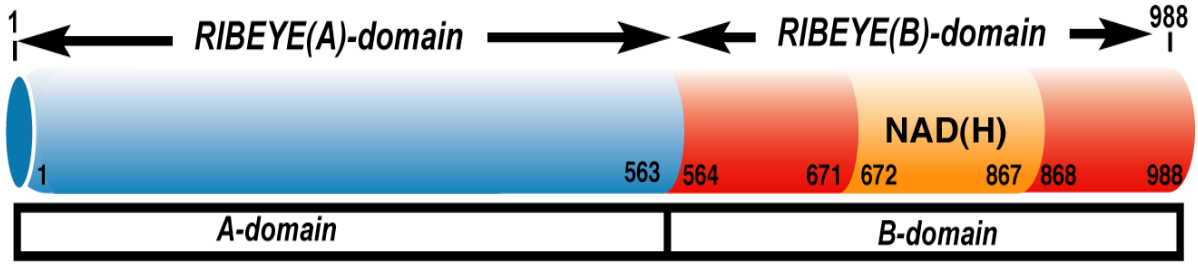

Figure.3. Schematic domain structure of RIBEYE
RIBEYE contains of a large amino-terminal A-domain and a carboxyterminal B-domain. The B-domain of RIBEYE contains the NADH-binding subdomain (NBD, depicted in yellow) and the substrate-binding subdomain (SBD, denoted in red). The A-domain comprises of 563 aa and the B-domain comprises of 425 aa.

The design of RIBEYE as a fusion protein of a novel domain with a pre-existing transcription factor suggests an intriguing evolutionary history, an accidental origin of RIBEYE in the vertebrate lineage by serependipitous addition of an exon encoding the A-domain to the pre-existing CtBP2 gene. However, further analyses indicate that the evolutionary history of RIBEYE may be even more complex and give a clue to the possible function of the B-domain (Schmitz *et al*., 2000). CtBP1 and CtBP2 themselves are not novel in terms of sequence but are significantly homologous to enzymes of the family of NAD^+-dependent 2-hydroxyacid dehydrogenases (Schmitz *et al*., 2000). In the nucleus, the CtBP family protein plays a role in transcription repression and in the cytosol, they perform diverse functions associated with membrane trafficking, central nervous system synapses and in regulation of the microtubule cytoskeleton (for review, see Chinnadurai, 2003 & 2005). Several studies indicated that RIBEYE is the major component of synaptic ribbons (Schmitz *et al*., 2000; Zenisek *et al*., 2002; Wan *et al*., 2005; Magupalli *et al*., 2008). Thus RIBEYE can be expected to exert a major influence on the function of synaptic ribbons.

1.4.2. The structural model of RIBEYE(B)-domain

The RIBEYE(B)-domain contains two globular domain, the NADH-binding subdomain (NBD) and substrate-binding subdomain (SBD). The dinucleotide-binding domain with an evolutionarily conserved structure forms the core homology domain among these proteins (for review, see Chinnadurai, 2003 & 2005). The NAD(P)-binding fold consists of two units of a mononucleotide-binding motif termed the Rossmann fold. The Rossmann fold is a conserved structural domain composed of three parallel β strands interconnected by α helices, forming a parallel twisted β sheet flanked by α helices with a βαβαβ topology. In the dehydrogenase domain, each repeated βαβαβ structural element binds a mononucleotide component of the NAD(P) coenzyme (for review, see Chinnadurai, 2003 & 2005). Like other dehydrogenases, these structures demonstrate that CtBPs, CtBP1, CtBP2 and RIBEYE(B)-domain can homo-dimerize through the dinucleotide-binding domain, forming an extensive, largely hydrophobic dimerization interface (Kumar *et al*., 2002; Nardini *et al*.,2003., Magupalli *et al*.,2008). Previous interaction mapping studies suggested that dimerization occurs through this domain (for review, see Chinnadurai, 2003 & 2005; Magupalli *et al*., 2008).

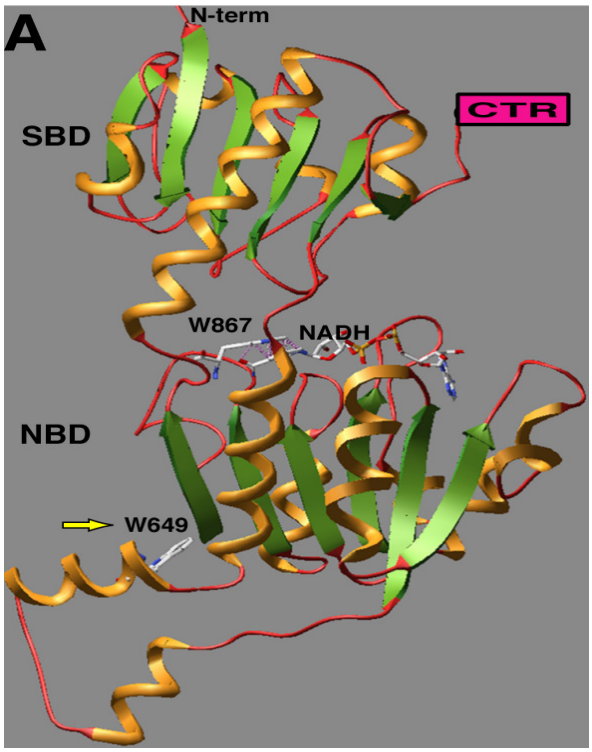

Figure.4. Predicted RIBEYE(B) domain structure using homology modelling with CtBP2
The RIBEYE(B)-domain contains two globular subdomain namely NADH-binding subdomain (NBD) and the substrate-binding subdomain (SBD). The NADH-binding subdomain has dimerization loop which is essential for RIBEYE(B)-RIBEYE(B) interaction. The NBD contains an excitable tryptophan residue at W867. The NBD binds with NADH as well as NAD^+. CTR- C terminal region which is un-structured in CtBP1, homologue of RIBEYE and CtBP2, has implicated in protein-protein interaction (Nardini *et al*., 2003; Schmitz, unpublished).

1.4.2.1. The substrate binding subdomain of RIBEYE(B)

In these structures, a deep cleft separates the SBD from the NBD, corresponding to a putative active site and the dinucleotide-binding pocket. For the D-2-hydroxyacid dehydrogenases, catalytic activity apparently proceeds through a "proton shuttle" between a histidine and a carboxylic acid residue (i.e., glutamate or aspartate) with the transfer of hydride ion between the substrate and coenzyme. An arginine residue located within proximity to the active site in 3PGDH interacts with the substrate carboxylic acid during catalysis. These residues are conserved in all D-2-hydroxyacid dehydrogenases (for review, see Chinnadurai, 2003 & 2005). All mammalian CtBP orthologues as well the *Drosophila* CtBP homologue also include these residues (hCtBP1 residues H315, E295, R266; corresponding residues in CtBP/BARS include H304, E284, and R255) indicating CtBP might retain oxo-reductase enzymatic activity (for review, see Chinnadurai, 2003 & 2005). Interestingly, most of the residues in the dehydrogenase consensus sequence are conserved in CtBPs and RIBEYE, including in particular the four residues that are involved in binding NAD^+ (GXGXXG-18-D) and the three amino acids that function in catalysis (R-30-E-19-H) (Schmitz *et al*., 2000). This conservation suggests that RIBEYE and CtBPs may still be partly or completely enzymatically active (Schmitz *et al*., 2000; Kumar *et al*., 2002).

1.4.2.2. The NADH/NAD^+ binding subdomain of RIBEYE(B)

In addition to a central essential role in metabolism as a carrier of reducing equivalents, the nicotinamide adenine dinucleotide coenzymes (NAD and NADP) play a pivotal role in cellular signalling (for review, see Chinnadurai, 2003 & 2005). It also serve as substrates for covalent protein modifications as well as precursors to the synthesis of intracellular calcium mobilizing second messenger molecules i.e. ADPR (for review, see Chinnadurai, 2003 & 2005). RIBEYE(B)-domain binds to NADH and NAD^+(Schmitz *et al*.,2000). Strong and specific binding of ^{14}C-labeled NAD^+ was also observed. Scatchard analysis uncovered a single class of binding site in RIBEYE/CtBP2 with an affinity of 1.3 μM NAD^+. ^{14}C-NAD^+ binding was completely inhibited by a 100-fold excess of unlabeled NAD^+ or by cibacron blue, which serves as a common ligand for NAD^+ binding site in many proteins but was unaffected by serine (Schmitz *et al*.,2000).

These results suggest that the homology of the RIBEYE(B) domain/CtBP2 to NAD^+-dependent 2-hydroxyacid dehydrogenases is functionally important, and that the domain may serve as an enzyme in synaptic vesicle priming on synaptic ribbons and in transcriptional repression (Schmitz *et al*., 2000).

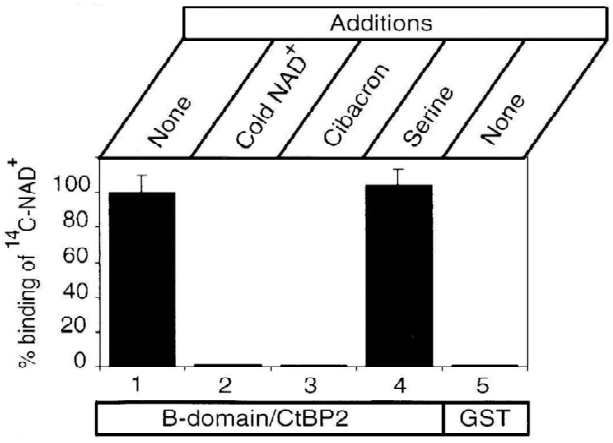

Figure.5. Binding of NAD^+ to the B Domain of RIBEYE/CtBP2

The Specificity of NAD^+ binding to the B-domain of RIBEYE. Binding of 10 µM ^{14}C-labeled NAD^+ in the absence of competitor (column 1, 100%) is displaced completely by 1 mM cold NAD^+ (column 2) or 1 mM Cibacron blue 3GA, an NAD^+ analog (column 3) but not by 1 mM serine (column 4).Column 5 shows binding to GST alone as background binding (Schmitz *et al*., 2000).

The binding NADH/ NAD^+ to CtBPs can be analysed by FRET experiment. The excitation of CtBP1 at 285 nm resulted in a typical tryptophan fluorescence emission with a peak at 340 nm (bold trace). The titration of NADH resulted in a decrease of tryptophan fluorescence at 340 nm and an increase in NADH fluorescence at 425 nm.

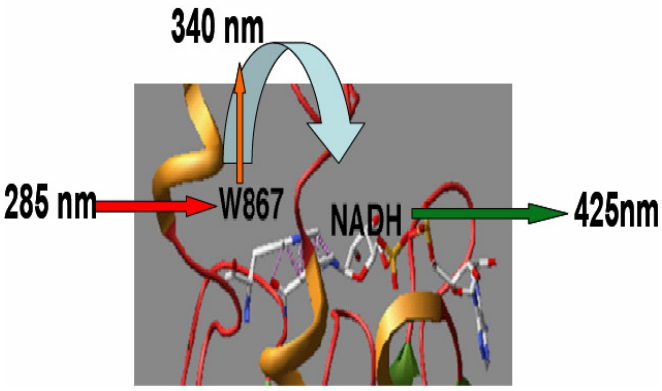

Figure. 6. Principle of FRET-NADH binding of RIBEYE(B) domain.
The tryptophan residue at W867 is excited at 285nm and the emission spectrum is measured at 340nm. The emission spectrum of NADH is measured at 425nm (Schwarz *et al*, submitted).

W318 demonstrated substantial FRET on the addition of NADH. This result agrees with the structural information suggesting that W318 is in position to excite the bound NADH (Fjeld *et al*., 2003). W867 is the corresponding tryptophan residue present in RIBEYE(B)-domain like W318 of CtBP1 (Schwarz *et al*, submitted).

1.4.3. The proposed functional role of RIBEYE in ribbon synapses

According to the model proposed by Schmitz *et al*., 2000, the N-terminal A-domain is involved in the formation of the assembled proteinaceous ribbon as a protein aggregate as suggested by the behaviour of the A-domain transfected into 293 cells. RIBEYE alone is not sufficient to organize ribbons but requires at least one additional protein component indicated in the model as an inner-core protein. The presence of such a protein component is suggested by the finding of a second unique protein in the biochemically purified ribbon fraction, which has not yet been identified (Schmitz *et al*., 2000). We have demonstrated that RIBEYE is a scaffolding protein with ideal properties to explain the assembly of synaptic ribbons as well as its ultra-structural dynamics via the modular assembly mechanism (Magupalli *et al*., 2008).

The RIBEYE(B)-domain binds NAD^+ with high affinity indicating that its homology with NAD^+-dependent dehydrogenases is functionally relevant and it may in fact serve as an enzyme. It is interesting that the CtBP1, a close homolog of CtBP2, was also suggested to function in membrane traffic under the name of "BARS" (brefeldin A-ADP ribosylated substrate) (Weigert *et al*., 1999). It was proposed that CtBP1, as BARS, has a role in membrane fission in the Golgi complex by functioning as a lysophosphatidic acid coenzyme A acyltransferase (Weigert *et al*., 1999). The close structural relationship of CtBPs with NAD^+-dependent dehydrogenases agrees well with the finding that CtBP is ADP ribosylated in an NAD^+-dependent reaction in parallel with GAPDH (another NAD^+-dependent dehydrogenase (Girolama *et al*., 1995). However, this relationship also makes it difficult to imagine how CtBP1 could function as a coenzyme A–dependent acyltransferases, since there is little chemical similarity between the reaction mechanisms of acyltransferases and dehydrogenases, raising questions about the precise enzymatic role of CtBP1 in Golgi membrane traffic (Schmitz *et al*., 2000).

Overwhelming evidence shows that CtBPs are transcriptional repressors in a large number of organisms, indicating that their NAD^+ binding and possible enzymatic function may be involved in executing this function (Schmitz *et al*., 2000). The binding sequences for CtBPs in their target proteins share a consensus sequence characterized by a PXDLS motif. By analogy, Schmitz *et al*., 2000 suggests that the B-domain of RIBEYE (which is identical with CtBP2) is displayed on the surface of the ribbons. On the ribbon surface, RIBEYE then is proposed to interact with a target sequence containing the consensus motif PXDLS of CtBPs. This model suggests that the target sequence may be in a synaptic vesicle protein and that this interaction may be involved in docking and/or translocation of vesicles. Furthermore, it is conceivable that an unknown enzymatic reaction of the B-domain may be involved in

priming. Although highly speculative at present, this model would provide a parsimonious explanation for how ribbons evolved and how they work (Schmitz *et al*., 2000). Identification of the binding partners for the B-domain on the ribbon surface and the role of NAD^+ binding in their function will give valuable insight into how this domain might perform this proposed function (Schmitz *et al*., 2000).

1.5. Munc119- a photoreceptor enriched protein

Munc119, a mammalian homolog of the *C. elegans* protein unc119 (also denoted as RG4; Higashide *et al*., 1996), is essential for normal vision and synaptic transmission at photoreceptor synapses (Higashide *et al*., 1996, 1998; Swanson *et al*., 1998). Munc119/RG4 was initially identified by a differential display screen and shown to be expressed at high levels in photoreceptor synapses (Higashide *et al*., 1996, 1998; Swanson *et al*., 1998). Swanson *et al* (1998) found evidence of alternative splicing of human and bovine UNC119 mRNA, but not of mouse UNC119 mRNA. Both rod and cone photoreceptors appeared to be expressing this gene (Higashide *et al*., 1996). Higashide *et al* (1998) localized Munc119 to the outer plexiform layer (OPL) of the retina in the synaptic termini of rod and cone photoreceptors The developmental profile of expression of this gene demonstrated that it begins to be significantly expressed around post natal day 5 (PND) in the developing rat retina when the photoreceptor differentiation begins to take place with the formation of the outer plexiform layer, outer nuclear layer, and the inner and outer segments (Higashide *et al*., 1996). The expression level increased rapidly throughout the remainder of the period of photoreceptor maturation and reached the maximal stable level by post natal day 23, when the retina was fully developed. The level remained the same thereafter. Throughout the developmental stage and adulthood, the site of expression was in the photoreceptors. This developmental pattern of expression is identical to that of other photoreceptor-specific genes such as rhodopsin, suggesting that HRG4/RRG4 may play a role in mature photoreceptors (Higashide *et al*., 1996). Results of the electron microscopic and immunocytochemical study showed that HRG4 is localized in the cytoplasm and on the pre-synaptic membrane of the horizontal and bipolar processes within the photoreceptor synapse (rod spherule) (Higashide *et al*., 1998). Thus, HRG4 certainly could be associated with synaptic vesicles, which are present in the cytoplasm and on the pre-synaptic membrane during docking and exocytosis (Higashide *et al*., 1998).

1.5.1. The molecular structure of Munc119

Munc119 contains 240 amino acid made up of α-helices, β-sheets, and turns (Higashide *et al*., 1996). Munc119 consists of amino terminal 77 amino acid long proline rich region and 163 amino acid long carboxy terminal that shares significant sequence homology to prenyl binding protein PrBP/δ (previously also designated as δ-subunit of photoreceptor cGMP dependent Phosphodiesterase (PDE6) (Higashide *et al*., 1996).The high degree of conservation between the human and the rat sequence suggests the importance of structural conservation for function of this retinal protein in different species.

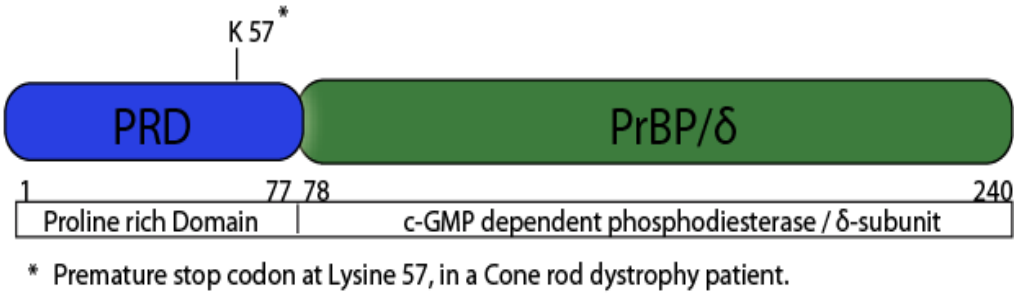

Figure.7. Schematic domain structure of Munc119

The proline-rich domain (PRD, aa1-77) is shaded in blue, the PrBP/δ-homology domain of Munc119 (aa78-240) in green. The lysine K57 indicates the site of a premature stop mutation that causes cone-rod-dystrophy in a human patient (Higashide *et al*., 1998)

The sizes of the protein in the SDS-poly acrylamide gel electrophoresis analysis were larger than the calculated sizes (27 kDa *versus* 35 and 33 kDa). The size discrepancy appears to be due to the primary characteristic of the proteins or due to post translation modification. It may be due to the proline-rich feature of these sequences, a phenomenon observed for other proteins. Of course, the native proteins may have still a different size due to post-translational modification (Higashide *et al*., 1996). The hydrophilic nature of the encoded gene product suggests that it could be a soluble phototransduction protein, but it does not contain any recognizable sequence motif for such a protein, nor does its expression show fluctuation with the light/dark cycle, as has been shown for a number of phototransduction proteins including opsin, transducin, and S antigen (Higashide *et al*., 1996).

The proline-rich amino terminal region of HRG4, which has several casein kinase II phosphorylation sites, may also be important in such interactions (Higashide *et al*., 1998). The absence of a hydrophobic membrane-insertion sequence tends to argue against HRG4 as an integral synaptic membrane protein, such as synaptotagmin, synaptobrevin, synaptophysin, or SNAP-25. It could, however, be a peripheral membrane associated protein (Higashide *et al*., 1998).

The homology of HRG4 with *unc-119* is consistent with the possibility that HRG4 may play an important role in the synaptic vesicle cycle. Although localization within the synapse or the function of *unc-119* in *C.elegans* has not yet been demonstrated, the existence of a defect in this gene leading to significant problems in movement, feeding, and chemosensation is consistent with a defect in neurotransmission (Maduro *et al*., 1995). Consistent with a nervous system role, unc-119 reporter genes are expressed throughout the *C. elegans* nervous system (Maduro *et al*., 1995). The *C.elegens* UNC-119 protein has strong sequence similarity to the predicted protein from a human gene, HRG4/HsUNC119, whose transcript is abundant in the retina (Higashide *et al*., 1999). The predicted *C. elegans*, human and *Drosophila* gene products are conserved across two domains. Expression of portions of HRG4/HsUNC-119 or DmUNC-119, directed by the unc-119 promoter, can fully rescue the *C. elegans* unc-119 mutant phenotype. UNC119, HRG4 and DmUNC119 constitute members of a new class of neural genes whose common function has been maintained through metazoan evolution (Maduro *et al*., 1995).

The UNC119 protein is expressed in various neural tissues in the developing zebra fish embryo and larva. Morpholino Oligonucleotides (MO)-mediated knockdown of unc119 results in a "curly tail down" phenotype (Manning *et al*., 2004). Examination of neural patterning demonstrates that these "curly tail down" zebra fish experience a constellation of neuronal defects similar to those seen in *C. elegans* unc-119 mutants: missing or misplaced cell bodies, process defasciculation, axon path finding errors, and aberrant axonal branching. These findings suggested that UNC119 may play an important role in the development and /or function of the vertebrate nervous system (Manning *et al*., 2004).

1.5.2. The physiological role of Munc119 in synaptic transmission

The essential function of Munc119 for synaptic transmission at photoreceptor synapses and for vision has been demonstrated in a cone-rod dystrophy patient with a premature termination codon mutation (Kobayashi *et al*., 2000). This termination codon mutation resulted in a Munc119 protein that lacked the PrBP/δ-domain. Consistently, a transgenic Munc119-mouse that reproduced this premature termination codon mutation of Munc119 also displayed severe disturbances of synaptic transmission at photoreceptor synapses and defects in vision. The transgenic model that expresses a mutant *HRG4* (identical with that found in a patient with late-onset cone–rod dystrophy) in the photoreceptor synapse shows a progressive decrease in the ERG b-wave (independent of the photoreceptor's ability to generate a c-wave), leading to retinal degeneration with prominent degeneration of the

synapses (Kobayashi *et al*., 2000; Kubota *et al*., 2002). The mechanism how Munc119 works in photoreceptor synapses is not known. The synaptic degeneration in the above mentioned patients was observed in the rod photoreceptor spherules, consistent with the expression of the transgene from the rhodopsin promoter. The presence of the disease mostly in the superior temporal quadrant also correlated with the highest expression of the transgene in this region of the retina (Kobayashi *et al*., 2000). Of interest, in the transgenic retina was the suggestion of trans-synaptic degeneration, which presumably occurred as a result of the photoreceptor synaptic degeneration. One of the postulated mechanisms for this phenomenon, which can be studied in the transgenic model, is the release of neuro-active material from the degenerating terminals that affects the postsynaptic neurons (Kobayashi *et al*., 2000).

1.5.3. The proposed functional role of Munc119 in the ribbon synapses

The specific decrease in three synaptic vesicle associated proteins in the HRG4 transgenic retina (synapsin IIa, synaptotagmin, and Doc2) further support the role of HRG4 in synaptic vesicle function (Kobayashi, *et al*., 2000). The time course of appearance of this reduction was consistent with the appearance of pathology in the transgenic model. Transgenic mice less than 1 year old do not manifest significant pathology in retinal function or morphology (Kobayashi, *et al*., 2000). The results of the Western blot analysis showed that levels of these synaptic proteins did not differ in the young transgenic and non-transgenic retinas (Kobayashi, *et al*., 2000).

Functional (reduced ERG b-wave) and structural (retinal disorganization/degeneration) defects begin to appear in the transgenic retina starting at approximately 1 year of age (Kobayashi, *et al*., 2000). In this study, reduction in the three synaptic vesicle proteins was demonstrated in the 13-month-old transgenic retina compared with normal control. One of these proteins, synaptotagmin, is present in the OPL, the site of localization of HRG4. Synaptotagmin, a postulated Ca^{2+}-regulated trigger of exocytosis (Perin *et al*., 1990) anchored in the synaptic vesicle through a 27-amino-acid trans-membrane domain. Synaptotagmin is an integral membrane protein. HRG4, however, was not shown to interact directly with synaptotagmin. The effect of HRG4 on synaptotagmin is most likely mediated by another protein with which HRG4 directly interacts (Kubota *et al*., 2002). It was interesting that in contrast to the reduction in three synaptic vesicle proteins, an increase in three cytoplasmic (rabaptin-5, rsec8, and rabphilin-3A) and two plasma membrane (syntaxin-4 and syntaxin-6) proteins was observed in the 13-month-old transgenic retina by Western blot analysis. The increase in syntaxin was confirmed by immunostaining in the transgenic IPL, despite its

reduced thickness compared with normal control (Kubota *et al*., 2002)**.** The observed increase in the IPL may be a compensatory increase in the presence of ineffective neurotransmission from the OPL in the transgenic retina. The increase, in fact, may not be restricted to the five proteins shown by the Western blot analysis. Because of the reduced thickness of the IPL in the transgenic retina, the two plasma membrane proteins, SNAP-25 and munc-18, which did not show a change in level by Western blot analysis, are probably also increased (Kubota *et al*., 2002)

The demonstrated interaction of PDEδ with ARL2 provides an interesting possibility for the function of HRG4. PDEδ, in addition to being a binding partner of ARL2 like HRG4, is homologous to HRG4 (Kobayashi *et al*., 2003). The two proteins are 23% identical overall and 30% identical in the COOH-terminal (Li *et al*., 1998). PDEδ is expressed ubiquitously, whereas HRG4 is predominantly expressed in the photoreceptors (Higashide *et al*., 1996; Florio *et al*., 1996). PDEδ was originally isolated from the soluble form of PDE6, the rod-specific cGMP Phosphodiesterase, but was found not to affect the catalytic activity of the enzyme (Gillespie *et al*., 1989; Florio *et al*., 1996). Rather, it was found to bind α and β subunits of PDE6 by their prenylated COOH ends and to solubilize them from the photoreceptor membrane (Florio *et al*., 1996). PDEδ has also been shown to interact with and solubilize Rab13, a small GTPase, involved in membrane trafficking in fibroblasts (Marzesco *et al*., 1998). PDEδ also interacts with the retinitis pigmentosa GTPase regulator (RPGR), the pathogenic gene for X-linked retinitis pigmentosa, RP3 (Linari *et al*., 1999). Cumulatively, these results point to a pattern of involvement of PDEδ in intracellular protein transport and localization (Kobayashi *et al*., 2003).

PDEδ was suggested to be a soluble transport factor for certain prenylated proteins which are mediated by interaction with ARL2-GTP (Hanzal-Bayer *et al*., 2002). HRG4 was shown not to be able to extract PDE6 from the photoreceptor outer segment membrane (Li *et al*., 1998), but it may play a role in the insertion/extraction of some other membrane protein. Because of its association with synaptic vesicles, it is tempting to speculate that HRG4 may be involved in the membrane trafficking of certain synaptic vesicle proteins (Kobayashi *et al*., 2003). Interestingly, Kubota *et al* (2002) demonstrated specific decrease in the levels of several peripheral membrane proteins of photoreceptor synaptic vesicles in a transgenic model expressing the identical truncation mutation of HRG4 as found in a human patient with late-onset cone–rod dystrophy. This phenomenon may be consistent with HRG4 playing a role in membrane trafficking of photoreceptor synaptic vesicle proteins.

Munc119 interacts with CaBP4 (calcium Binding Protein 4; Haeseleer, 2008). This interaction is compelling because both of these two proteins reportedly involved in neuronal development and synaptic transmission (Haeseleer, 2008). This study raises the possibility that CaBP4 interacts with multiple synaptic proteins that play roles in mechanisms important for normal neurotransmitter release, including Cav1.4 and Unc119 (Haeseleer, 2008). Although Unc119 is prominent in the retina, it is also expressed in myeloid and lymphoid cells (Cen *et al*., 2003) where it activates src-type tyrosine kinases important for eosinophil survival and T-cell function (Cen *et al*., 2003; Gorska *et al*., 2004).

1. 6. Protein-protein interactions in the synaptic vesicle cycle of ribbon synapses

In the biological system most of the protein, function as along with other proteins to build a functional cellular task depending upon certain external stimuli and stage of the cell. Synaptic vesicle cycles are orchestrated by protein-protein interactions in every step of exocytosis and endocytosis. As like conventional synapse many of the key protein interaction are not ruled out in ribbon synapse, since many important synaptic proteins are present in different isoform in ribbon synapse. In order to better understand the molecular mechanism of synaptic transmission in ribbon synapse, identification and characterization of protein-protein interaction is important. This information will be useful for the better understanding of the physiology of ribbon synapse.

Synaptic ribbons are dynamic organelle suggested to be the prerequisite for the fast synaptic vesicle exocytosis and endocytosis based upon electron microscopic and physiological observations (for review, see sterling and Matthews, 2005; Heidelberger *et al*., 2005). RIBEYE is a major component of synaptic ribbon. But how this synaptic ribbon orchestrates ultra-fast mechanism in ribbon synapse is still not known. In order to better understand the molecular composition and physiological role of synaptic ribbons, we performed YTH screen using RIBEYE(B)-domain as bait. In this screen I identified Munc119 as a potential RIBEYE interacting protein. I corroborated the RIBEYE-Munc119 interaction by various independent approaches in this study.

CHAPTER 2

MATERIALS & METHODS

2.1. Cells

2.1.1. Bacterial strains

Strain	Genotype	Source& Reference
DH10B	F- *mcr*A Δ(*mrr-hsd*RMS-*mcr*BC) φ80*lac*ZΔM15 Δ*lac*X74 *rec*A1 *end*A1 *ara*D139 Δ (*ara, leu*)7697 *gal*U *gal*K λ- *rps*L *nup*G	Invitrogen, Grant *et al*.,1990
BL21(DE 3)	F- *omp*T *hsd*SB (rB-mB-) *gal dcm* (DE3)	Invitrogen , Grodberg and Dunn, 1988

2.1.2. Yeast strains

Strain	Genotype	Source& Reference
AH109	MATa, trp1-901, leu2-3, 112, ura3-52, his3-200, Gal4Δ, gal80Δ, LYS2::GAL1UAS-GAL1TATA-HIS3, GAL2 UAS-GAL2 TATA-ADE2, URA3::MEL1UAS-MEL1TATA-lacZ	Clontech, James *et al*., 1996
Y187	MATα, ura3-52, his3-200, ade2-101, trp1-901, leu2-3, 112, gal4Δ,. met, gal80Δ, URA3:GAL1UAS-GAL1TATA-lacZ	Clontech, Harper *et al*., 1993

2.1.3. COS-7 cell line

Strain	Description	Reference
COS-7	Fibroblast-like cells growing as monolayer. African green monkey kidney derived from CV-1, a simian cell line (*Cercopithecus aethiops*), by transformation with an origin-defective mutant of SV-40; cells were described to support the growth of SV-40 viruses	Gluzman, 1981

2.1.4. R28 cell line

Strain	Description	Reference
R28	R28, an immortalized retinal precursor cell line derived from P6 rat retinal tissue. The 12S portion of the E1A gene was used for immortalization. It was shown to display characteristics consistent with photoreceptor, ganglion, and even Muller cell phenotypes.	Seigel,1996

2.2. Vectors

2.2.1. Bacterial expression vector

Name	Description	Reference
pMAL-C2	The pMAL-C2 vector facilitates the expression and purification of foreign proteins/peptides in Escherichia coli by fusion to maltose-binding protein. It contains *E.Coli* mal gene, Lac I and tac promoter. It has ampicillin resistance gene.	Invitrogen
pGEX-KG	The pGEX-KG vector contains coding sequence for Glutathione S Transferase (GST), MCS, pBR322 origin, and ampicillin resistance, Ptac is Transcription promoter for the Expression of the GST or GST Fusions proteins, chemically inducible by IPTG, high-level expression. An internal lac I^q gene for use in any E. coli host. Very mild elution conditions for release of fusion proteins from the affinity matrix, thus minimizing effects on antigenicity and functional activity. PreScission™, thrombin, or Factor Xa protease recognition sites for cleaving the desired protein from the fusion product.	Basal-vector from Pharmacia & pGEX-KG from T.C.Sudhof lab.

2.2.2. Yeast Two Hybrid vector

Name	Description	Reference
pACT2	The pACT2 vector expresses a hybrid protein by a fusion of the GAL4 AD, at high levels in yeast host cells from the constitutive ADH1 promoter (*P*); transcription is terminated at the ADH1 transcription termination signal; contains HA epitope tag. The protein is targeted to the yeast nucleus by the nuclear localization sequence from SV40 T-antigen. It is a shuttle vector that replicates autonomously in both *E. coli* and *S. cerevisiae* and carries the *bla* gene, which confers ampicillin resistance in *E. coli.* It also contains the *LEU2* nutritional gene that allows yeast auxotrophs to grow on limiting synthetic media.	Clontech Laboratories Inc.
pGBKT7	The pGBKT7 vector expresses proteins fused to GAL4 DNA binding domain (DNA-BD). In yeast, fusion proteins are expressed at high levels from the constitutive *ADH1* promoter	Clontech Laboratories Inc.

	(*PADH1*); transcription is terminated by the T7 and *ADH1* transcription termination signals. It also contains the T7 promoter and a c-Myc epitope tag, It is a shuttle vector replicates autonomously in both *E. coli* and *S. cerevisiae* from the pUC and 2 μ ori, respectively. It has Kan^r for selection in *E. coli* and the *TRP1* nutritional marker for selection in yeast.	
pSE1111	The pSE1111 vector expresses proteins fused to GAL4 activation domain. It used as negative control vector (prey vector) for checking auto-activation of bait constructs	Bai & Elledge, 1996
pSE1112	The pSE1112 vector expresses proteins fused to GAL4 DNA binding domain. It used as negative control vector (bait vector) for checking auto-activation of prey constructs	Bai& Elledge, 1996

2.2.3 Mammalian expression vector

Name	Description	Reference
pEGFPN1	The vector pEGFP-N1 encodes a red-shifted variant of wild-type GFP which has been optimized for brighter fluorescence and higher expression in mammalian cells. (Excitation max= 488 nm; emission max = 507 nm). Sequences flanking EGFP have been converted to a Kozak consensus translation initiation site. The MCS in pEGFP-N1 is between the immediate early promoter of CMV (PCMV IE) and the EGFP coding sequences. The vector backbone also contains an SV40 poly adenylation signals, SV40 origin for replication in mammalian cells, and pUC origin of replication and an f1 origin. It contains neomycin and kanamycin resistance genes.	Clontech laboratories Inc.
pEBG1	It's a mammalian expression vector. Non viral type. It has EF-1alpha promoter and GST tag at N terminal. It contains ampicillin resistance gene. Derived from pEF-BOS, BstXI-NotI stuffer fragment of pEF-BOS replaced with polylinker containing BamHI site, PCR to generate GST fragment from pGEX-2T with 5' BglII site, eukaryotic ribosome binding site and 3' BamHI site, inserted into BamHI site to generate pEBG.	Thiel and Cibelli,1999

2.3. Oligonucleotides

Name	No	Sequence	Res. site
Munc119 Ntem For	611	TTTTCCATGGATATGAAGGTGAAGAAGGGCG	NcoI
Munc119 Ntem Rev	612	TTTTGGATCCGCACAGGTAGTCGCCCGT	BamHI
Munc119 (PrBP/δ) For	613	TTTTCCATGGATTCCCCTGAGGAGAATATCTA	NcoI
Munc119 (PrBP/δ) Rev	614	TTTTGGATCCCCCGCTGTAGGAATAGTCA	BamHI
Munc119 For	702	TTTTGGATCCATGAAGGTGAAGAAGGGCGG	BamHI
Munc119 Rev	703	TTTTACTAGTGGGCGTCCCGCTGTAGGA	SpeI
RE(B) D758N For	866	TACTTACAG**AAC**GGGATAGAGCGG	
RE(B) D758N Rev	867	CCGCTCTATCCC**GTT**CTGTAAGTA	
RE(B) E844Q For	868	CATGAGTCT**CAG**CCCTTCAGCTTT	
RE(B) E844Q Rev	869	AAAGCTGAAGG**GCT**GAGACTCATG	
RE(B) F848W For	870	CCCTTCAGC**TGG**GCTCAGGGCCCA	
RE(B) F848W Rev	871	TGGGCCCTGAGC**CCA**GCTGAAGGG	
RE(B) K854Q For	872	GGCCCATTG**CAG**GATGCTCCAAAT	
RE(B) K854Q Rev	873	ATTTGGAGCATC**CTG**CAATGGGCC	
RE(B) I796A For	876	CACCACCTC**GCC**AATGACTTCACC	
RE(B) I796A Rev	877	GGTGAAGTCATT**GGC**GAGGTGGTG	
RE(B) E790Q For	874	AATCTGAATCAACACAACCACCAC	
RE(B) E790Q Rev	875	GTGGTGGTTGTGTTGATTCAGATT	
RE(B) E842Q For	882	GATGTGCAT**CAG**TCTGAGCCCTTC	
RE(B) E842Q Rev	883	GAAGGGCTCAGA**CTG**ATGCACATC	
RE(B) D820N For	884	GGCCTGGTG**AAC**GAGAAAGCCTTA	
RE(B) D820N Rev	885	TAAGGCTTTCTC**GTT**CACCAGGCC	
RE(B) R815Q For	928	GTGAATGCA**GCC**CAAGGTGGCCTG	
RE(B) R815Q Rev	929	CAGGCCACCTTG**GGC**TGCATTCAC	
RE(B) H864F For	930	ATCTGCACA**CCA**TTTACAGCCTGG	
RE(B) H864F Rev	931	CCAGGCTGTAAA**TGG**TGTGCAGAT	
RE(B) SBD For	523	AACATCCCATCTGCTGCAGGAGGATCTTACAG CGAACAAGCATCA	
RE(B) SBD Rev	522	TGATGCTTGTTCGCTGTTAGATCCTCCTGCAGC AGATGGGATGTT	
RE(B) NBD For	508	TTTTGAATTCTTATCCCATCTGCTGCAGT	EcoRI
RE(B) NBD Rev	509	TTTTCTCGAGGCTGTACCAGGCTGTGT	XhoI
Moazed outward For	353	GTTCCATGGAGATCCGCCCCCAGATCAT	NcoI
Moazed outward Rev	354	GTTCTCGAGCTATTGCTCGTTGGGGT	XhoI
RE(B) ACT2/GBK For	405	TTTTCCATGGTTATCCGCCCCCAGATCATGA	NcoI
RE(B)ACT2/GBK Rev	406	TTTTCTCGAGCTATTGCTCGTTGGGGTGCT	XhoI

2.4. Plasmid constructs

Plasmid name	Protein	Amino acid	Restriction site	Oligos
Munc119pACT2	Munc119	240	NcoI/XhoI	
Munc119 (PrBP/δ) pACT2	Munc119	77	NcoI/BamHI	611/612
Munc119 (PrBP/δ) pACT2	Munc119	163	NcoI/BamHI	613/614
Munc119-GSTpEBG	Munc119	240	BamHI/SpeI	702/703
Munc119pGEX	Munc119	240	EcoRI/XhoI	Sub Cloning
RE (B) pGBKT7	RIBEYE	425	NcoI/XhoI	405/406
RE (B) NBDpGEX-KG	RIBEYE	196	NcoI/XhoI	508/509
RE (B) NBDpGBKT7	RIBEYE	196	NcoI/SalI	Sub Cloning
RE(B)SBDpGBKT7	RIBEYE	229	NcoI/salI	353/354,523/524
RE(AB)pGBKT7	RIBEYE	988	NdeI/SalI	227/264
RE(B)pMal-C2	RIBEYE	425	EcoRI/XbaI	96/979
RE(B)E844QpGEX	RIBEYE	425	NcoI/xhoI	353/354,868/869
RE(B)E844QpGBKT7	RIBEYE	425	NcoI/SalI	353/354,868/869
RE(B)F848WpGEX	RIBEYE	425	NcoI/XhoI	353/354,870/871
RE(B)F848WpGBKT7	RIBEYE	425	NcoI/SalI	353/354,870/871
RE(B)K854QpGEX	RIBEYE	425	NcoI/XhoI	353/354,872/873
RE(B)K854QpGBKT7	RIBEYE	425	NcoI/SalI	353/354,872/873
RE(B)D758NpGEX	RIBEYE	425	NcoI/xhoI	353/354,866/867
RE(B)D758NpGBKT7	RIBEYE	425	NcoI/SalI	353/354,866/867
RE(B)I796ApGEX	RIBEYE	425	NcoI/XhoI	353/354,876/877
RE(B)I796ApGBKT7	RIBEYE	425	NcoI/SalI	353/354,876/877
RE(B)D820NpGEX	RIBEYE	425	NcoI/XhoI	353/354
RE(B)D820NpGBKT7	RIBEYE	425	NcoI/SalI	353/354
RE(B)E842QpGEX	RIBEYE	425	NcoI/XhoI	353/354
RE(B)E842QpGBKT7	RIBEYE	425	NcoI/SalI	353/354
RE(B)E790QNpGEX	RIBEYE	425	NcoI/XhoI	353/354
RE(B)E790QNpGBKT7	RIBEYE	425	NcoI/SalI	353/354
RE(B)R815QpGEX	RIBEYE	425	NcoI/XhoI	353/354
RE(B)R815QpGBKT7	RIBEYE	425	NcoI/SalI	353/354
RE(B)H864FpGEX	RIBEYE	425	NcoI/XhoI	353/354
RE(B)H864FpGBKT7	RIBEYE	425	NcoI/SalI	353/354
RE(B)ΔHDLpGBKT7	RIBEYE	398	NcoI/Sali	353/354,504/505
RE(B)pGEX	RIBEYE	425	NcoI/XhoI	405/406

2.5. Antibodies

Primary antibody	Anti- EGFP (Polyclonal) T3743	Gift by Prof. T.C. Südhof , Dallas
	Anti-RIBEYE(B) domain (polyclonal) U2656	Schmitz *et al*.,2000
	Anti-Munc119 (Polyclonal) UNC119 V2T2.120	Our lab made antibody
	Anti-MBP (Monoclonal)	New England Biolab Inc.
	Anti-GST (Monoclonal)	Sigma Inc.
	Anti-CtBP2 (Monoclonal)	BD Biosciences.
Secondary antibody	GAR POX	Sigma Inc.
	GAM IgG HRP	Sigma Inc
	GAM Cy3	Sigma Inc.
	GAR Cy2	Sigma Inc.

2.6. Chemicals

Agar-Agar	Roth
Agarose	Roth
3-Amino-1,2,4-triazol	Sigma
Ampicillin	Roth
BSA	Sigma
Chloroquine	Sigma
Coomassie Brilliant Blue R 250	Roth
DEAE-Dextran	Sigma
N,N-Dimethylformamid	Roth
Disodium Hydrogen phosphate	Roth
Dithiothreitol (DTT)	Sigma
EDTA	Roth
Ethidiumbromide	Roth
Glucose	Roth
Glutathione-Sepharose	Sigma
Glycerine	Roth
Glycine	Roth

IPTG	Roth
Potassium chloride	Roth
Potassium hydrogen phosphate	Roth
Lithiumacetate	Sigma
Lysozyme	Sigma
Magnesium chlorid Hexahydrate	Roth
β-Mercaptoethanol	Roth
Sodium azide	Sigma
Sodium carbonate	Roth
Sodium chloride	Roth
Sodium dihydrogenphosphate	Roth
NPG (n-Propylgallate)	Sigma
ONPG (o-Nitrophenyl-β-D-galactoside)	Sigma
Phenylmethylsulfonylfluoride (PMSF)	Roth
Ponceau-S	Roth
Saccharose	Roth
Sorbitol	Roth
Tris	Roth
Triton X-100	Fluka
X-Gal(5-Brom-4-Chlor-3-indoyl-β-galactoside)	Roth

2.7. Buffers & Media

Acetate buffer (P3)	3 M Potassium acetate, pH 5.5
3-Amino-1,2,4-triazol	10 mM in dd H_2O
Ampicillin	50 mg/ml dd H_2O, filtersteriled
Bradford-Reagenz Roti®-Quant	Carl Roth
Breaking Buffer	100 mM Tris-HCl pH 8,0 1 mM β-Mercaptoethanol 20 % Glycerol
100 x BSA 10 mg/ml (Restriction digestion)	New England Bio labs
Coomassie-Brilliant blue stain	600 ml Isopropanol, 1560 ml dd H_2O. 240 ml acetic acid

	0.6 g Coomassie Brilliant Blue R 250
Dulbecco´s modified Eagle's Medium (DMEM)	Invitrogen 4 mM Glutamine 1.5 g/l Sodium Bi carbonate 4.5 g/l Glucose 1 mM sodium pyruvate + 50 ml FCS (Invitrogen)
ECL-solution	ECL-I (for 100 ml aliquot) Tris 1M pH 8.5 10 ml Luminol stock 1 ml PCA 440 µl. Made up to 100 ml with dd H_2O ECL-II Tris 1M pH 8.5 10 ml H_2O_2 64µl Made up to 100 ml with dd H_2O
De-staining solution for coomassie stain gel	100 ml acetic acid, 300 ml Ethanol Made up to 1 litre with dd H_2O
Loading buffer for Agarose gel	10 µl 100mM EDTA 490 µl dd H_2O 500 µl Glycerol
LiAc/TE/DTT	20 ml 1 M Lithium acetate 10 ml 200mM DTT 20 ml TE (0,1M Tris-HCl, 10mM EDTA) Made up to 200 ml with dd H_2O- Filter steriled
IPTG stock solution	0.1M in PBS
Lysis Buffer for *E. coli* (P2)	200 mM NaOH, 1% SDS
COS-Cell lysis buffer	1.0% TritonX-100 100 mM Tris HCl pH 7,9 150 mM NaCl,1 mM EDTA
LB Nutrient medium for Bacteria	Invitrogen
Na_2CO_3	1M in dd H_2O

ONPG-Stock solution	4 mg/ml in Z-Buffer
5x PBS	40 g NaCl 1 g KCl 7.2 g Na_2HPO_4 1.2 g KH_2PO_4 Make up to 1 litre with dd H_2O
PMSF-Stock solution	40mM in 100% Isopropanol
Polyacrylamide gel 10% (minigel)	1 ml dd H_2O, 1.27 ml 1 M Tris pH 8.8 1.67 ml 30% Acrylamide 50 µl 10% SDS,1 ml 50% Glycerol 3.3 µl TEMED 25 µl 10% APS
Ponceau S-stain	30 g Trichloroaceticacid 5 g Ponceau S Make up to 1 litre with dd H_2O
R28 cell medium	500ml DMEM 50ml NCS (10%) 5ml MEM vitamins(100X) 5ml MEM Non essential amino acid (100X) 25ml Sodium bicarbonate (7.5%) 1.25ml of 200mM Glutamine
Resuspensions Buffer P1	50 mM Tris-HCL, pH 8.0 10 mM EDTA, 100 µg/ml RNase A
SD-Dropout-Medium (Minimal medium) -L SD Dropout-liquid medium -W SD Dropout-liquid medium -LW SD Dropout-liquid medium -ALWH SD Dropout- liquid medium	26.7 g/l +0.69 g -Leu-DO Supplement (BD) +0.74 g -TRP-DO Supplement (BD) +0.64 g-Leu-TRP-DO Supplement(BD) +0.6 g-Ala-Leu-Trp-HIS-Supplement (BD) All medium was make up to 1 litre with ddH_2O. Adjusted pH 5.8

SDS-PAGE-Electrophoresis buffer	3.03 g Tris 14.4 g Glycine,1.0 g SDS Make up to 1 litre with ddH_20
SDS-loading buffer 4 x	1,6 g SDS 4 ml β-Mercaptoethanol 2 ml Glycerol 2 ml 1M Tris pH 7 4 mg Bromo phenol blue 2 ml of ddH_2O
Taq-Buffer	Peqlab
2 x TBS	28 ml 5 M NaCl, 3 ml 1 M KCl 1 ml 1 M $CaCl_2$ 0.5 ml $MgCl_2$ 4,5 ml 200 mM Na_2PO_4, pH 7.4 20 ml 1 M Tris-HCl, pH 7.9 Make up to 500 ml with filter steriled water
1xTAE-Buffer	40 mM Tris pH 7,8 10 mM Sodium acetate 1 mM EDTA
Transfer Buffer (Western Blot)	Tris 15.125 g ,Glycine 72.05 g Methanol 1 litre Make up to 5 litres with ddH2O
X-Gal-solution	20 mg/ml in N,N-Dimethylformamid
X-Gal detection solution	340µl X-Gal- solution 54 µl β-Mercaptoethanol Make up to 20 ml with Z-Buffer
YPD-Medium(Clontech)	50g YPD dissolved in 1 litre of ddH2O.Autoclaved
Z-buffer	60mM Na_2HPO_4 40mM NaH_2PO4 10mM KCl, 1mM MgSO4 50mM 2-mercaptoethanol pH 7.0

2.8. Recombinant DNA techniques

2.8.1. Polymerase Chain Reaction

The following criteria were changed according to need.

Primers were designed manually according to basic principles. The Tm value of primer was kept around 50-55°C. Primer length was usually not more than 20-22 bases. The restriction sites were added to the primers along with overhang ends for efficient digestion of PCR products and cloning in to the specific vectors. Primers were diluted in sterile ddH_2O to get a 100 µM stock concentration. 100-200 ng of DNA was used as a template.

PCR master mix

10x PCR buffer-5µl

10mM dNTPs-1µl

Template DNA-100ng

100µM Forward primer-0.5µl

100µM Reverse primer-0.5µl

Taq Polymerase (5U/µl)-1µl

Sterile water to make up to 50µl

PCR cycling condition

Initial Denaturation-95°C for 2 mins

8 cycles

Denaturation- 95°C for 30 sec

Annealing- 55°C for 30 sec

Extension-72°C (approximately 1 min for 1000bp)

30 cycles

Denaturation- 95°C for 30 sec

Annealing- 65°C for 30 sec

Extension-72°C (approximately 1 min for 1000bp)

Final extension-72°C for 7 mins

2.8.2. Agarose gel electrophoresis

Agarose gel electrophoresis is used for separation, purification and identification of plasmid DNA and DNA fragments. The size of a DNA fragment was determined by comparison with standard DNA Marker. Rough estimation of the DNA concentration can be

made by comparing the band intensity of the sample and a reference marker DNA band upon staining with ethidium bromide. Depending on the size of the DNA molecules, the agarose concentration chosen was between 0.8 % and 1.2 % (w/v). DNA-samples were mixed with 10x DNA loading buffer and applied into the wells of the gel. In parallel, a marker was loaded. 1X TAE buffer was used for agarose solution and as electrophoresis buffer. The electrophoretic separation was done at 5volts/cm. DNA was visualized by UV-light and documented using BIO-RAD Gel Doc apparatus.

2.8.3. Agarose gel extraction

The DNA fragments were extracted from agarose gel using QIA®quick gel extraction kit. The specific DNA band was cut out from the gel. 1 ml of QX1 buffer and 5µl of QX1 suspension were added to the gel band. This mixture was kept at 55°C shakers for 30 mins. Then the mixture was centrifuged at 13,000 rpm for 1 min and the supernatant was removed. To the pellet 1 ml of QX1 buffer was added and mixed. The centrifugation step was repeated. To the pellet 1 ml of PE wash buffer was added and mixed. The mixture was centrifuged at 13,000 rpm for 1 min and the supernatant was removed. This step was repeated and the pellet was dried at room temp for 15 mins. Then 30 ml of pre-warmed 1mM Tris HCl pH8.4 was added and kept at 55°C in thermal shaker for 10 mins. This mixture was centrifuged at 13000 rpm for 2 mins and the supernatant which contains DNA was used for further experiment.

2.8.4. Restriction digestion & ligation (cloning)

Restriction Digestion mixture

Plasmid	10.0µl
10X buffer	3.0µl
10X BSA	3.0µl
Enzyme I	0.5µl
Enzyme II	0.5µl

Sterile dd H_2O was added to make up 30µl

The insert and vector were digested with appropriate enzymes for 2 to 3 hours at 37°C. The digested products were fractionated by agarose gel electrophoresis. Then appropriate band excised from the gel and eluted using Qiagen gel extraction method. The concentration of eluted insert and vector DNA was measured. The insert to vector concentration used for ligation is 3:1 weight ratio.

Ligation mixture

Insert	12µl (approx.400ng)
Vector	4µl (approx.100ng)
10X ligase buffer	2µl
T4 DNA ligase	1µl
Sterile dd H_2O to make up	20µl

The ligation mixture was incubated at room temp for over night. The amounts of restriction enzyme and DNA, the buffer and ionic concentrations, and the temperature and duration of the reaction vary depending upon the specific application. Then 2 µl of ligation mixture was electroporated to *E.Coli* DH10B bacteria. The colonies were selected on respective antibiotic plates and plasmids were isolated from mini culture and the insert was checked by restriction digestion and confirmed by sequencing.

2.8.5. Precipitation of ligation mixture

The DNA was purified from high salt concentrations for an efficient transformation into *E. coli* DH10B by electroporation. Precipitation was done with 3M sodium acetate. (1 volume ligation mixture, 1/10 volume 3M sodium acetate (pH 5.0) and 10 volumes of ice cold ethanol). The DNA pellet was washed once with 70% ethanol and resuspended in a suitable volume of ddH_2O.

2.8.6. Determination of DNA concentration

The DNA molecules in solution can absorb UV-light and this absorption can be measured by a spectrophotometer. The optical density at 260nm is directly proportional to the DNA concentration. The following relationship exists between the optical density (OD) and the DNA concentration: Double stranded DNA: 1 $OD_{\mathbf{260\ nm}}$ = 50µg/ml

2.8.7. Bacterial transformation

2.8.7.1. Preparation of electrocompetent *E. coli* DH10B & BL21 bacteria

All procedures were carried out in sterile and aseptic environment. Glycerol stock of *E.coli* cells was freshly streaked on LB plate and incubated overnight at 37°C. 50 ml LB preculture was grown at 37°C, 160 rpm for overnight after single colony inoculation. 500 ml main culture (in 2 liters flask) was prepared with inoculation of 20 ml overnight grown preculture. Cells were grown at 37°C, 160 rpm till an $OD_{\mathbf{600nm}}$ 0.9-1.0 was achieved. Electro competent cells were prepared at 4°C. The cultures were transferred to a sterile falcon tubes

and centrifuged at 3,500rpm, 15min at 4°C. The cell pellet was washed thrice in the ice-cold, sterile, double-distilled water and centrifuged at 3,500rpm, 15min at 4°C. The final washed pellet (~4ml) was resuspended in 5 ml sterile, ice-cold 10% glycerol (made in sterile water). Aliquot's of (50µl) cell suspension was made in prechilled 1.5 ml eppendorf tube, and frozen in liquid nitrogen. Electro competent cells were stored at -80°C for long term storage. Using this method, we routinely got approximately 6 – 8 (10^8) transformants / µg DNA

2.8.7.2. Transformation of elecrtocompetent bacteria *E.coli*

The LB medium was kept at room temperature for 30 mins. The electroporation cuvette was kept in the ice for 10 mins. The competence bacteria were thawed on the ice for 1 mins. 2 µl of ligated DNA or plasmid DNA was added to the competence bacteria and this sample added to the pre chilled cuvette. Electric shock was given at 1200V for 5 msec. Immediately after electric shock, 1 ml of antibiotic free LB medium was added and the sample was transferred to the test tube and incubated at 37◦C for 1 hr. After incubation, the sample was spreaded on suitable antibiotic selection plate and incubated for over night at 37◦C. A single colony can be expanded in LB medium containing specific antibiotic and this culture was used for plasmid preparation.

2.8.8. Isolation of plasmid DNA

2.8.8.1. Mini preparation

Plasmid DNA was isolated from bacterial cultures using alkaline lysis method. Single bacterial colony was allowed to grow over night in 5 ml of LB medium with appropriate amount of specific antibiotic at 37◦C. 1 ml of culture was stored at 4◦C for maxi preparation. 4 ml cultures were centrifuged in a 15 ml falcon tube at 4,000 rpm for 10 mins at 4◦C. The pellet was resuspended with 250 µl of buffer I. This mixture was transferred to 1.5 ml of microfuge tube. 250 µl of buffer II was added to that and mixed After incubating at room temperature for 5 mins, 350 µl of buffer III was added and incubated for 10 mins at room temperature. This sample was centrifuged at 13,000 rpm for 15 mins at 4◦C. 600 ul supernatant was removed and mixed with 800 µl of isopropanol. This sample was centrifuged at 13,000 rpm for 20 mins. The supernatant was removed and the pellet was washed with 1 ml of 70% ethanol, air dried and resuspended in 40 µl of 1 mM Tris HCl pH8.5.

2.8.8.2. Maxi preparation

The plasmid isolated using mini preparation was checked for specific insert by restriction digestion. 200 µl of bacterial culture from storage culture was inoculated in to 100

ml of LB medium with appropriate antibiotic and incubated for overnight at 37°C. The cells were harvested by centrifugation at 4000 rpm for 20 mins at 4°C. The pellet was resuspended in 5 ml of buffer I by vortexing. Then, 5 ml of buffer II was added to that and incubated for 10 mins at room temp. There after, 8 ml of buffer III was added and mixed thoroughly. This sample was centrifuged at 8500 rpm for 20 mins until no pellet appears. The supernatant was transferred to 50 ml Beckman centrifuge tube and 15 ml of isopropanol was added to that. After centrifugation at 13,000 rpm,1 hr, supernatant was removed and the pellet was washed with 15 ml of 70% ethanol; air dried and resuspended in 1 ml of 1mM Tris HCl (pH 8.5).

2.8.9. Purification of plasmid DNA for sequencing

100 µl of plasmid DNA was mixed with 500 µl of binding buffer and added to the column and kept for centrifuge at 13000 rpm for 1 min. the supernatant removed and 500 µl of PE wash buffer was added and centrifuged at 13000 rpm for 1 min. the supernatant removed and the above step repeated again. Finally only the column was centrifuged to remove the traces of alcohol. 50µl of prewarmed (at 55°C) 1 mM Tris HCl (pH8.4) was added to the column kept for incubation at room temp for 5 mins and centrifuged. The supernatant collected contain plasmid DNA. The OD value of DNA was measured by spectrophotometer. Approximately 2 µg of DNA was sent for sequencing to MWG sequencing service centre.

2.8.10. Site directed mutagenesis

Site-directed mutagenesis involves the introduction of mutations at the DNA level to alter the primary amino acid sequence of proteins. COMBO PCR methods for site-directed mutagenesis utilize four oligonucleotides primers in two rounds of PCR. In the first round of PCR external forward and mutant reverse primers was used in one reaction (N-terminal PCR product); external reverse and mutant forward was used in another reaction (C-terminal PCR product). Pfu polymerase was used in this first round. In the second round of PCR, the two PCR products (N and C-terminal) were annealed after denaturation and amplified using external forward and external reverse primers. Taq polymerase was used in this second round PCR.

1st round-Mutagenesis PCR

PCR Master Mix-I

10X Pfu buffer……...5.0µl

10mM dNTPs …….. 1.0µl

100µM Forward Primer (#353)……0.5µl

100µM Reverse Primer (Mutagenic)……0.5µl

Template cDNA…….....0.5µl

Pfu Polymerase…….0.5µl

Sterile ddH_2O……..42.0µl

PCR Master Mix-II

10X Pfu buffer……..5.0µl

10mM dNTPs …….....1.0µl

100µM Forward Primer (Mutagenic)…….....0.5µl

100µM Reverse Primer (#354)…….....0.5µl

Template……...0.5µl

Pfu Polymerase…….....0.5µl

Sterile ddH_2O……..42.0µl

PCR cycling condition

95°C -2 mins

8 cycles

95°C -30 secs; 55°C -30 secs ; 72°C -1 min

30 cycles

95°C -30 secs ; 65°C -30 secs ; 72°C -1 min

1 cycle

72° C -7 mins

2nd round-combo PCR

10X PCR buffer…….5µl

10mM dNTPs……1µl

25mM MgCl2……1µl

100µM Forward Primer (353)…….....1µl

100µM Reverse Primer (354)……1µl

Template (PCR-I)……..4µl

Template (PCR-II)…….4µl

Taq Polymerase……..1µl

Sterile ddH_2O……35µl

PCR cycling condition

95°C -5 mins

1 cycle

70°C -5 mins ; 65° C-5 mins ; 60°C -2 mins ; 72°C-3 mins

30 cycles

95°C-3 mins ; 95°C -30 secs ; 65°C-30 secs ; 72°C-1:30 mins

1 cycle

72°C -10 mins

2.9. Yeast Two Hybrid methods

For Yeast-Two-Hybrid (YTH) analyses, the Gal4-based Matchmaker Yeast-Two-hybrid System (Clontech) was used according to the manufacturer's instructions. For the YTH screening we used a bovine retinal YTH cDNA library from the retina (Tai *et al*., 1999). The cDNA of the respective bait proteins were cloned in frame with the Gal4-DNA-binding domain of pGBKT7. The cDNA of the indicated prey proteins were cloned in frame with the Gal4-activation domain of pACT2 or pGADT7. The bait and prey plasmids confer tryptophan and leucine prototrophy to the respective auxotrophic yeast strains.

2.9.1. Yeast cell transformation

2.9.1.1. Preparation of electrocompetent yeast

Preparation of electrocompetent yeasts and electroporation of yeasts were done as described by Helmuth *et al*., 2001. For identifying transformants, yeasts were plated on the respective selective plates to identify the resulting convertents to the respective prototrophy (drop out media Clontech / QBiogene).

The yeast strain AH109 and Y187 were streaked from the glycerol stock on YPD plate and incubated at 30◦C till the colony appears. Precultures were made by inoculating the single colony in 10 ml of YPD medium by incubation over night at 30◦C. From this, all steps were carried out in ice. The cells were harvested by centrifugation at 2000 rpm for 10 mins at 4◦C. The cell pellet was washed twice with sterile cold distilled water. The cells were collected from washing each time by centrifugation at 2000 rpm for 10 mins at 4◦C. Then the cells were treated with 1M sorbitol followed by centrifugation at 2000 rpm for 10 mins at 4◦C. Then, the cells were incubated with 20 ml of incubation mixture containing 100 mM LiAc, 10 mM β-mercaptoethanol and 1X TE buffer at 30◦C for 30 mins at 250 rpm. The cells were collected by centrifugation at 2000 rpm for 5 mins at 4◦C. 1 M sorbitol washing step was

repeated once. The pellet was bathed in 100-200 µl of 1M sorbitol and it was used for electroporation.

2.9.1.2. Electroporation

120 µl of electro competent yeast cells were mixed with 1 µl of plasmid DNA and electroporated at 1800 V for 5 msec. 1 ml of YPD medium was added to the mixture and incubated at 30°C for 1 hr at 600 rpm. After incubation, 100 µl of sample was spreaded on selection plates (AH109 -W plate; Y187 –L plate) and incubated at 30°C for 2-3 days

2.9.2. Yeast mating

Yeast strains Y187 and AH109 were used that contain distinct auxotrophic marker genes: AH109 [MATa, trp1-901, leu2-3, 112, ura3-52, his3-200, Gal4Δ, gal80Δ, LYS2::$GAL1_{UAS}$-$GAL1_{TATA}$-HIS3, $GAL2_{UAS}$-$GAL2_{TATA}$-ADE2, URA3::$MEL1_{UAS}$-$MEL1_{TATA}$-lacZ] (James *et al*., 1996); Y187 [MATα, ura3-52, his3-200, ade2-101, trp1-901,leu2-3,112, gal4Δ,. met, gal80Δ, URA3::$GAL1_{UAS}$-$GAL1_{TATA}$-lacZ] (Harper *et al*., 1993). The bait (pGBKT7) and prey (pACT2/pGADT7) plasmids confer tryptophan and leucine prototrophy to the respective auxotrophic yeast strains. Bait plasmids were always electroporated into AH109 yeast, and grown in –W plate whereas all prey plasmids were transformed into Y187 and grown in –L plate. For interaction analyses, AH109 yeasts containing the respective bait plasmid were mated with Y187 yeasts containing the respective prey plasmid. For the mating, pSE1111 and pSE1112 (Bai *et al*., 1996) as well as the empty bait and prey vectors were used as negative controls. The control plasmid pCtiP-ACT2 served as a positive control (Yu *et al*, 2000). Single colony from -L and –W plate (respective prey and bait construct) were added to the 1 ml of YPD medium and mixed. This sample was incubated at 30°C for 6 hours. After incubation, the samples were pelleted down by centrifugation at 3000 rpm for 5 mins at 4°C. The supernatant was discarded and keep the cell pellet in 100 µl of remaining supernatants. 50 µl of cells were spreaded on selection plate –LW; and another 50 µl of cells were spreaded on selection plate –ALWH +100 µl of 10mM ATZ. The plates were incubated at 30°C until colony appeared.

2.9.3. β-galactosidase assay

Expression of β-galactosidase (β-gal) marker gene activity was qualitatively analyzed by filter assays and quantitatively with liquid assays as described (Stahl, *et al*., 1996).

2.9.3.1. Colony lift filter assay

To rule out the false positive that grown on dropout medium (-ALWH), this test was performed to determine which of the positive colonies are also LAC Z positive, by screening for blue colour colonies in β- galactosidase assay. The whatman filter paper was laid on to the yeast colonies. The filter paper was removed using forceps and immersed in liquid nitrogen by facing colony side up. The Petri dish was prepared with 20 ml of Z buffer containing 340 µl of 50 mg/ml X-gal. A replica of the yeast colonies were made with whatman filter (#1). The yeast on the filter was cracked in liquid nitrogen and then placed on the Z buffer, by colony faced up with out air bubbles. Cover the bottom of the dish and place at room temperature.

2.9.3.2. Liquid assay

The single colony from the mating selection plate (-LW) was inoculated in 5 ml of selection medium (-LW) and allowed to grow overnight at 30°C. The cells were harvested by centrifugation at 2000 rpm for 5 mins. The cells were kept on the ice from this point. The supernatant was discarded and the pellet was resuspended in 250 µl of breaking buffer and transferred to 1.5 ml microfuge tubes. The glass beads were added until the beads reach a level just below the meniscus of the liquid. 12.5 µl of PMSF stock solution was added. The tube was vortexed 6 times at top speed in 15 second bursts. The tube was chilled on ice in between bursts. Again 250 µl of breaking buffer was added and mixed well.

The liquid extract was extracted using 1000 µl pipette by plunging to the bottom of the tube. The extract was clarified by centrifugation at 13000 rpm for 15 mins. 100 µl of extract was added to 0.9 ml of Z buffer. The mixture was incubated in thermal shaker at 28°C for 5 mins. The reaction was initiated by adding 0.2 ml of ONPG stock solution and incubation was continued until the mixture has acquired a pale yellow colour. The reaction was terminated by adding 0.5 ml of Na_2CO_3 stock solution. The precise time between starting and terminating the reaction was noted. The optical density was measured at 420 nm. The protein concentration was measured using the dye binding assay of Bradford (1976). The specific activity of the extract was expressed according to the following formula:

$$\frac{OD420 \times 1.7}{0.0045 \times \text{protein} \times \text{extract volume} \times \text{time}}$$

OD420 is the optical density of the product, o-nitro phenol, at 420nm

The factor1.7 is the correction for reaction volume

The factor 0.0045 is the optical density of a 1 nmole/ml solution of O-nitro phenol

Protein concentration expressed as mg/ml

Extract volume is the volume assayed in ml

Time is in minutes

Specific activity is expressed as nmoles/minute/mg of protein

2.10. Expression and purification of recombinant protein

2.10.1. Expression of fusion proteins

The plasmid constructs, pGEX-KG, pMunc119-GEX-KG, pMBP-C2 and pRIBEYE(B)MBP-C2 to BL21 were electroporated into the electro competent bacteria BL21(DE3) at 1200 volt for 5 ms. 1 ml of LB medium was added to these bacteria and incubated for 1 hr at 37°C, 220 rpm. The bacterial cultures were spreaded on LB-Amp plates and incubated at 37°C overnight. The precultures were prepared by inoculating the overnight grown isolated colonies in 5 ml of LB medium with 10 µl of ampicillin (50mg/ml) and incubated for over night at 37°C at 220 rpm.

5 ml of precultures were transferred to 500 ml of LB medium with 1 ml of ampicillin (50mg/ml) and incubation was continued until an OD_{600} of 0.8-0.9 at 37°C at 220 rpm. After reaching the appropriate OD (OD_{600} equals 0.9 to 1.0 is optimum for induction) the cultures were incubated at room temperature for 30 mins with shaking at 220rpm. 600 µl of 100 mM IPTG was added to the growing culture for the induction of protein expression and incubation was continued for 5 hours at room temperature. From this step all experiments were done at 4°C. The cells were harvested by centrifugation at 3,500 rpm for 20 mins.

The pellet was washed thrice by resuspension with 50ml of ice cold PBS and centrifuged at 3,500 rpm for 15 mins. Then, the pellets were incubated with 500µl of 10 mg/ml freshly prepared lysozyme in a total volume of 20ml of PBS for 1 hr at 4°C. The cell membrane was disrupted by sonication. The supernatants were collected by centrifugation at 13,000 rpm for 1 hr. This procedure was repeated until no pellet appears.

2.10.2. Purification & elution of fusion proteins

1 ml of glutathione agarose beads or 200µl of amylose beads were washed thrice with ice cold PBS and added to the supernatant containing the GST, Munc119-GST protein and MBP, RIBEYE(B)-MBP respectively. These samples were incubated for over night at 4°C in cold room for binding of GST and GST fusion protein to glutathione agarose beads; MBP and MBP fusion protein to amylose beads. Then the samples were centrifuged at 1500 rpm at 4°C

for 2mins and the supernatant was removed. The pellets were washed thrice with 50 ml of ice cold PBS for three times by shaking for 30 mins at 4°C. After last washing the beads were saved as bathed in 500 µl of PBS. 20 µl of beads were loaded on to the 10% SDS-PAGE for checking the expression. The MBP and MBP fusion protein was eluted using elution buffer containg 10 mM TRIS-HCl pH (8.5), 10% maltose in PBS in different fractions and checked it on 10% SDS-PAGE. The GST and GST fusion proteins were eluted in buffer containg 10mM reduced glutathione, 50 mM TRIS-HCl pH (8.5)

2.10.3. Measurement of protein concentration

The Bradford Mini assay was used to calculate the protein concentration (Bradford, 1975). The absorbance for the protein-specific dye, Coomassie brilliant blue G-250, shifts from 465 nm to 595 nm when binding to protein occurs. The measured absorbance at 595 nm was blotted against a reference curve obtained with known concentrations of BSA.

2.11. SDS-PAGE

SDS PAGE was done by following Mannitis *et al*, 2005. One dimensional gel electrophoresis under denaturing conditions in presence of 0.1% SDS separates proteins according to their molecular size. The polyacrylamide gel is casted as a separating gel topped by a stacking gel. Sample proteins were solubilized by boiling in 6X SDS loading buffer. Coomassie brilliant blue R- 250 binds non-specifically to almost all proteins, which allows detection of protein bands in polyacrylamide gels. Gels were stained with Coomassie staining solution with gentle shaking for 30 min at room temperature. The background was subsequently reduced by soaking the gel in Acrylamide gel destaining solution. After that, gels were documented using either HP scanner or BIO RAD Gel Doc apparatus.

2.12. Western blotting

Proteins were separated by SDS-PAGE and transferred from the polyacrylamide gel to a PVDF or nylon membrane with a constant voltage (3 hrs, 50 volt at 4). After electro blotting, the membrane was stained with ponceau-S for 2 mins. The ponceau S stained membrane was documented using scanner. Then the membrane was destained using PBS and blocked with 5% MMP for 1 hour. For immunodetection of proteins, the primary antibodies were diluted in 5% MMP and the membrane was incubated for over night in cold room with constant mild shaking. Then the membrane washed with PBS 3 times. After that, the secondary antibody was diluted in 5% MMP and the membrane was incubated at room temp

for 1 hour. Then the membrane was washed with PBS 3 times. Then finally the membrane was incubated with ECL1 and ECL2 mixture (1:1 ratio; chemiluminescence's detection solution) and the signals were documented with BIO RAD Gel Doc apparatus. Also the band intensity was quantified using BIO RAD Gel Doc apparatus.

2.13. Cell culture

2.13.1. COS-7 cell culture

COS-7 cells were cultured in DMEM medium with 10% FCS. For sub-culturing, the medium from the 4 days old culture was removed and the cells were washed once with 5 ml of PBS. The cells were incubated with 1ml of 0.25% trypsin. The culture flask was gently taped and 10 ml of DMEM medium with 10% FCS was added and mixed. To the new flask, 5 ml of DMEM medium with 10% FCS along with 500µl of trypsinized cells were added and incubated for 4 days at 37°C. For transfection 1 ml of trypsinized cells were added to the 6 ml of DMEM medium with 10% FCS and incubated for 24 hours at 37°C. For Immunocytochemistry, 2 ml of medium and 500 µl of trypsinized cells were added to the cover slip containg small Petri dish and allowed to grow for one day at 37°C.

2.13.2. R28 cell culture

R28 cells were cultured in specific medium (see materials section 2.7 for composition). For sub-culturing, the medium from the 7 days old culture was removed and the cells were washed twice with 5 ml of PBS. The cells were incubated with 1ml of 0.25% trypsin. The culture flask was gently taped and 10 ml of R28 medium was added and mixed. To the new flask, 5 ml of R28 medium along with 500µl of trypsinized cells were added and incubated for 7 days at 37°C. For transfection 1 ml of trypsinized cells were added to the 6 ml of R28 medium and incubated for 24 hours at 37°C. For Immunocytochemistry, 2 ml of R28 medium and 500 µl of trypsinized cells were added to the cover slip containg small Petri dish and allowed to grow for one day at 37°C

2.14. COS-7 cells transfection

Transfection of COS-7 cells was performed using the DEAE Dextran method as previously described by Schmitz *et al*, 2000. The COS-7 cells were allowed to grow for 24 hrs, to get a 50 % confluency. The plasmid-DNA mixture was prepared by adding 1254 µl of Sterile H_2O; 1650 µl of 2X TBS; 330 µl 0.5M DEAE-Dextran and 2.5 µg (25 µl of 0.1 mg/ml) of purified plasmid DNA. This mixture was incubated at room temperature for 10

mins. The DMEM medium was removed from the Petri dish and the cells were washed twice with 5 ml of PBS. Then the cells were incubated with plasmid DNA mixture for 45 mins at 37°C. After incubation, the plasmid DNA mixture was removed. After that, the cells were incubated with 6 ml of DMEM medium with 10 % FCS containg 6 µl of 100 mg/ml of chloroquine for 3 hours at 37°C. The chloroquine-DMEM medium was removed and cells were washed twice with 5ml of PBS. Then, 6 ml of DMEM medium (without FCS) containg 20% glycerol was added to the cells and incubated for 2 mins at room temperature. The DMEM medium (without FCS) with 20% glycerol was removed from the plate and the cells were washed twice with 5 ml of PBS. Finally the cells were incubated with 6 ml of DMEM medium with 10% FCS at 37°C for 48 hrs.

2.15. GST pull-down assay

2.15.1. Bacterial fusion proteins GST pull-down assay

GST and Munc119-GST bound to glutathione agarose beads was used as an immobilized partner (bait). The eluted MBP and RE (B)-MBP fusion protein was used as a prey for this assay. The eluted RE(B)-MBP fusion protein and MBP protein (control) were incubated with eluted Munc119-GST fusion protein and GST protein (control) in equivalent - molar concentration in a total volume of 500 µl incubation buffer (100 mM TRIS HCl pH 7.9 ,150 mM NaCl,1 mM EDTA and 0,25% TritonX-100). These samples were incubated for 4 to 6 hrs at 4°C. After incubation, the samples were centrifuged to remove the supernatant. The pellets were washed 5 times with incubation buffer. Every washing step was followed by centrifugation at 13000 rpm for 1 min at 4°C. The pellet was boiled in SDS-PAGE loading buffer at 96°C for 5 mins. The eluted proteins were subjected to 10% SDS-PAGE followed by coomassie staining. And in parallel reaction, one fifth of the eluted proteins were subjected to 10% SDS-PAGE for western blotting. The membrane was first detected with MBP antibody followed by GST antibody after stripping.

	Lane	Protein	Vol. (µl)	(%) in total	Protein	Vol. (µl)	(%) in total
Input	1	GST	3	50			
	2	MBP	15	50			
	3	Munc119-GST	7	50			
	4	RE(B)-MBP	15	25			
Pellet	1	GST	6	100	MBP	30	100
	2	GST	6	100	RE(B)-MBP	60	100
	3	Munc119-GST	14	100	MBP	30	100
	4	Munc119-GST	14	100	RE(B)-MBP	60	100

Protein	Nature	Concentration (mg/ml)	Protein used for each experiment (µg)
GST	Immobilized	1.7	10
Munc119-GST	Immobilized	1.5	20
MBP	Eluted	0.5	15
RE(B)-MBP	Eluted	0.5	30

Input-protein used in the experiment

Pellet – the proteins bound with GST empty or Munc119-GST (glutathione sepharose beads bound) which is settled after incubation followed by washing

2.15.2. COS-7 cells GST pull-down assay

The COS-7 cells were allowed to grown 24 hours after splitting. The cells were co transfected with Munc119-GST and RE(B)-EGFP or GST and RE(B)-EGFP constructs. After 48 hrs of incubation, cells were scrapped off from the plate and pelleted by centrifugation at 6000 rpm for 5 mins. The pellets were transferred to sterile 1.5 ml microfuge tube and washed with ice cold PBS for 2 times. The cells were incubated with 500 µl of ice cold Lysis buffer (100mM TRIS , 150mM NaCl, 1mM EDTA and 1% TritonX-100) for 30 mins at 4°C After incubation, the samples were centrifuged at 13000 rpm for 15 mins. The supernatant was removed and the centrifugation step was repeated. 100 µl of glutathione sepharose beads was washed in the lysis buffer 3 times. The Munc119-GSTand RIBEYE(B)-EGFP, GST and RE(B)-EGFP supernatants were incubated with 100 µl of washed glutathione sepharose beads for over night at 4°C. After the incubation, the samples were centrifuged at 13000 rpm for 1 mins and the pellets were washed three times with lysis buffer. The final pellets were boiled in 30 µl of SDS loading buffer for 3 mins at 96°C and subjected to 10% SDS-PAGE followed by western blotting with anti-GFP and anti-GST antibodies.

Fraction	lane	Co transfection	Vol. (µl)	(%) in total
Input	1	GST+ RE(B)-EGFP	40	10
	2	Munc119-GST+ RE(B)-EGFP	40	10
Pellet	3	GST+ RE(B)-EGFP	400	100
	4	Munc119-GST+ RE(B)-EGFP	400	100

Input- proteins used in the experiment

Pellet – the proteins bound with GST empty or Munc119-GST (glutathione sepharose beads bound) which is settled after incubation followed by washing

2.15.3. GST pull-down assay in presence of NADH/NAD$^+$

GST and Munc119 bound to glutathione agarose beads as an immobilized bait protein and the eluted RE (B)-MBP as a prey protein were used for this assay. The eluted RE (B) MBP were incubated with Munc119-GST or GST in equivalent -molar concentration in a total volume of 500 µl incubation buffer containing 0.25% Triton X-100. The NADH/NAD$^+$ was added as an increasing concentration in µM (0µM,5µM,10µM,15µM) in the incubation mixture of Munc119-GST and RE(B)-MBP. These samples were incubated for 4 to 6 hrs at 4^{o}C. Then, the samples were centrifuged and the pellets were washed 3 times with incubation buffer. Every washing step was followed by centrifugation at 13000 rpm for 1 min at 4^{o}C. The pellet was boiled in SDS-PAGE loading buffer at 96^{o}C for 5 mins. The eluted proteins were subjected to 10% SDS-PAGE followed by western blotting. The membrane was detected with anti-MBP and detected with anti GST antibody after stripping.

	lane	Protein	Vol.(µl)	% in total	Protein	Vol.(µl)	% in total	NADH Conc. (µM)
Input	1	GST	0.5	10				
	2	RE(B)-MBP	2	10				
	3	Munc119-GST	1	10				
Pellet	4	Munc119-GST	10	100	RE(B)-MBP	20	100	0
	5	Munc119-GST	10	100	RE(B)-MBP	20	100	5
	6	Munc119-GST	10	100	RE(B)-MBP	20	100	10
	7	Munc119-GST	10	100	RE(B)-MBP	20	100	15
	8	GST	5	100	RE(B)-MBP	20	100	0

Protein	nature	Concentration (mg/ml)	Protein used in each experiment (µg)
GST	Immobilized	1.5	7.5
Munc119-GST	Immobilized	1.5	15
RE(B)-MBP	Eluted	1.2	22.5

2.16. Co-immunoprecipitatation

2.16.1. R 28 cells co-immunoprecipitation

The R28 cells were grown up to 75% confluent in R28 cells medium.6 flasks of R28 cells were scrapped off from the flask. The samples were centrifuged at 3500 rpm for 20 mins at 4^{o}C. The supernatant medium was removed. The cell pellet was transferred to 1.5 ml microfuge tube by adding 1ml of cold PBS. Then the sample was centrifuged and the supernatant removed. The cell pellet was washed with 1ml of cold PBS. The supernatant

removed after centrifugation at 6000rpm for 10 mins at 4°C. The cell pellet was added with 1 ml of lysis buffer (100mM Tris-HCl pH7.9, 150mMNaCl, 1mM EDTA, 1% TritonX-100) and lysed by inverting the tube up and down for 20 times. The sample was incubated in the ice for 45 mins.

Then the sample was centrifuged at 13000 rpm for 15 min at 4°C.The supernatant was removed and transferred to another fresh tube. This centrifugation step was repeated once again. The final supernatant was incubated with 10 µl of preimmune serum (PIS) for 1 hr at 4°C in rotation. Then 20 µl of protein A sepharose beads was washed with 1 ml of PBS . The lysate with preimmune serum was added to the beads and the incubation was continued for 1hr at 4°C in rotation. Then the samples were centrifuged at 13000 rpm for 1 min. The supernatant (pre-cleared lysate) was removed and used for the immunoprecipitation experiment. Roughly 1ml of pre cleared lysate was divided in to 500µl each in two 1.5ml microfuge tube.10µl of Immune Serum (U2656) was added to one sample and 10µl of preimmune serum (PIS) was added to another sample.

And these samples were incubated at 4C for over night in rotation. After over night incubation, the samples were incubated with 20µl of protein A sepharose beads (pre washed with PBS) and the incubation was continued for another 2 hours. Then the samples were centrifuged at 13000 rpm for 1 min. The pellets were washed with 1 ml of cold PBS for 3 times. The final pellets were resuspended in 30µl of SDS loading buffer and boiled for 3mins at 96°C subjected to 10% SDS PAGE followed by western blotting with anti-Munc119 antibody.

2.16.2. Bovine retina co-immunoprecipitation

All steps were performed at 4°C if not denoted otherwise. For each immunoprecipitation, a bovine retina was incubated with 2ml of lysis buffer (100 mM Tris HCl, pH 7.9, 150 mM NaCl, 1mM EDTA) containing 1% TritonX-100 for 30 min at 4°C. Then the sample was centrifuged at 13000 rpm for 15 mins at 4◦C. Then, the samples were transferred to 2ml syringes and forcefully ejected through 23 gauge needles to mechanically disrupt the retinal tissue. Mechanical crushing through 23 gauge needles was repeated 40-50 times. The mechanical disruption is essential to fractionate synaptic ribbons and to make them accessible for immunoprecipitation. Without mechanical treatment no RIBEYE immuno reactivity was observed in the respective tissue lysate. After mechanical disruption, lysis was allowed to proceed for further 30min on ice. Afterwards, samples were centrifuged twice at 13,000 rpm for 30 min. The supernatant was incubated with 10 µl of Munc119 pre-immune

serum for 1 hour at 4°C and 20 µl of washed protein A-sepharose beads. Afterwards, the sample was centrifuged at 13,000 rpm for 15 min and the pre-cleared lysate was divided into two aliquot and incubated either with 10µl of Munc119 immune serum (Munc119 V2T2.120) or with Munc119 pre-immune serum (IgG control) together with 20µl of washed protein A sepharose beads (overnight). After overnight incubation, samples were centrifuged at 3000rpm (2min) to pellet the protein A-sepharose beads. The pellet was washed three times with 1 ml of lysis buffer. The final pellet was boiled with SDS loading buffer and subjected to SDS-PAGE followed by western blotting.

2.17. Immunocytochemistry

The transfected COS-7 cells, were briefly washed with PBS and fixed with 1% formaldehyde in PBS for 30 mins at room temperature. Cells were treated with blocking buffer for 45 mins at room temperature. The primary antibodies were diluted in blocking buffer (1:500 dilutions) and added to the cells for overnight incubation at 4 C. Thereafter the cells were washed with PBS (3 times, each for 5 mins) and incubated with secondary antibody (Cy2/Cy3 conjugated goat-anti-rabbit antibody for polyclonal rabbit primary antibody; Cy2/Cy3 conjugated goat-anti-mouse antibody for monoclonal mouse primary antibody) diluted in blocking buffer (1:1000 dilution) for 1 hr at room temperature. The cells were washed with blocking buffer (4 times, each for 5 mins) and followed by PBS (3 times, each for 5 mins). The cells were mounted in 60% glycerol contained n-propylgallate in order to retard photo bleaching.

2.18. Purification of synaptic ribbons (Schmitz *et al*, 1996)

2.18.1. Purification of photoreceptor synaptic complexes (OPL-fraction)

As a first step in the purification of photoreceptor synapses, a crude synaptic membrane fraction was prepared as described previously (Schmitz *et al*., 1993). Briefly, retinae freshly isolated from bovine eyes (obtained from a local slaughterhouse within 30 min post-mortem) and detached from pigment epithelium were disrupted by shear forces exerted by an Ultraturrax for 3 min on ice (Type TP 18/10; Janke and Kunkel, Staufen, Germany) in hypotonic homogenization buffer containing 15mM Na_2HPO_4, pH 7.4, 1mM EGTA, 1mM $MgCl_2$, and 1mM phenylmethylsulfonyl fluoride for 3 min at 4°C. Thirty-five ml of homogenization buffer were used for eight isolated retinae. For preparation of crude synaptic membranes, 20 ml of homogenate was over layered on 10 ml of a sucrose cushion containing 50% sucrose (w/v) in homogenization buffer and centrifuged for 50 min at 15,000 rpm

(~27,200 × g_{max}) at 4°C in a JA20 rotor (Beckman, Palo Alto, CA). At the interface between the sucrose cushion and the supernatant, a broad opaque band of membranes was visible and used for the subsequent purification of photoreceptor synapses. This band was removed carefully with a Pasteur pipette and diluted with approximately twofold its volume with homogenization buffer. This diluted suspension was spun in a JA20 rotor at 20,000 rpm (~48,400 × g_{max}) for 10 min (4°C). The supernatant was discarded, and the pellet was resuspended with approximately the same volume of homogenization buffer. For convenience, this resulting membrane suspension containing crude synaptic membranes (CSMs) was denoted CSM-fraction. The CSM-fraction was over layered on a linear sucrose gradient ranging from 35 to 50% sucrose (w/v) in homogenization buffer. Membranes were spun at 13,000 rpm (~30,000 × g_{max}) for 1.5 hr at 4°C in an SW40 rotor. After this spin, two bands and a large pellet were visible. A membrane fraction that was recovered as a broad band at a sucrose density of ~40% (w/v) in homogenization buffer (sucrose density calculated by its distance between the top and bottom of the gradient) was denoted OPL-fraction and characterized as described below. Membrane fractions were analyzed by immunoblotting and immunofluorescence microscopy with the ribbon antiserum. To analyze the retinal fractions by immunofluorescence, microscopy samples were diluted with the twofold volume of homogenization buffer, sedimented in an Eppendorf centrifuge (model 5415C, Eppendorf, Hamburg, Germany) at 14,000 rpm (~15,900 × g_{max}) at 4°C for 10 min, and flash-frozen in liquid nitrogen. From these frozen samples, 10-µm-thick cryostat sections were cut and immunolabeled with the ribbon antiserum as described above.

2.18.2. Purification of synaptic ribbons from the OPL fraction.

OPL membranes were diluted with the twofold volume of homogenization buffer and spun in a JA20 rotor at 11,000 rpm (~14,600 × g_{max}) for 10 min at 4°C. The resulting sediment was resuspended in homogenization buffer containing 1% Triton X-100 (w/v) to a protein concentration of ~1 mg/ml. The pellet was homogenized three times with a tight-fitting Teflon pestle and kept on ice for ~30 min. After this incubation period, the Triton-insoluble fraction of photoreceptor synapses was sedimented in a JA20 rotor at 11,000 rpm (~14,600 × g_{max}) for 10 min at 4°C. The sediment was resuspended with approximately the same volume of homogenization buffer containing 20% sucrose. This suspension was over layered on a sucrose step gradient containing 2 ml of each of the following sucrose concentrations (in homogenization buffer): 30, 40, 50, and 70%. Then the sample was centrifuged in an SW40 rotor at 11,000 rpm (~20,000 × g_{max}) for 75 min at 4°C. The opaque

protein bands at the respective interfaces of the sucrose step gradient were tested for the presence of synaptic ribbons by immunofluorescence and electron microscopy. The retinal subfraction between the 50 and 70% sucrose step contained the highest density and purity of synaptic ribbons and was denoted SR-fraction

2.19. Ribbon fractions pull-down assay

The ribbon fraction was incubated with increasing concentration of Munc119-GST) or GST (maximum concentration equal to Munc119-GST) in final volume of 500 µl of PBS which contains 0.5 % of Triton X-100. The sample was incubated for over night at 4^{o}C. Then the sample was centrifuged at 5000 rpm for 1 min and the pellet was washed thrice with 1 ml of PBS. The final pellet was boiled with 30µl of SDS-loading buffer and subjected to SDS-PAGE followed by western blotting. The membrane was detected with anti–GST. Then the membrane was stripped and detected with CtBP2/RIBEYE.

	Lane	Protein	Vol. (µl)	(%) in total	Protein	Vol. (µl)	(%)In total
Input	1	GST	0.3	10			
	2	Munc119-GST	1.5	10			
	3	Ribbon fraction	2	10			
Pellet	4	GST	37.5	3.0µM	Ribbon fraction	20	100
	5	Munc119-GST	30	0.6µM	Ribbon fraction	20	100
	4	Munc119-GST	60	1.2µM	Ribbon fraction	20	100
	5	Munc119-GST	90	1.8µM	Ribbon fraction	20	100
	4	Munc119-GST	120	2.4µM	Ribbon fraction	20	100
	5	Munc119-GST	150	3.0µM	Ribbon fraction	20	100

The western blot signals were digitally captured using ChemiDOC XRS Gel documentation system (BIORAD). For semi quantitative analysis of binding of Munc119 to purified, isolated synaptic ribbons, the intensity of bands on the western blot was quantified by the Quantity one 1D analysis software (version 4.5). The volume tool in Quantity one 1D analysis software was used to measure the indicated protein bands. The density was measured as intensity units (INT) under identical conditions (same exposure time, area size of protein band and background area).

The background signal was subtracted from the experimental protein band signal using Local background subtraction method. For the final analysis of binding of Munc119-GST to isolated, purified synaptic ribbons, the bound Munc119-GST (determined as above) was normalised by the intensity of RIBEYE signal present in the bait ribbon fraction to correct the potential difference in the amount of synaptic ribbons used as baits in the experiment. For this purpose, the bound Munc119-GST was expressed as the intensity ratio of Munc119-GST(as

detected by anti-GST antibody) and RIBEYE(B) and (as detected by anti-RIBEYE antibody U2656). GST served as a control protein. The ratio among the GST empty (3µM) and various concentration of Munc119-GST (0.6, 1.2, 1.8, 2.4 and 3.0µM) binding to the synaptic ribbon was statistically analysed using two tailed student's t-test.

2.20. Fluorescence Resonance Energy Transfer (FRET) assays

RIBEYE(B) is identical to CtBP2 except for the first 20 amino acids (Schmitz *et al*.,2000) and RIBEYE(B) / CtBP2 is highly homologous to CtBP1(Chinnadurai,2003 & 2005).CtBP1 has been crystallised and its structure has been determined(Kumar *et al*.,2002; Nardini *et al*.,2003). Based on the crystal structure of CtBP1 and homology modelling, tryptophan W867 of RIBEYE is located within the Förster distance of energy transfer from W867 to the nicotinamide moiety of bound NADH. Tryptophan W867 of RIBEYE corresponds to tryptophan W318 of CtBP1 which has been previously shown to be an efficient FRET donor in NADH binding analyses of CtBP1(Fjeld *et al*.,2003).

RIBEYE(B)-domain contains three tryptophan (W649; W867; W911).Tryptophan W867 was determined as FRET donor in RIBEYE(B) FRET as judged by the analysis of the respective tryptophan point mutants. The mutation of tryptophan W867 abolished FRET transfer whereas point mutants of W649 and W911 still showed a robust FRET (Schwarz *et al*., submitted; data not shown). FRET analysis of NADH bound to RIBEYE(B) was performed as previously described (Fjeld *et al*.,2003). FRET experiments were performed using LS55 spectrophotometer. The GST empty, wild type RE (B)-GST and the mutant RE (B)-GST were expressed in BL21. These proteins were purified using glutathione sepharose beads. Then these proteins were eluted and the purity was analysed by SDS-PAGE followed by coomassie staining. The concentration was measured by Bradford assay. The Trp residue was excited at 285 nm (excitation slit width of 2.5nm). The emission spectra were collected between 300 to 500 nm. FRET based emission appeared as second peak at 425nm in addition to tryptophan emission peak at 340nm 1µM of fusion protein in 500 µl of PBS (pH7.4) was used in the experiment. The titration of NADH (0µM, 200µM, 400µM, 600µM, 800µM, 1000µM, 1200µM) was performed by constant stirring and at constant temp. The increase in fluorescence at 425 nm was analyzed. At all NADH concentration used no unspecific, FRET unrelated emissions at 425nm were present as checked by lack of protein independent emission at 425nm.

Titration	Final 10 µM NADH (vol.)	Final conc. of NADH (nM)	Protein conc.
1st	0	0	1µM fusion protein
2nd	10	200	
3rd	20	400	
4th	30	600	
5th	40	800	
6th	50	1000	
7th	60	1200	

2.21. Radioactive ^{14}C-NAD binding assays

The NAD binding property of RIBEYE(B) was assessed by radioactive ^{14}C-NAD$^+$ binding experiment. The radioactive NAD$^+$ binding assay were performed largely as previously described (Schmitz *et al*., 2000). The binding experiments were performed with purified GST fusion proteins (RIBEYE(B)-GST and RE(B)E844Q-GST). Immobilized GST alone served as negative control. For the binding assay the respective fusion protein were used at equimolar concentrations (0.7µM). ^{14}C-NAD$^+$ as added to the fusion protein at a chemical concentration of 0.9µM. The amounts of proteins were used according to the following table:

Protein	Amount of protein used in each experiment
GST	9µg
RE(B)-GST WT	27µg
RE(B)-GST E844Q	27µg

The required amounts of fusion proteins were centrifuged at 13000 rpm for 2 mins at 4^{o}C to pellet the beads. The supernatant was removed. 0.5µl of radioactive ^{14}C-NAD$^+$ was added to the each fusion protein beads .The samples were incubated at 4^{o}C by constant shaking for over night. After incubation the samples were centrifuged at 13000 rpm for 2 mins at 4 C. the supernatant removed. The beads were washed with ice cold PBS for 5 times at 13000 rpm for 2 mins at 4^{o}C. The final beads were mixed with 7.5 ml of ROTISZINT scintillation solution and transferred to scintillation vials. The samples were kept at scintillation counter and bound radioactivity was determined. Each binding assay was repeated five times.

CHAPTER 3

RESULTS

3.1. Identification of Munc119 as a RIBEYE interacting protein

In order to identify novel RIBEYE interacting proteins, RIBEYE(B)-domain (aa 564-988) was used as bait in YTH screen of bovine retina cDNA library. We identified three independent clones which encode Munc119, as potential RIBEYE interacting protein. From these Munc119 prey clones one encoded for full length cDNA and 2 clones encoded for PrBP/δ homology domain of Munc119 starts at aa93 and 94 respectively. All Munc119 clones were shown not to be auto-activating as demonstrated by the respective control matings (Fig.8). The two truncated Munc119 prey clones suggested that the PrBP/δ homology domain of Munc119 is responsible for interaction with RIBEYE (Fig.8). Next, we tested this hypothesis by further YTH analysis. I cloned the PRD and PrBP/δ homology domain of Munc119 in pACT2 and tested these constructs in the YTH system using RIBEYE(B) as bait.

Indeed, the PrBP/δ homology, but not the PRD interacted with RIBEYE(B) in these analyses as shown by the growth of the respective yeasts on –ALWH plates and by expression of β-galactosidase marker gene activity. All clones were not auto-activating as shown by the respective control matings. As outlined in the introduction, RIBEYE(B) consists of NADH-binding subdomain (NBD) and a substrate-binding subdomain (SBD). I tested whether the NBD or the SBD is involving the interaction with Munc119. In the YTH system, I could show that the NBD is responsible for interaction with Munc119 as shown by the growth of respective yeasts on –ALWH plate and expression of β-galactosidase marker gene activity (Fig.8). None of the employed clones were auto activating as shown by the respective control matings (Fig.8) indicating the specificity of the Munc119-RIBEYE interaction in the YTH system.

Since RIBEYE expresses endogenously as a full length (A+B domain) *in vivo*, we also tested the full length RIBEYE (A-domain and B-domain) interaction with Munc119 full length. It shows interaction as similar to RIBEYE(B)-domain as well as NADH- binding sub domain (NBD) indicating that the A-domain of RIBEYE is not inhibiting the interaction of RIBEYE(B)-domain with Munc119 (Fig.9A & 9B). This verifies the functional interaction between RIBEYE and Munc119 full length protein and also NADH-binding sub domain of RIBEYE and PrBP/δ homology domain of Munc119 mediates the interaction. In YTH assay, the confirmation of bait and prey plasmids in the yeast was confirmed by growth on –LW plates. The interactions were judged by the growth on -ALWH selection plates, selective for protein interaction (Fig.8A & 9A) as well as by qualitative (Fig.8A & 9A) and quantitative assessment of β-galactosidase marker gene expression (Fig. 8B & 9B).

A

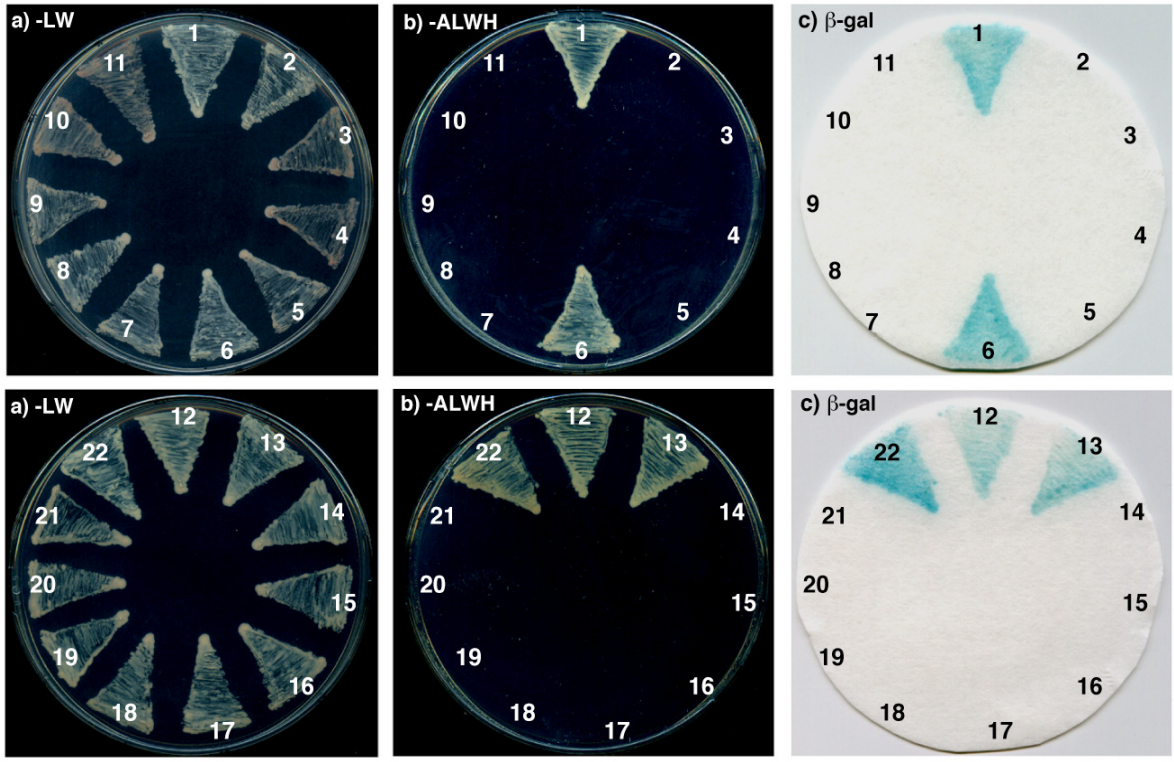

B

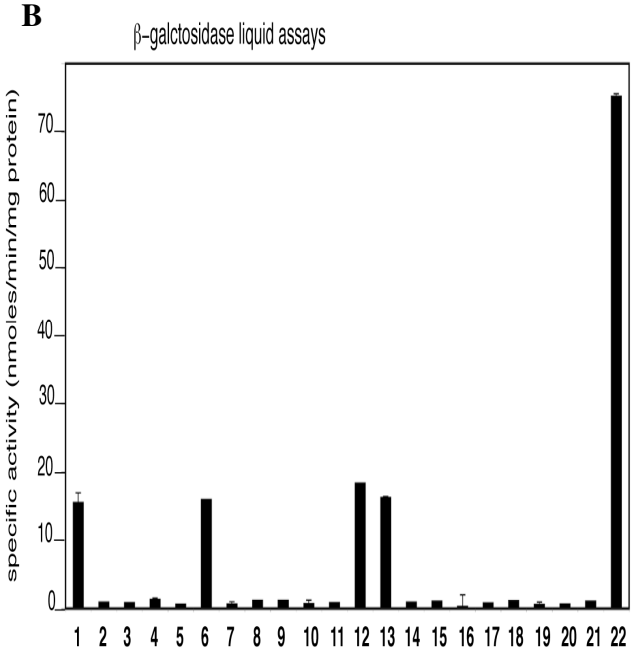

mating	bait	prey	-ALWH	βGal
1	RE(B)	Munc119(1-240)	+	+
2	RE(B)	pACT2	–	–
3	RE(B)	pSE1111	–	–
4	pGBKT7	Munc119(1-240)	–	–
5	pSE1112	Munc119(1-240)	–	–
6	RE(B)	Munc119(78-240)	+	+
7	pGBKT7	Munc119(78-240)	–	–
8	pSE1112	Munc119(78-240)	–	–
9	RE(B)	Munc119(1-77)	–	–
10	pGBKT7	Munc119(1-77)	–	–
11	pSE1112	Munc119(1-77)	–	–
12	RE(B)NBD	Munc119(1-240)	+	+
13	RE(B)NBD	Munc119(78-240)	+	+
14	RE(B)NBD	Munc119(1-77)	–	–
15	RE(B)NBD	pACT2	–	–
16	RE(B)NBD	pSE1111	–	–
17	RE(B)SBD	Munc119(1-240)	–	–
18	RE(B)SBD	Munc119(78-240)	–	–
19	RE(B)SBD	Munc119(1-77)	–	–
20	RE(B)SBD	pACT2	–	–
21	RE(B)SBD	pSE1111	–	–
22	RE(B)	CtIP	+	+

Figure. 8. RIBEYE(B) interacts with PrBP/δ homology domain of Munc119 in YTH

A. Summary plates of YTH analyses obtained with the indicated bait and prey plasmids. For convenience, experimental bait-prey pairs are under layered in colour (green in case of interacting bait-prey pairs; yellow in case of non-interacting bait-prey-pairs; control matings are non-coloured). RIBEYE(B) interacts with full length Munc119. The interaction is mediated via the NBD of RIBEYE and the PrBP/δ homology domain of Munc119, Munc119 (78-240) (Fig. A; matings #1,6 & 12,13). Mating #22 denotes an unrelated positive control mating (pCtIP). B. Quantification of β-galactosidase activities in liquid assays of the indicated mated yeast.

A

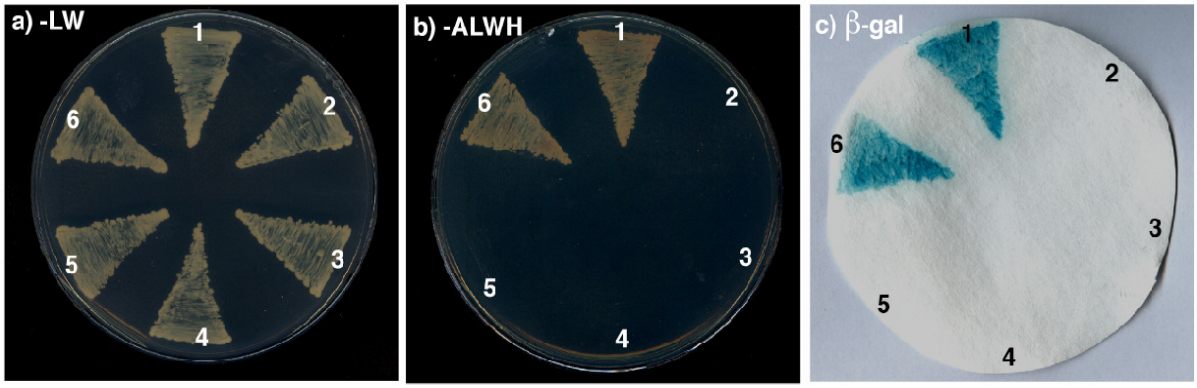

B

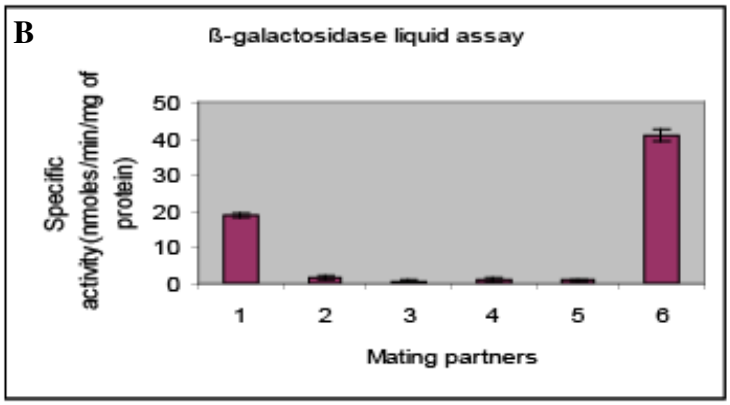

mating	bait	prey	-ALWH	βGal
1	RE(AB)	Munc119(1-240)	+	+
2	RE(AB)	pACT2	-	-
3	RE(AB)	pSE1111	-	-
4	pGBKT7	Munc119(1-240)	-	-
5	pSE1112	Munc119(1-240)	-	-
6	RE(B)	CtIP	+	+

Figure.9. RIBEYE (AB) interacts with Munc119 in the YTH

A. Summary plates of YTH analyses obtained with the indicated bait and prey plasmids. For convenience, experimental bait-prey pairs are under layered in colour (green in case of interacting bait-prey pairs; yellow in case of non-interacting bait-prey-pairs; control matings are non-coloured). Full-length RIBEYE (RIBEYE (AB) interact with full length Munc119 (Figure A; matings #1). Mating #6 denote an unrelated positive control mating (pCtIP). B. Quantification of β-galactosidase activities in liquid assays of the indicated mated yeast.

3.2. Munc119 interacts with RIBEYE in GST pull-down assays

We used various independent approaches to verify the Munc119-RIBEYE(B) interaction. To confirm the interaction at biochemical level, we have performed two different GST pull-down assays. In the first assay, we used bacterially expressed and purified fusion proteins. We used GST-tagged proteins (GST and Munc119-GST) as immobilized bait proteins and MBP-tagged proteins (MBP and RIBEYE(B)-MBP) as soluble prey proteins. In this assay, Munc119-GST effectively interacted with RIBEYE(B)-MBP but not MBP alone as judged by protein pull-down analyses (Fig.10). In the control, GST alone does not pull-down RIBEYE(B)-MBP as well as MBP demonstrating the specificity of interaction. Specificity of interaction in these fusion protein pull-downs was consistently shown by SDS-PAGE and western blot analyses. In western blotting, the membrane was first incubated with anti-MBP to show the binding of RIBEYE(B) to Munc119-GST and then the same blot was incubated with anti-GST (after stripping) to show the equal loading of bait proteins.

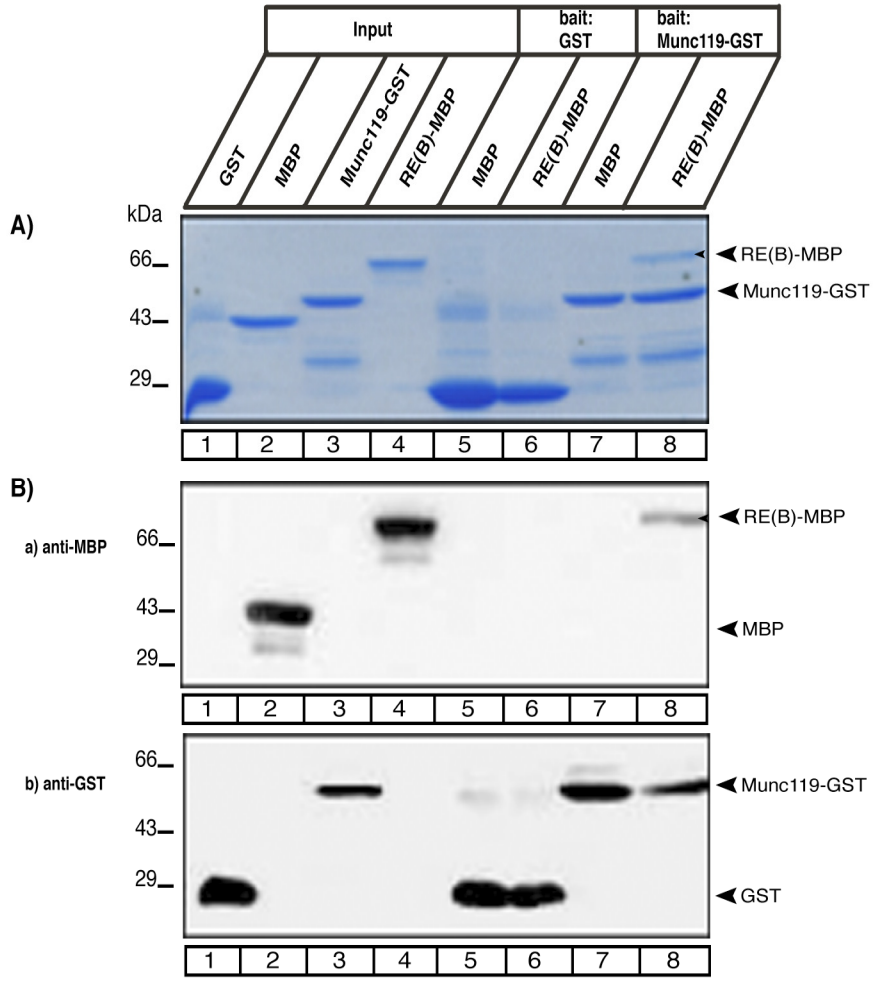

Figure.10. RIBEYE(B) interacts with Munc119 in GST pull-down assays

Pull-down analyses of RIBEYE/Munc119 complexes using bacterially expressed fusion proteins. In Fig.A Pull-down experiments were analyzed by Coomassie-stained SDS-PAGE and in Fig.B by western blot analysis with indicated antibodies. Lanes 1-4 show the indicated purified fusion proteins (input fractions). All input lanes, except lane4, represent 50% of the input fraction. Lane4 represents 25% of the input fraction. GST-tagged fusion proteins were used as immobilized bait proteins and MBP-tagged proteins as soluble prey proteins. Only Munc119-GST (lane 8), pulled down RE (B)-MBP but not GST alone (lane 6).Munc119-GST has a similar though clearly different running position than MBP alone. Already SDS-PAGE demonstrated that Munc119-GST does not pull-down MBP alone (Fig. A). Also the western blot analysis with anti-MBP antibodies (Fig.B) clearly shows that only RE(B)-MBP(lane8) but not MBP alone(lane7) is pulled down by Munc119-GST.GST alone does not pull-down RE(B)-MBP(lane6) as well as MBP alone(lane5).The specific interaction was both shown by Coomassie Blue-stained polyacrylamide gels (SDS-PAGE) (A) as well as by western blotting with the indicated antibodies (B). In Fig. Bb the same blot as analyzed in Fig. Ba (with anti-MBP) was reprobed (after stripping) with anti-GST to show equal loading of the bait proteins.

In another assay, we analysed whether RIBEYE(B) interacts with Munc119 in transfected COS-7 cells. For this purpose, COS-7 cells were co-transfected with the indicated eukaryotic expression plasmids that encoded for RIBEYE(B)-EGFP and GST-tagged Munc119 (experiment) or GST alone (control). Munc119-GST but not GST alone pulls down the RIBEYE(B)- EGFP from crude cell extracts of transfected COS-7 cells shown in western blotting with respective antibodies (Fig.11) further demonstrating the specific interaction between Munc119 and RIBEYE.

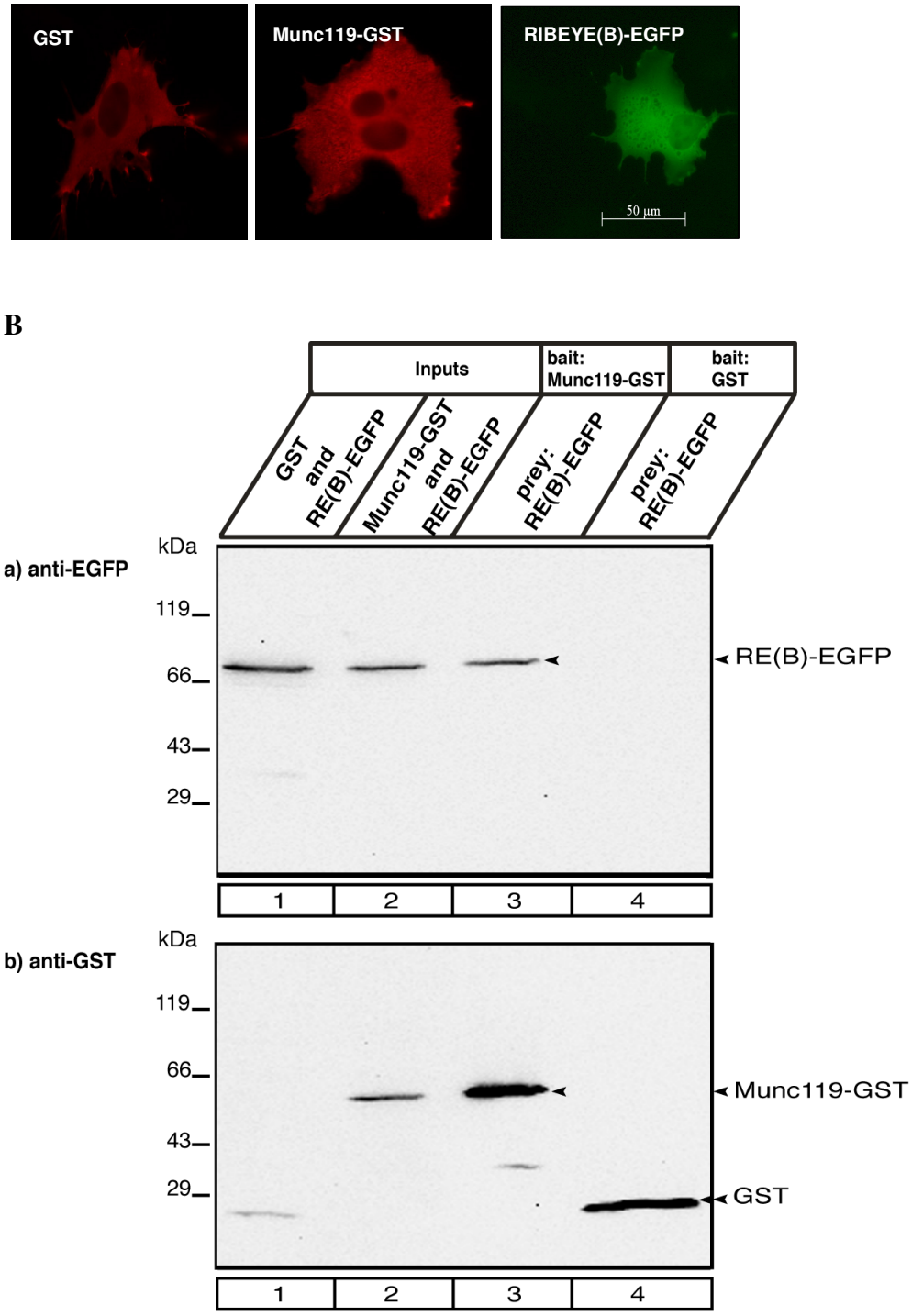

Figure.11. RIBEYE(B) interacts with Munc119 in transfected COS cells

A. Immunocytochemistry of COS cells transfected with GST, Munc119-GST and RIBEYE(B)-EGFP. This clearly demonstrates the soluble nature of Munc119 and RIBEYE(B) in COS cells. B. COS cells co-transfected either with Munc119-GSTpEBG and RIBEYE(B)-EGFP (experimental assay) or with GST-pEBG and RIBEYE(B)-EGFP (control assay). Glutathione beads were added to the respective cell lysates. Protein bound to the glutathione beads were analysed via western blotting with antibodies against GST and EGFP. Munc119-GST pulls down RIBEYE(B)-EGFP(lane3) but not GST alone (lane 4) demonstrating the specific interaction of Munc119 and RIBEYE(B). Lane 1&2 show the respective input fractions (10% of total input). In Fig. Bb the same blot as shown in Fig. Ba (with anti-EGFP) was reprobed (after stripping) with anti-GST to show equal loading of the samples.

3.3. Co-immunoprecipitation of Munc119 and RIBEYE from R28 retinal precursor cells

R28 cells endogenously express Munc119 (Fig12; Seigel, 2004) and RIBEYE in a Triton X-100 soluble fraction (Fig.12). Therefore, to analyse the interaction between RIBEYE and Munc119 at *in vivo* situation, we performed co-immunoprecipitation analysis using protein extracts from R28 cells (retinal precursor cell line). The R28 cells extracts was precipitated with anti-RIBEYE (U2656 immune serum) and IgG control (U2656 pre-immune serum) and tested for the co-immuno precipitation of Munc119 with the respective antibody. RIBEYE immune serum (lane2) but not RIBEYE pre-immune serum(lane3) specifically co-precipitated Munc119 confirming the interaction between the RIBEYE and Munc119 also in cellular context (Fig.14).

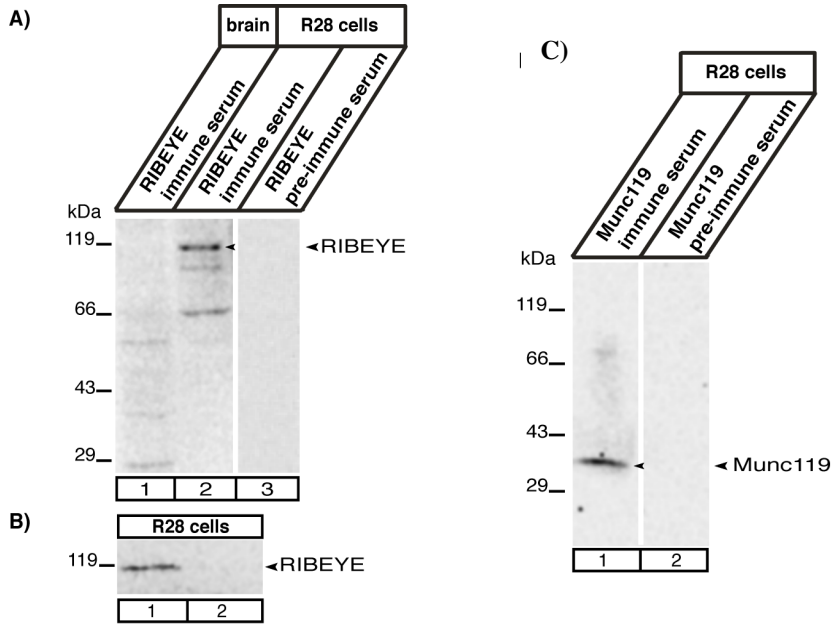

Figure.12. R28 retinal progenitor cells express RIBEYE that can be solubilized by TritonX-100.

R28 retinal progenitor cells were tested for the presence of RIBEYE(B)y western blotting with RIBEYE immune and pre-immune serum. The presence of the 120kDa RIBEYE protein in R28 cells is clearly detected by the immune- (A, lane 2) but not by the pre-immune serum (A, lane 3). Rat cortex that does not contain ribbon synapses served as a negative control (lane 1). Rat cortex did not show a RIBEYE signal. **B)** Most of the endogenous RIBEYE in R28 cells can be solubilized by Tx-100 (B, lane 1, and data not shown) and recovered in TritonX-100 – soluble extract (B, lane1) whereas little of the endogenous RIBEYE is found in a TritonX-100-insoluble fraction (B, lane 2). Thus, for co-immunoprecipitation experiments with R28 cells we used a TritonX-100 lysate of R28 cells (Fig. 4). The expression of RIBEYE in R28 cells were confirmed by RT-PCR experiments (data not shown). **C**) Characterization of the Munc119 antiserum (V2T2.120) in R28 cells. The Munc119 band at 35kDa is clearly detected in R28 cells by the Munc119 immune serum V2T2.120 (lane 1), but not by the Munc119 pre-immune serum (lane 2).

For this assay, we generated antibody against Munc119 and tested in COS-7 cells transfected with Munc119-GST, R28 cells and bovine retina for the specificity of antibody . The antibody we used for the immunoprecipitation studies specifically detects the Munc119 in R28 cells

and in bovine retina at 35 kDa as reported previously (Fig.12). We verified the specificity of this Munc119 antibody, Munc119 V2T2.120 in COS-7 cells transfected with Munc119–GST. Anti-Munc119 (Munc119 V2T2.120 immune serum) detects the Munc119–GST in Munc119-GSTpEBG transfected COS-7 cells (Fig.13)

.

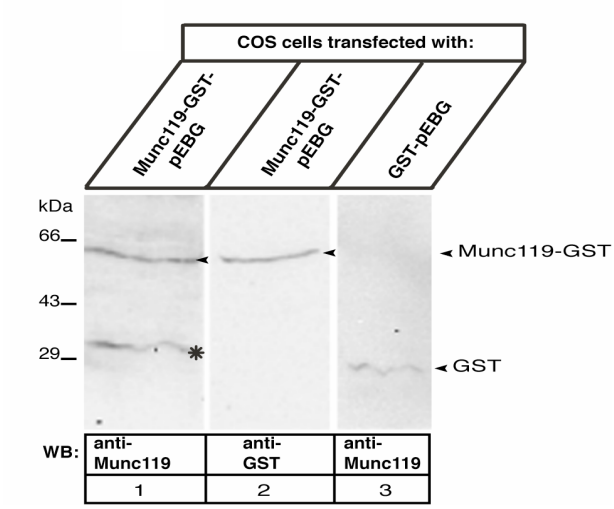

Figure.13. Characterization of the Munc119 antiserum (V2T2.120) in transfected COS cells.

Western blot analyses of COS cells tansfected with the indicated eukaryotic expression plasmids using the DEAE dextran transfection method (2). The Munc119 antiserum V2T2.120 specifically detects Munc119-GST in COS cells transfected with the Munc119-GST-expression plasmid (lane 1) but not in control-transfected COS cells (lane 3). The Munc119-GST band is detected by Munc119 antiserum as well as by a monoclonal GST antibody (lane 2). The asterisk in lane 1 denotes a breakdown product of Munc119-GST

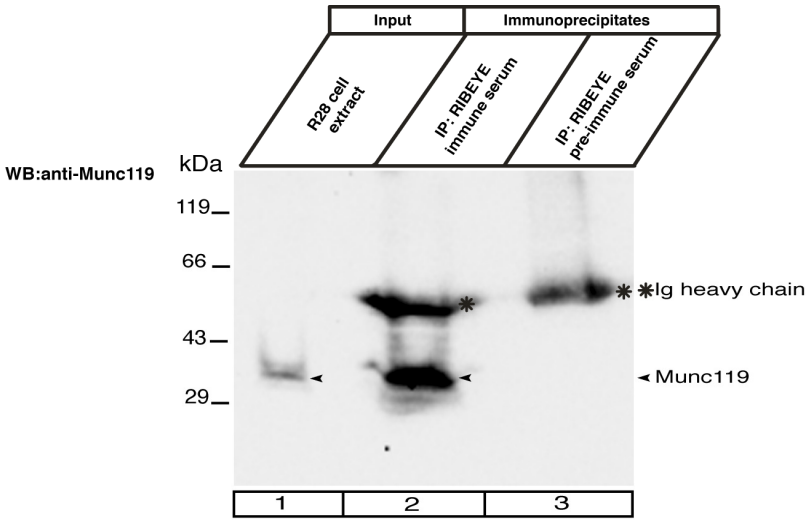

Figure.14. Co-immunoprecipitation of RIBEYE and Munc119 in R28 retinal precursor cells.

R28 retinal progenitor cells endogenously express soluble Munc119 and RIBEYE which can be readily solubilized from R28 cells by Triton X-100 lysis as describes in materials and methods. Munc119 was co-immunoprecipitated by antibodies against RIBEYE from extracts of R28 retinal progenitor cells (lane 2). The RIBEYE pre-immune serum did not co-immunoprecipitate Munc119 (lane 3) demonstrating the specificity of the co-immunoprecipitation.lane1 shown the input fraction (5% of the total input). Asterisks indicate the immunoglobulin heavy chains

3.4. Co-immunoprecipitation of Munc119 and RIBEYE from bovine retina

Next, I tested whether RIBEYE and Munc119 could co-immunoprecipitated from extracts of the bovine retina. The extract was precipitated with anti-RIBEYE (U2656 immune serum) and IgG control (U2656 pre-immune serum). The anti-RIBEYE (U2656 immune serum) efficiently precipitate the RIBEYE and also co precipitate Munc119 but IgG control (U2656 pre-immune serum) was not precipitate either RIBEYE or Munc119 as judged by western blotting with respective antibodies(Fig.15).

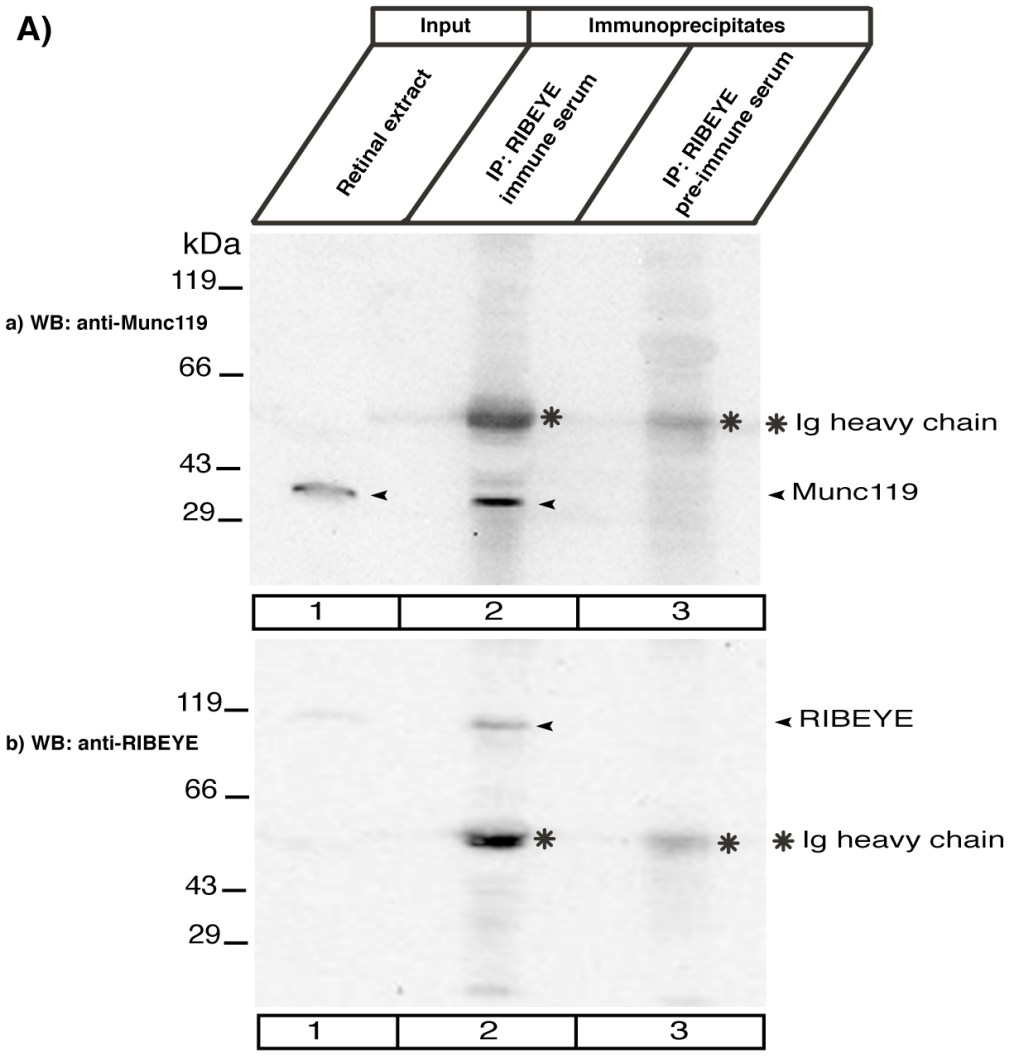

Figure.15.A. Co-immunoprecipitation of RIBEYE and Munc119 from the bovine retina

In Figure A, RIBEYE immune serum and RIBEYE pre-immune serum were tested for their capability to co-immunoprecipitate Munc119. Munc119 is co-immunoprecipiated by RIBEYE immune serum (lane 2, Fig 15Aa) but not by RIBEYE pre-immune serum (lane 3, Fig. 15Aa). Fig.15Ab) shows the same blot as in Fig. 15.Aa but reprobed with anti-RIBEYE antibodies. This blot shows the presence of RIBEYE precipitated by the immune serum (lane 2) but not by the preimmune serum (lane 3). Asterisks indicate the immunoglobulin heavy chains.

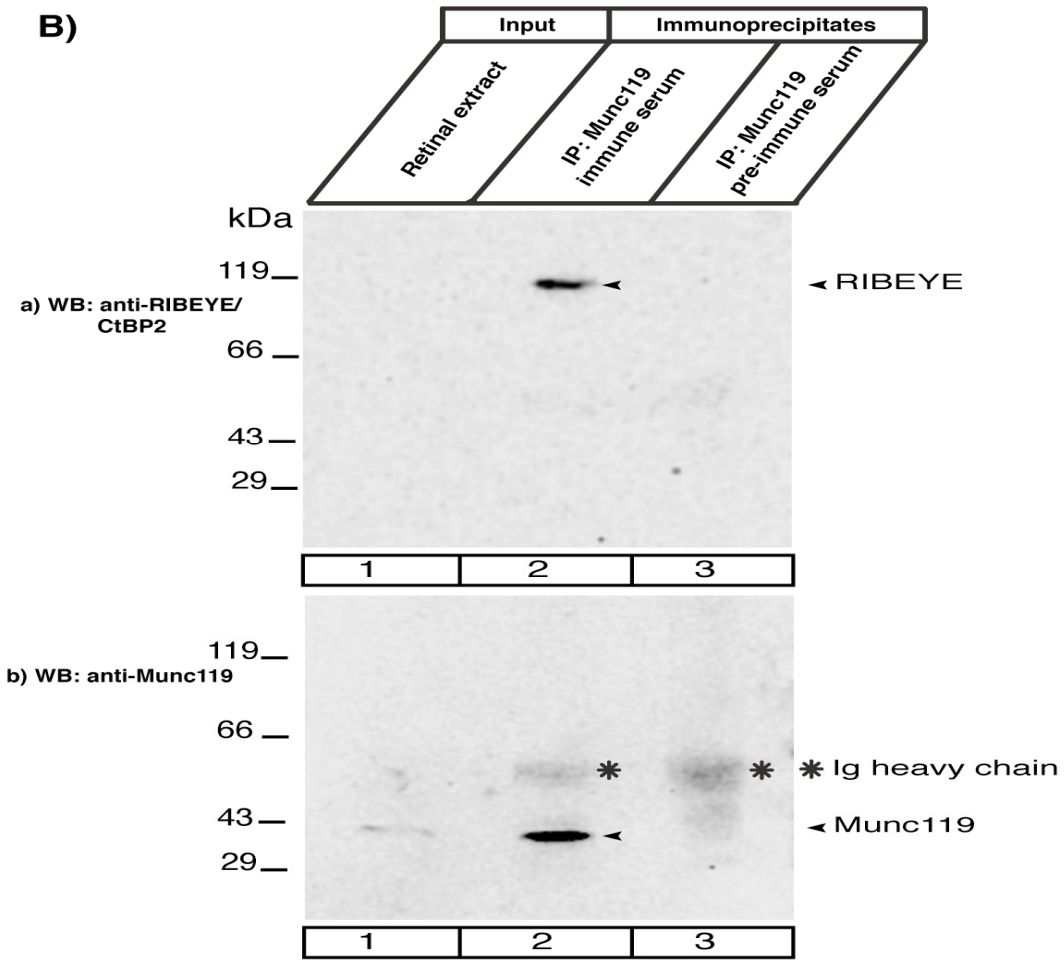

Figure 15.B.Co-immunoprecipitation of RIBEYE and Munc119 from the bovine retina

In Figure B, Munc119 immune serum and Munc119 pre-immune serum were tested for their capability to co-immunoprecipitate RIBEYE. RIBEYE is co-immunoprecipitated by Munc119 immune serum (lane 2, Fig 15Ba) but not by Munc119 pre-immune serum (lane 3, Fig. 15Ba). Fig15Bb) shows the same blot as in Fig. 15Ba but reprobed with anti Munc119. This blot shows the presence of Munc119 immunoprecipitated by the immune serum but not by the preimmune serum. Lane1 shows the input fraction (2% of the total input).Asterisks indicate the immunoglobulin heavy chains. The loaded input fraction corresponds roughly to 200µg of total proteins (in a volume of approx.20µl). Considerably more input fraction could not be loaded on the gel for volume reason and also not to overload the gel. Further more synaptic ribbons are mechanically stable, Triton X-100 insoluble structures which can only be extracted to a certain extent from the bovine retina by the combination of mechanical and chemical lysis. Therefore the RIBEYE signal is weak in the input fractions. RIBBEYE is highly enriched in the experimental immunoprecipitate (lane2) but absent in control immunoprecipitate (lane3).

3.5. Munc119 and RIBEYE interaction is independent of dimerization of RIBEYE and NADH/NAD$^+$ binding

Previous YTH analyses demonstrated that the NADH-binding sub domain (NBD) of RIBEYE(B) is mediating the interaction with Munc119. The binding of NADH causes conformational changes in CtBP to trigger its dimerization consequently an increase in its binding to proteins such as E1A and ZEB (Zhang *et al*., 2002). Due to this nature, the binding of CtBP with its partner protein is regulated by NADH/NAD$^+$ levels in turn by dimerization

(Zhang *et al*., 2002). Since the RIBEYE(B)-domain is highly homologous to CtBP2 as well as CtBP1, we have taken this model (Fig.16) as an example and tested the interaction between Munc119 and RIBEYE in presence of NADH/NAD^+ as well as in absence of dimerization loop. The dimerization loop is essential for RIBEYE(B) dimerization like other CtBP family proteins (Schwarz *et al*., submitted).

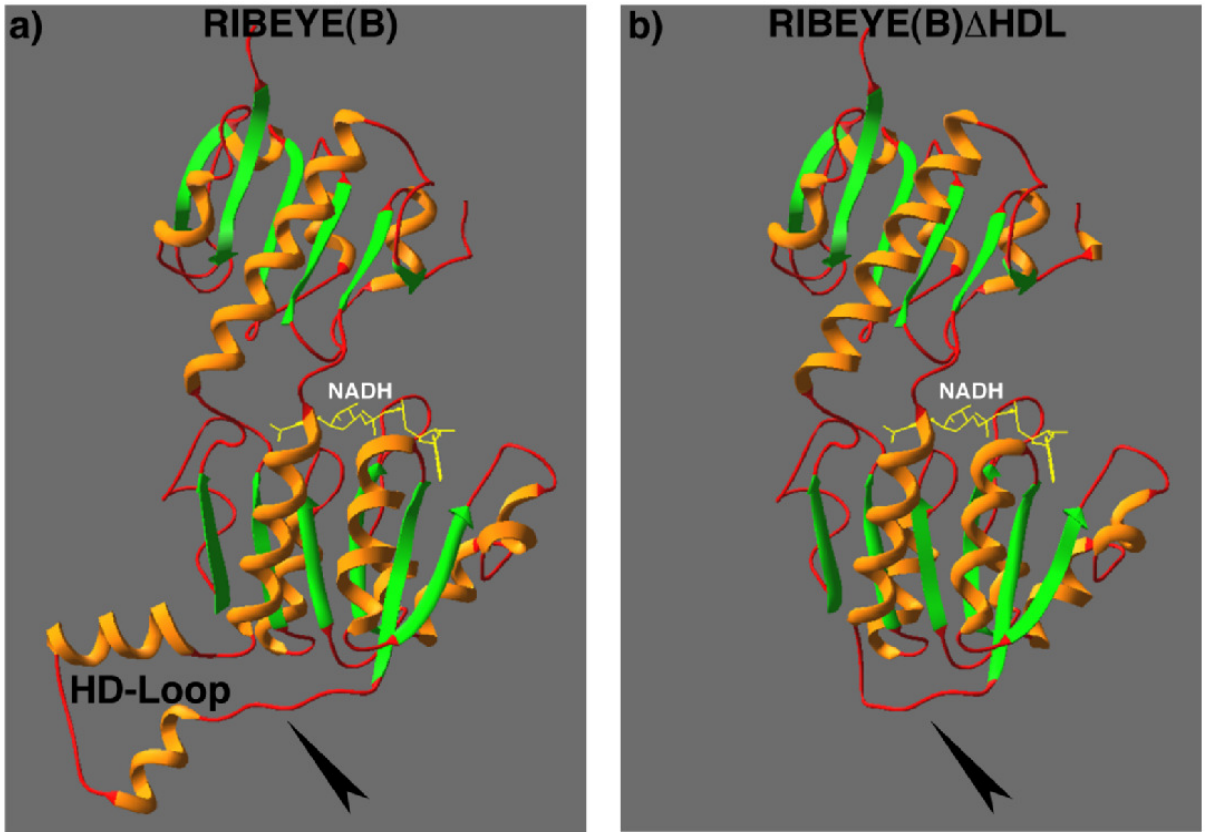

Figure.16.The predicted model of RIBEYE dimerization loop and RE (B) ΔHDL

Fig.A. The HD loop which is essential for dimerization present NADH binding domain of RIBEYE as well as other CtBP family proteins. Fig.B, shows the predicted structure of RIBEYE(B)ΔHDL , RIBEYE with out HD loop (Schmitz, unpublished)

We examined the effect of dimerization on RIBEYE interaction with Munc119 by YTH assays and the effect of NADH/NAD^+ levels by YTH assays and GST pull-down assays. In YTH assay, Munc119 interacts with RIBEYE(B)-domain full-length as well as RIBEYE(B)ΔHDL (delta homo-dimerization loop). From our lab, we have also shown that in the absence of dimerization loop, RIBEYE(B)-RIBEYE(B) interaction was abolished as observed in the control experiment (Schwarz *et al*., submitted). The interactions in the YTH were judged by the growth on -ALWH selection plates selective for protein interaction as well as by qualitative assessment of β-galactosidase marker gene expression (Fig.17). We generated point mutants of NADH-binding domain of RIBEYE. In order to further map the

interaction site of Munc119 on RIBEYE(B), we analyzed these point mutants for their ability to interact with Munc119 in the YTH system. RIBEYE(B)G730 is an essential component of the NADH-binding motif and the RIBEYE(B) point mutant RIBEYE(B)G730A does not bind significant levels of NADH (Schmitz *et al*., 2000; Magupalli *et al*.,2008; Schwarz *et al*., submitted). In contrast to the NADH-binding deficiency, RIBEYE(B)G730A still interacted with Munc119 in YTH analyses indicating that NADH binding is not important for binding of Munc119 to RIBEYE(B)-domain (Fig.19).

mating	bait	prey	-ALWH	βGal
1	RE(B)-NBD	Munc119(1-240)	+	+
2	pGBKT7	Munc119(1-240)	-	-
3	pSE1112	Munc119(1-240)	-	-
4	RE(B)ΔHDL	Munc119(1-240)	+	+
5	RE(B)-NBD	pACT2	-	-
6	RE(B)-NBD	pSE1111	-	-
7	RE(B)ΔHDL	pACT2	-	-
8	RE(B)ΔHDL	pSE1111	-	-
9	RE(B)-NBD	Munc119(78-240)	+	+
10	pGBKT7	Munc119(78-240)	-	-
11	pSE1112	Munc119(78-240)	-	-
12	RE(B)ΔHDL	Munc119(78-240)	+	+

Figure.17.The binding of Munc119 to RIBEYE(B) is independent of RIBEYE(B) dimerization

Summary plates of YTH analyses obtained with the indicated bait and prey plasmids. For convenience, experimental bait-prey pairs are under layered in colour (green in case of interacting bait-prey pairs; control matings are non-coloured. The Dimerization deficient RIBEYE RE(B)point mutant RE(B)ΔHDL (mating # 4,12) interacts with Munc119 and PrBP/δ in YTH indicating that RIBEYE dimerization is not essential for the binding of Munc119.

In addition, the effect of NAD^+ or NADH on Munc119-RIBEYE(B) interaction was tested in GST pull-down assay. Munc119-GST,GST empty (control) were used as bait proteins. RIBEYE(B)-MBP, MBP empty (control) were used as prey proteins. The pull-down assay was setup to test the interaction at increasing concentration of NADH/NAD^+ up to 15µM. Increasing concentrations of NADH or NAD^+ did not significantly influence the binding of Munc119 to RIBEYE(B) (Fig.18).

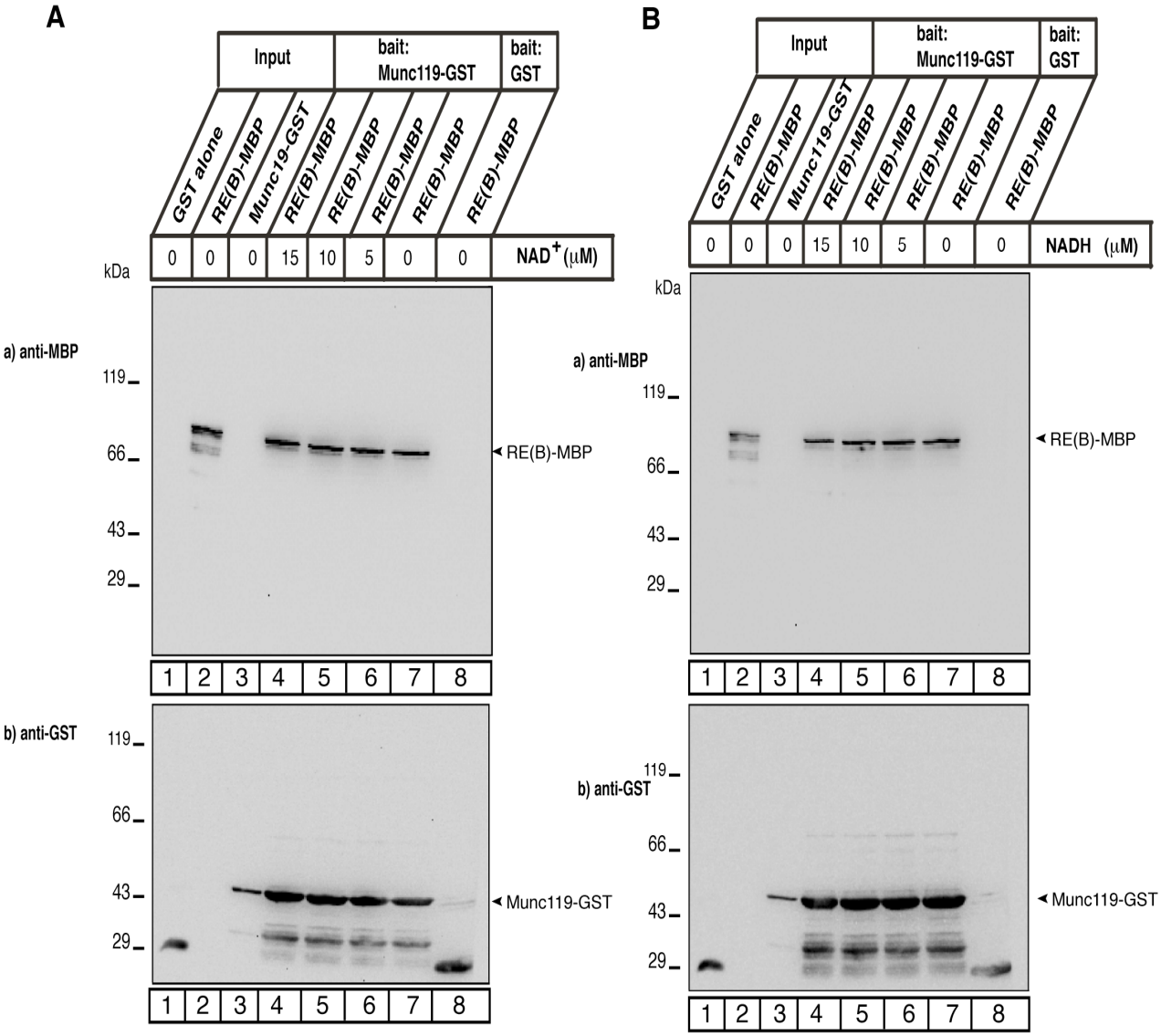

Fig.18.The binding of Munc119 to RIBEYE(B) is independent of NADH binding

The binding of RIBEYE(B)-MBP (0.5µM) to Munc119-GST (0.5 µM) was analyzed in the presence of increasing concentrations of NAD^+ (A) or NADH (B). Neither addition of NAD^+ nor addition of NADH affected the binding of RIBEYE(B) to Munc119-GST. The blots in Figure Ab) and Bb) represent the same blots as shown in Aa) and Ba) respective but reprobed with antibodies against GST to show equal loading of the bait proteins.

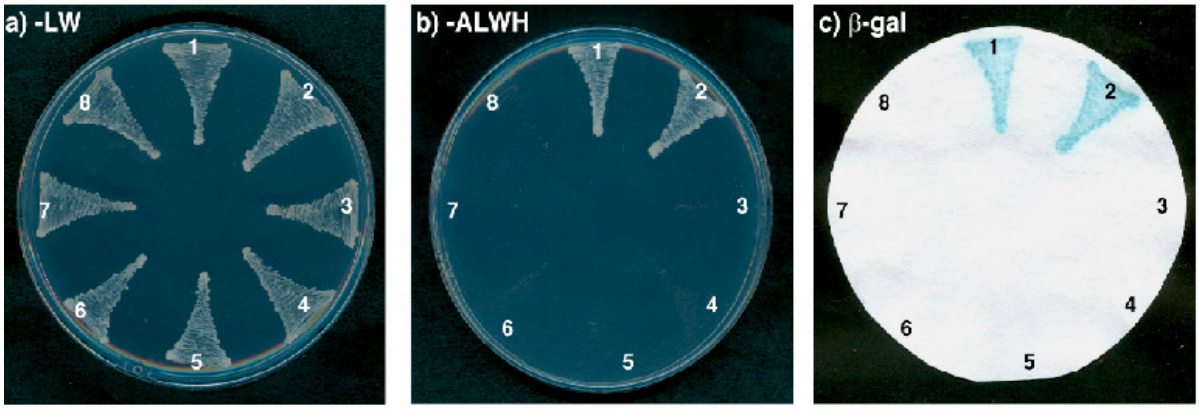

mating	bait	prey	-ALWH	βGal
1	RE(B)	Munc119(1-240)	+	+
2	RE(B)G730A	Munc119(1-240)	+	+
3	pGBKT7	Munc119(1-240)	-	-
4	pSE1112	Munc119(1-240)	-	-
5	RE(B)	pACT2	-	-
6	RE(B)	pSE1111	-	-
7	RE(B)G730A	pACT2	-	-
8	RE(B)G730A	pSE1111	-	-

Figure.19. RIBEYE(B)-Munc119 interaction is independent of NADH binding of RIBEYE(B)

Summary plates of YTH analyses obtained with the indicated bait and prey plasmids. For convenience, experimental bait-prey pairs are under layered in colour (green in case of interacting bait-prey pairs; control matings are non-colored. The NADH-binding deficient RIBEYE point mutant RE(B)G730A (mating #2) interacts with Munc119 in YTH indicating that NADH binding to RIBEYE is not essential for the binding of Munc119.

3.6. Identification of critical amino acid residues for RIBEYE–Munc119 interaction

We generated further point mutants located on the NADH-binding domain of RIBEYE, namely RE(B)D758N, RE(B)E844Q, RE(B)F848W, RE(B)K854Q RE(B)I796A, RE(B)E842Q, RE(B)D820N RE(B)E790Q, (Fig.20) to further map the docking site of Munc119 on the NBD of RIBEYE(B). All of these latter point mutants still interact with Munc119 except for RE(B)E844Q pointing that this amino acid is crucial for the interaction with Munc119 (Fig.20). Glutamate E844 is located close to the NADH-binding cleft of RIBEYE (Schmitz *et al.*, 2000; Nardini, 2003; Kumar *et al.*, 2002). As judged by NADH-dependent FRET experiments (Fjeld *et al.*, 2003) and ^{14}C NAD^+ binding experiment (Schmitz *et al.*, 2000) this mutant still binds NADH (Fig.23 & 24). Based on these data, we assume that the Munc119 binding pocket of RIBEYE is topographically closely related to the NADH binding cleft of RIBEYE(B). But binding of Munc119 is not dependent on NADH binding

and vice versa. Additionally, all the point mutants able to homo-dimerize with wild type RIBEYE(B) (Magupalli *et al*., 2008).

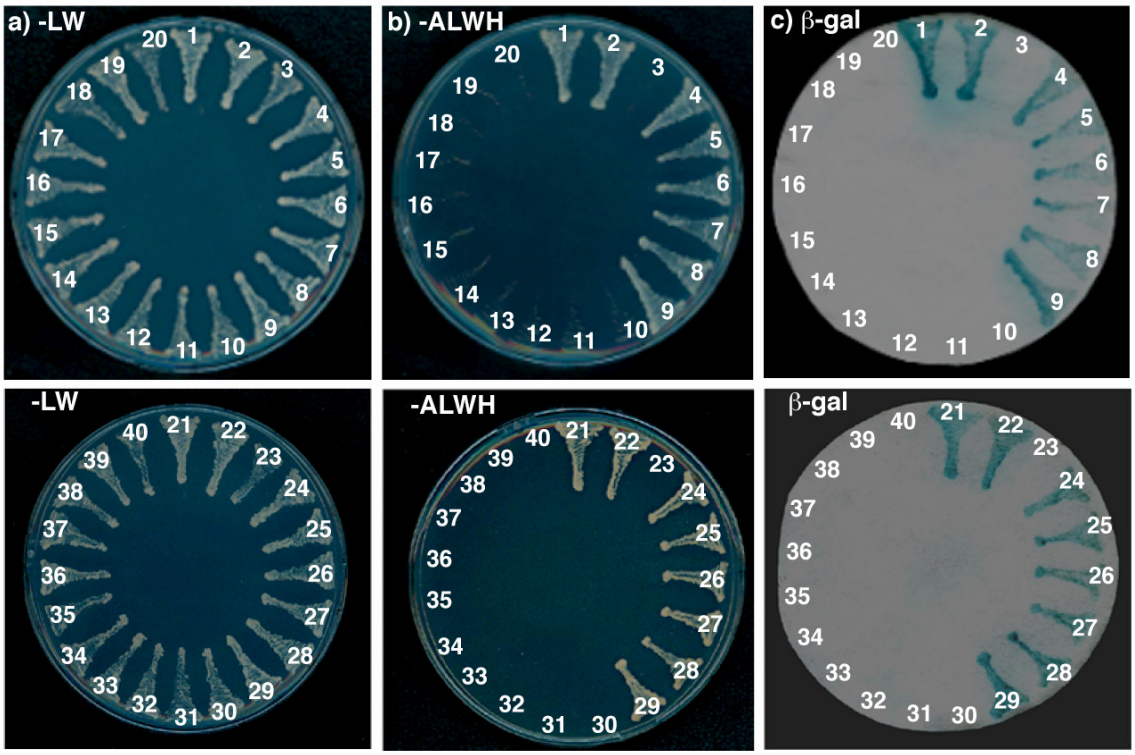

mating	bait	prey	-ALWH	βGal
1	RE(B)	Munc119(1-240)	+	+
2	RE(B)D758N	Munc119(1-240)	+	+
3	RE(B)E844Q	Munc119(1-240)	-	-
4	RE(B)F848W	Munc119(1-240)	+	+
5	RE(B)K854Q	Munc119(1-240)	+	+
6	RE(B)I796A	Munc119(1-240)	+	+
7	RE(B)E842Q	Munc119(1-240)	+	+
8	RE(B)D820N	Munc119(1-240)	+	+
9	RE(B)E790Q	Munc119(1-240)	+	+
10	pGBKT7	Munc119(1-240)	-	-
11	pSE1112	Munc119(1-240)	-	-
12	RE(B)	pACT2	-	-
13	RE(B)D758N	pACT2	-	-
14	RE(B)E844Q	pACT2	-	-
15	RE(B)F848W	pACT2	-	-
16	RE(B)K854Q	pACT2	-	-
17	RE(B)I796A	pACT2	-	-
18	RE(B)E842Q	pACT2	-	-
19	RE(B)D820N	pACT2	-	-
20	RE(B)E790Q	pACT2	-	-

mating	bait	prey	-ALWH	βGal
21	RE(B)	Munc119(78-240)	+	+
22	RE(B)D758N	Munc119(78-240)	+	+
23	RE(B)E844Q	Munc119(78-240)	-	-
24	RE(B)F848W	Munc119(78-240)	+	+
25	RE(B)K854Q	Munc119(78-240)	+	+
26	RE(B)I796A	Munc119(78-240)	+	+
27	RE(B)E842Q	Munc119(78-240)	+	+
28	RE(B)D820N	Munc119(78-240)	+	+
29	RE(B)E790Q	Munc119(78-240)	+	+
30	pGBKT7	Munc119(78-240)	-	-
31	pSE1112	Munc119(78-240)	-	-
32	RE(B)	pSE1111	-	-
33	RE(B)D758N	pSE1111	-	-
34	RE(B)E844Q	pSE1111	-	-
35	RE(B)F848W	pSE1111	-	-
36	RE(B)K854Q	pSE1111	-	-
37	RE(B)I796A	pSE1111	-	-
38	RE(B)E842Q	pSE1111	-	-
39	RE(B)D820N	pSE1111	-	-
40	RE(B)E790Q	pSE1111	-	-

Figure.20. Mapping of RIBEYE/Munc119 interactions using point mutants of RIBEYE(B)-domain.

Summary plates of YTH analyses obtained with the indicated bait and prey plasmids. For convenience, experimental bait-prey pairs are under layered in colour (green in case of interacting bait-prey pairs; yellow in case of non-interacting bait-prey pairs); control matings are non-colored. The analyzed Munc119 constructs interact with all point mutants of RIBEYE(B) domain (matings #2, 4-9, 22, 24-29) except for RIBEYE(B)E844Q (matings #3, 23). The respective control matings (auto activation controls; yeast matings #10-20, 30-40) did not show growth on -ALWH plate and expression of β-galactosidase activity. Growth on –LW plates (Fig.20.Aa) demonstrates the presence of the bait and prey plasmids in the mated yeast.

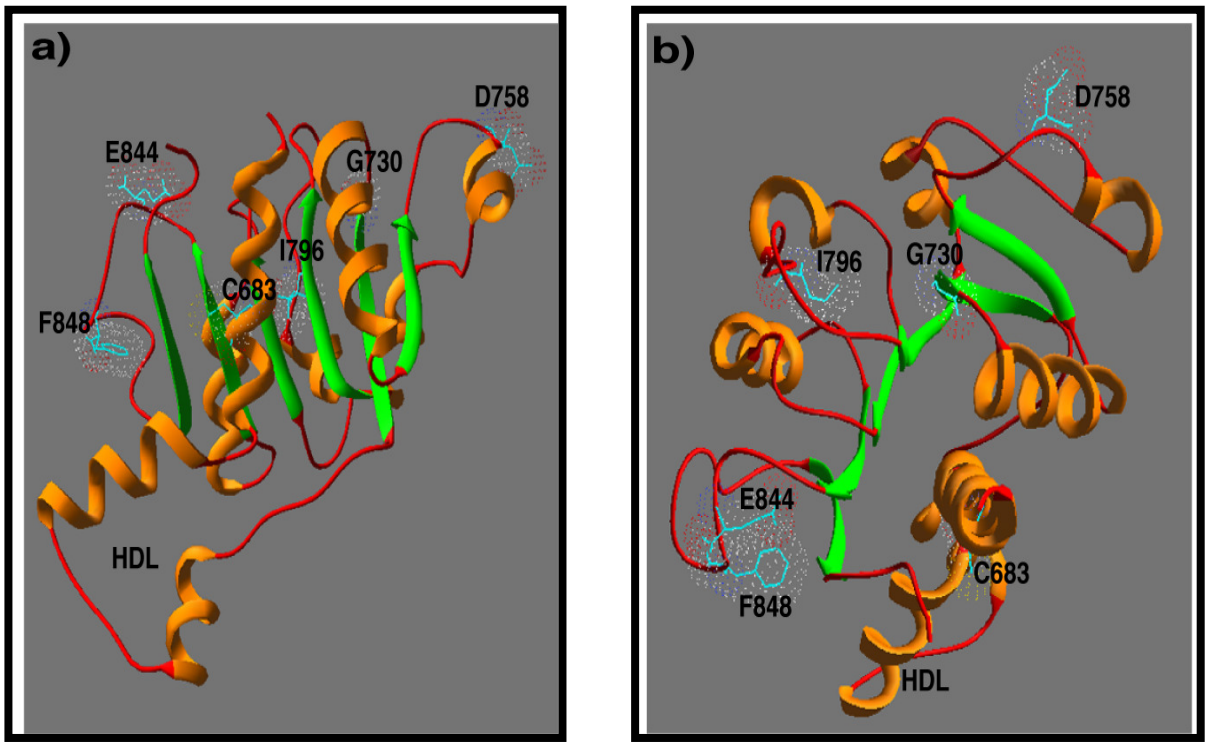

Figure.21. Location of point mutants in NADH-binding subdomain of RIBEYE(B)

This is the model of NADH binding subdomain made by homology modelling with CtBP1. This model shows the position of RIBEYE(B) NADH binding domain point mutants in front view(a) and in top view (b) add more. The mutants made in such a way that should not affect the secondary structure of protein and also the mutant protein is properly folded.

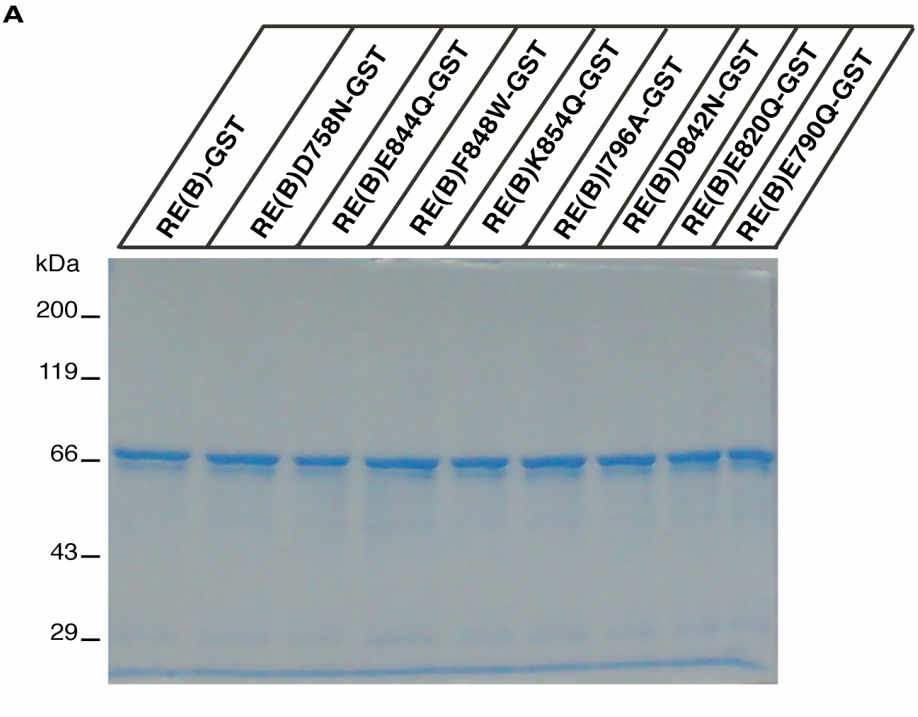

Figure.22. SDS-PAGE of RIBEYE(B) wild type and point mutants

Coomassie Blue-stained SDS-PAGE of the indicated RIBEYE(B) wild type protein and RIBEYE(B) point mutants. All mutant protein expressed nicely as like wild type RIBEYE(B)

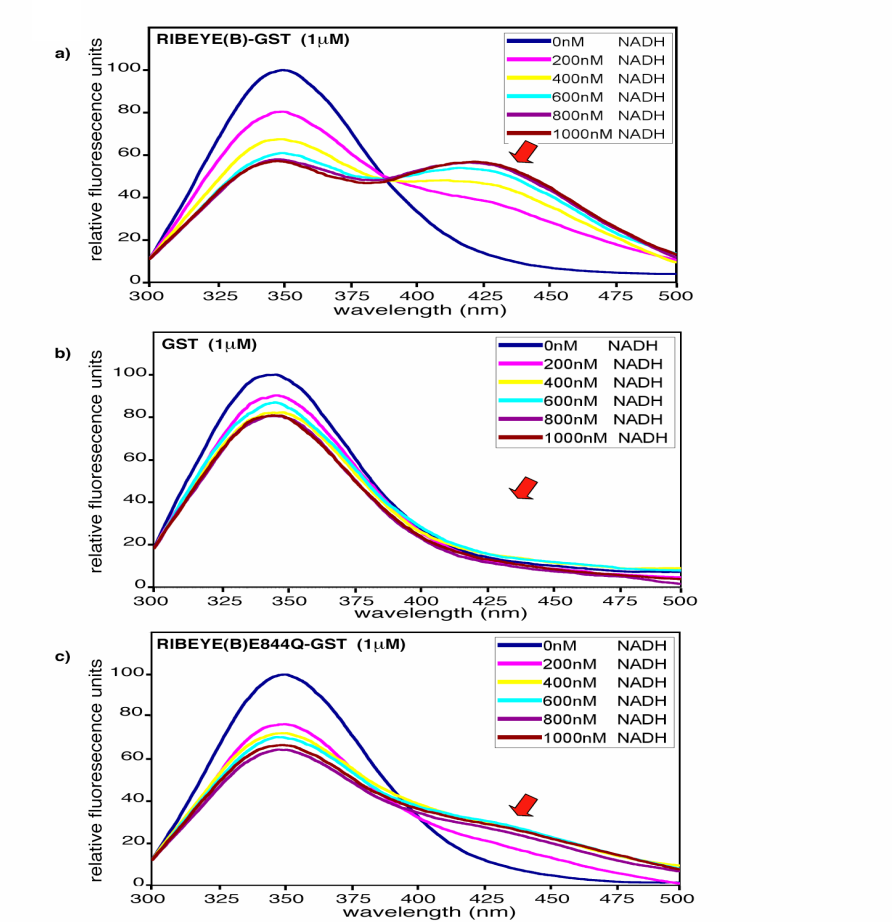

Figure.23. NADH binding of wild type and mutant RIBEYE(B) by FRET analysis

The purified fusion proteins were tested for the presence of NADH-dependent energy transfer performed as described by Fjeld *et al*., 2003. The emission peak at 430nm indicates binding of NADH to RIBEYE(B) and energy transfer from tryptophan W867 to NADH. RIBEYE wild type fusion protein (1µM) showed a strong, FRET peak at 430nm which increased in size with increasing concentrations of NADH. GST did not display FRET emission at 430nm. RIBEYE(B)844Q also showed a clear FRET peak at 430nm (arrow) although the FRET peak was smaller in size than the wild type protein. The FRET peak of RIBEYE(B) E844Q clearly demonstrates that this point mutant of RIBEYE(B) is properly folded.

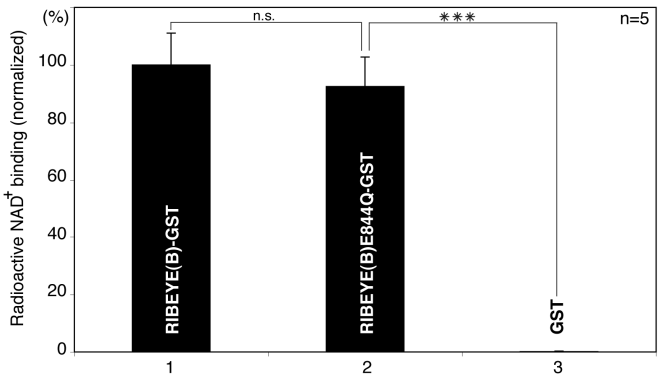

Figure.24. Radioactive ^{14}C-NAD^{+} Binding of RIBEYE(B)

The RIBEYE(B) E844Q mutant protein binds with ^{14}C-NAD^{+} as like wild type RIBEYE(B) protein. The control GST protein showed no binding of ^{14}C-NAD^{+}.The radioactive NAD^{+} binding data as well as FRET data of RIBEYE(B)E844Q clearly demonstrate that this point mutant of RIBEYE(B) is properly folded.

3.7. RIBEYE(B)E844Q is critical for Munc119 binding

We identified the glutamate E884 residue in the RIBEYE(B)-domain is a crucial site for Munc119 interaction. In order to rule out the consequence of catalytic sites on RIBEYE – Munc119 interaction, we made further mutants in two other catalytic sites, aa R815 and H864 and tested these mutants for Munc119 interaction in YTH assays. Except E844Q mutant other mutants H864F and R815Q were interacted with Munc119 (Fig.25)

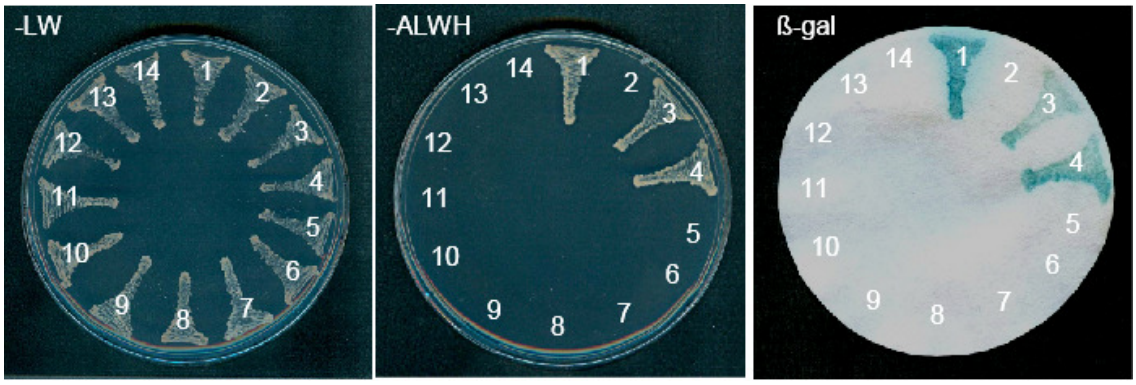

mating	bait	prey	-ALWH	βGal
1	RE(B)WT	Munc119(1-240)	+	+
2	RE(B)E844Q	Munc119(1-240)	-	-
3	RE(B)R815Q	Munc119(1-240)	+	+
4	RE(B)H864F	Munc119(1-240)	+	+
5	pGBKT7	Munc119(1-240)	-	-
6	pSE1112	Munc119(1-240)	-	-
7	RE(B)WT	pACT2	-	-
8	RE(B)E844Q	pACT2	-	-
9	RE(B)R815Q	pACT2	-	-
10	RE(B)H864F	pACT2	-	-
11	RE(B)WT	pSE1111	-	-
12	RE(B)E844Q	pSE1111	-	-
13	RE(B)R815Q	pSE1111	-	-
14	RE(B)H864F	pSE1111	-	-

Figure.25. Munc119 interaction with RIBEYE(B) catalytic mutants

Summary plates of YTH analyses obtained with the indicated bait and prey plasmids. For convenience, experimental bait-prey pairs are under layered in colour (green in case of interacting bait-prey pairs; yellow in case of non-interacting bait-prey pairs); control matings are non-colored. The analyzed Munc119 constructs interact with catalytic point mutants of RIBEYE(B) domain RIBEYE R815Q and RIBEYE H864F (matings #3, 4) except for RIBEYE(B)E844Q (matings #2). The respective control matings (auto activation controls; yeast matings #5-14) did not show growth on -ALWH plate and expression of β-galactosidase activity. Growth on –LW plates demonstrates the presence of the bait and prey plasmids in the mated yeast.

3.8. Munc119 is specifically recruited to purified synaptic ribbons

The co-immunoprecipitation experiments from bovine retina demonstrated the presence of Munc119 on synaptic ribbons (Fig.15). Additionally, the immunolabelling data showed that there are large amounts of Munc119 in the presynaptic terminals at ribbon sites and also at sites close to the synaptic ribbon (Fig.26). Interestingly, purified synaptic ribbons

isolated from bovine retina specifically recruited externally added soluble Munc119-GST fusion protein (Fig. 27). The binding of Munc119 to synaptic ribbons was specific because the control protein, GST did not bind to synaptic ribbons. Since the amount of Munc119 on purified synaptic ribbons was low, Munc119 appears to be a peripheral protein component of synaptic ribbon that can relatively easily dissociate from synaptic ribbons.

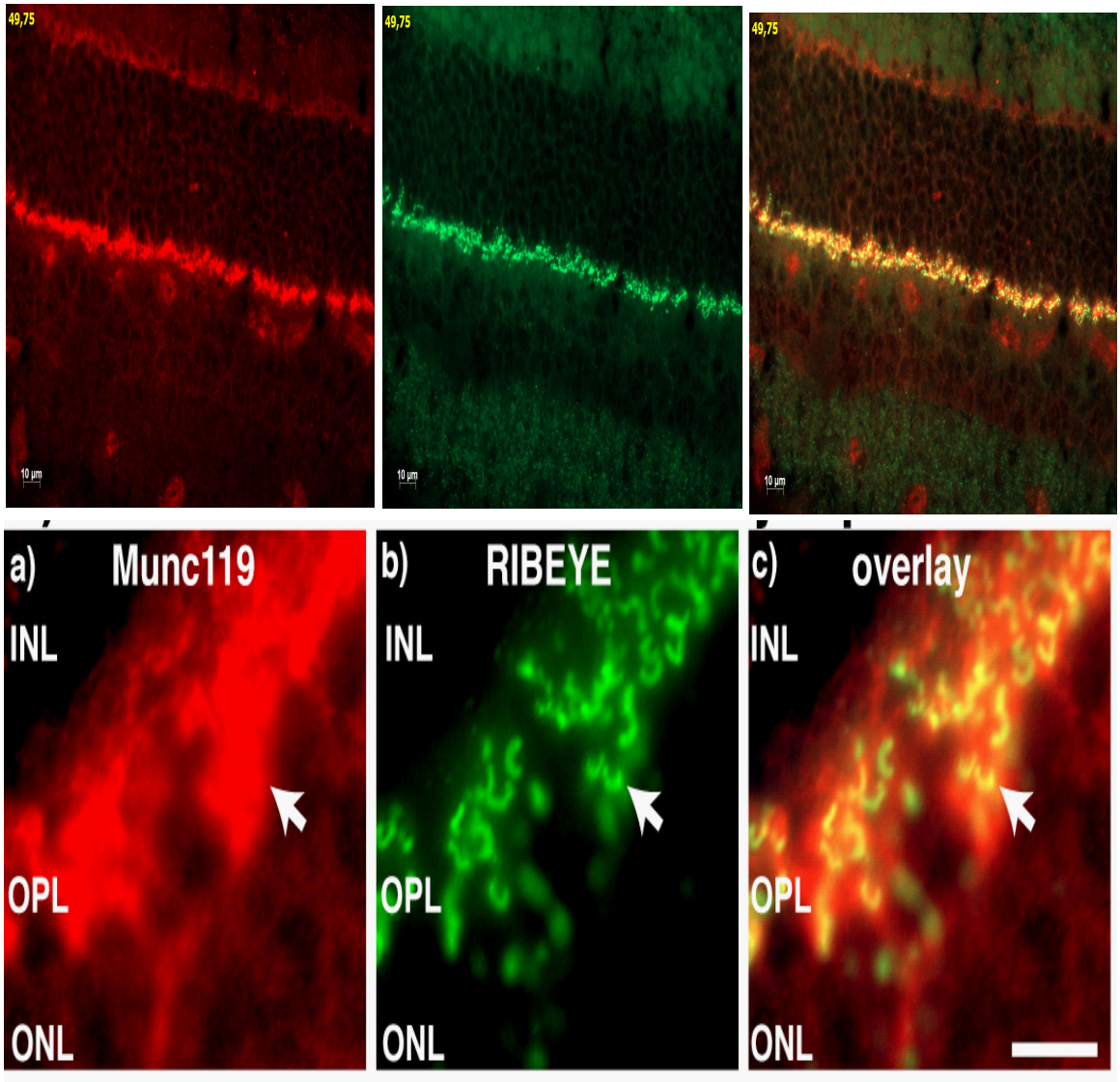

Figure.26. Munc119 co-localize with RIBEYE in synaptic ribbon of bovine retina

Immunolabelling of the outer plexiform layer of the bovine retina that contain photoreceptor ribbon synapses with polyclonal antibodies against Munc119 and monoclonal antibodies against RIBEYE(B)/CtBP2. Strong immunosignals of Munc119 were found at synaptic ribbons and in close vicinity to synaptic ribbons. Abbreviations: ONL, outer nuclear layer; OPL, outer plexiform layer; INL, inner nuclear layer. Scale bar:10 µm.

(Contributed by Stephanie Keppel as part of her MD thesis work)

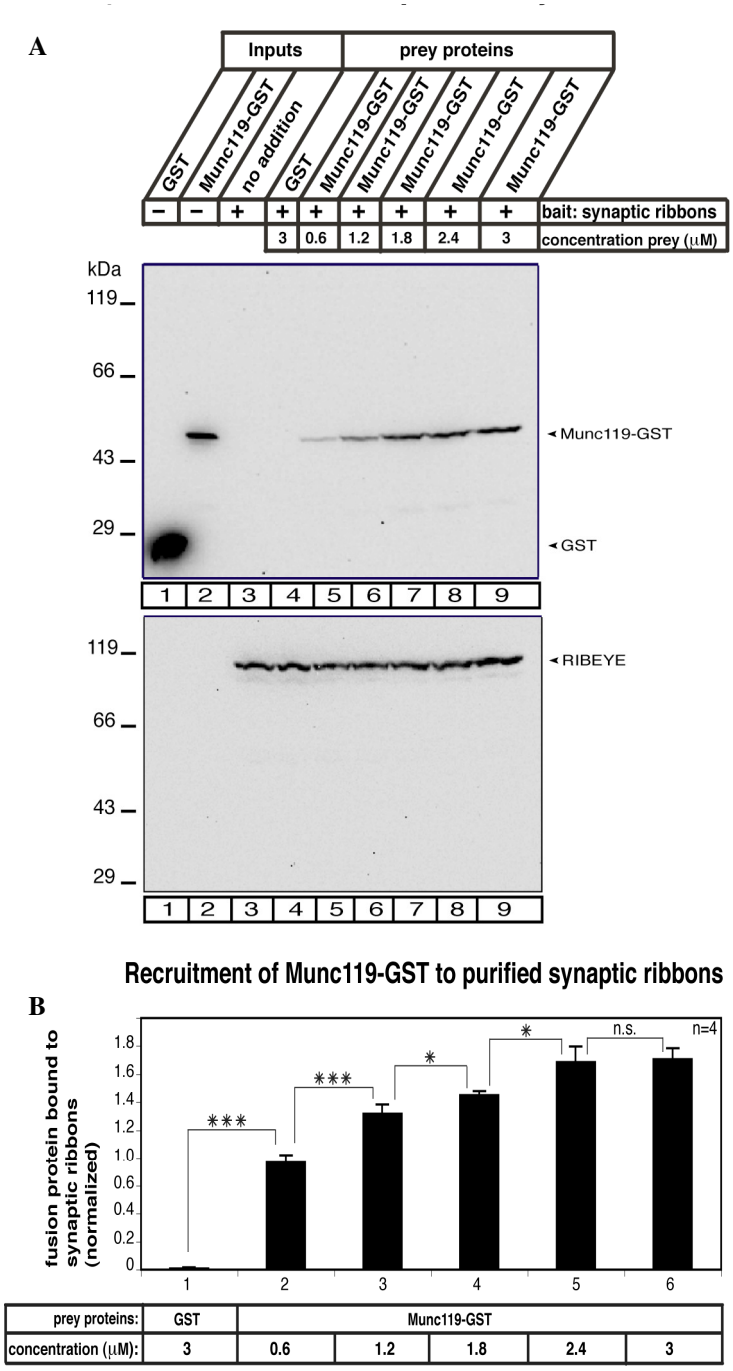

Figure.27. Purified synaptic ribbons specifically recruit Munc119

A. 20µg of purified synaptic ribbons were tested for their capability to bind soluble Munc119 fusion protein at the indicated concentrations, ranging from 0.6 to 3µM. GST alone (at a concentration of 3µM) was used as a control. Purified ribbons specifically bound Munc119-GST but not GST (Fig. 7A). The two depicted blots show representative examples of 4 different experiments which all showed the same result. The lower blot is stripped and reprobed with antibodies against RIBEYE to show equal loading of ribbons. B. Quantification of binding of the indicated concentration of Munc119 (ranging from 0.6µM to 3µM) to a fixed amount of synaptic ribbons. With increasing concentration of munc119,the binding to ribbons increased in an asymptotic manner. The binding of Munc119-GST is saturating indicating a limited, fixed amount of binding sites for Munc119 on synaptic ribbons. Abbreviations: ***, highly significant (α=0.001); weakly significant (α=0.05); n.s. non-significant. Error bars s.e.m.

CHAPTER 4

DISCUSSION

Synaptic ribbons are dynamic organelles suggested to be the prerequisite for the fast synaptic vesicle exocytosis and endocytosis in ribbon synapse based upon electron microscopic and physiological observations (for review, see Sterling and Matthews, 2005; Heidelberger *et al*., 2005). But how the synaptic ribbon orchestrates ultrafast mechanism in ribbon synapse is still unknown. RIBEYE is a major and unique component of synaptic ribbon (Schmitz *et al*., 2000). In line with proposed role by Schmitz *et al.*, 2000, a step towards the understanding of molecular function of RIBEYE in ribbon synapse, we identified Munc119 as one of the potential interaction partners of RIBEYE. This Munc119-RIBEYE interaction provides the molecular link between RIBEYE and membrane trafficking machinery in synaptic transmission at photoreceptor ribbon synapse.

4.1. Munc119-RIBEYE interaction, an essential molecular event in synaptic transmission at photoreceptor ribbon synapses

In the present study, we identified Munc119 as one of the potential interaction partners of RIBEYE through yeast two hybrid screens. We corroborated this interaction by GST pull-down assays, co-immunoprecipitation and synaptic ribbon recruitment assays. Munc119 directly interacts with RIBEYE(B)-domain and it associates with RIBEYE *in vivo* in bovine retina and R28 retinal progenitor cells. We have also shown that the NADH-binding subdomain of RIBEYE interacted with PrBP/δ homology domain of Munc119.

Although the physiological importance of Munc119 for the synaptic transmission has been well documented, it is not yet clear how Munc119 works at the molecular level in ribbon synapse. Interestingly, a patient with cone-rod dystrophy had the heterozygous premature termination mutation in HRG4 (human UNC119) leads to the expression of truncated protein which lacks the PrBP/δ homology domain. This domain was identified as an interaction sub domain with RIBEYE in our study. Electroretinogram studies of this patient had shown reduced b wave and normal c wave like PrBP/δ knock out animal (Zhang *et al*., 2007). This reduced b wave of ERG corresponds to the defect in photoreceptor synaptic transmission, suggested the possible role of Munc119 in synaptic transmission. Since RIBEYE interacts with the PrBP/δ homology domain, we assume that both proteins interact at specific molecular event in photoreceptor synaptic transmission.

4.2. NADH/NAD$^+$ binding of RIBEYE is not an essential requirement for Munc119–RIBEYE interaction

RIBEYE consists of two functional domains, the amino terminal A-domain and the carboxy terminal B-domain. The A-domain was suggested to be the prerequisite for assembly of synaptic ribbon. The B-domain binds to NADH/NAD$^+$, may serve as an enzyme (Schmitz *et al*, 2000). We demonstrated that RIBEYE is a scaffolding protein with ideal properties to explain the assembly of synaptic ribbons as well as its ultra-structural dynamics via a modular assembly mechanism (Magupalli *et al*., 2008). NADH-binding domain of RIBEYE interacts with PrBP/δ homology domain of Munc119. Specific protein-protein interactions of CtBP family proteins was regulated by NADH/NAD$^+$ (for review, see Chinnadurai, 2003 & 2005). The NADH/NAD$^+$ binds to CtBP family proteins and induce structural conformation. This modulates the interaction between CtBP family proteins and its interaction partners (for review, see Chinnadurai, 2003 & 2005). Since the RIBEYE(B)-domain is structurally homologue to CtBP2 and CtBP1 (Schmitz, unpublished), we addressed the RIBEYE-Munc119 interaction in presence of NADH/NAD$^+$. Increasing concentration of (physiological cellular concentration range) both NADH and NAD$^+$ did not significantly influence the binding of Munc119 to the RIBEYE(B) in GST pull-down assays. RIBEYE(B)G730 is an essential component of the NADH-binding motif and the RIBEYE(B) point mutant RIBEYE(B)G730A does not bind significant levels of NADH (Magupalli *et al*,2008). In contrast to the NADH-binding deficiency, RIBEYE(B)G730A still interacted with Munc119 in YTH analyses indicating that NADH-binding is not important for binding of Munc119 to RIBEYE(B)-domain. This clearly demonstrated that NADH/NAD$^+$ binding of RIBEYE is not an essential factor for Munc119-RIBEYE(B) interaction.

4.3.The NADH/NAD$^+$ binding site and Munc119 interaction site of RIBEYE are topographically closely related

Previous YTH analyses demonstrated that the NADH-binding subdomain of RIBEYE(B) is mediating the interaction. Interestingly, mutational analysis of key residues in NADH-binding sub domain (NBD) showed that Glutamate E844 is crucial for Munc119 interaction with RIBEYE. Glutamate E844 is the component of catalytic triad (R-E-H). The Arg/Glu(Asp)/His triad is conserved in all D2-HDHs and implicated as the centre for substrate binding and dehydrogenase activity (for review, see Chinnadurai, 2003 & 2005). Kumar *et al*, 2002 showed that mutation of catalytic residues affect the binding of E1A to CtBP. The two other catalytic site mutants R815Q and H864F still interacted with Munc119

in yeast two hybrid assays. From these findings, we assume that R815 and H864 are not crucial as E844 for Munc119 interaction. As judged by NADH dependent FRET experiments and $C^{14}NAD^+$ binding analyses, the mutant RIBEYE(B)E844Q still able to bind $NADH/NAD^+$. The catalytic site E844 is not essential for NADH-binding but crucial for Munc119 interaction. Based on these data, we suggested that Munc119 binding region of RIBEYE appears to be topographically close to the NADH-binding cleft of RIBEYE(B). Since RIBEYE may contain enzymatic activity (Schmitz *et al*.,2000), the impact of Munc119 biding to RIBEYE at catalytic site to be ruled out in further analysis. Furthermore, we assume from these results that RIBEYE may binds to the $NADH/NAD^+$ at different physiological event compared to Munc119 binding or $NADH/NAD^+$ binding is a parallel event to Munc119-RIBEYE interaction in synaptic transmission.

4.4. RIBEYE(B) dimerization is dispensable for Munc119 interaction

The CtBP family proteins have the property of NADH-binding and dimerization (for review, see Chinnadurai, 2003 & 2005). The homo-dimerization and NADH-binding process are dependent on each other. The dimerization loop present in NADH-binding domain is essential for dimerization (for review, see Chinnadurai, 2003 & 2005). Dimerization is implicated in protein-protein interaction of CtBP family proteins (for review, see Chinnadurai ,2003 & 2005). RIBEYE(B)-domain homo-dimerize like other CtBP family proteins and also the dimerization loop is important for RIBEYE(B) homo-dimerization (Magupalli *et al*., 2008). RIBEYE(B)ΔHDL (delta homo-dimerization loop) is a mutant which is not able to form RIBEYE(B)-RIBEYE(B) dimers. RIBEYE(B)ΔHDL mutant still interacted with Munc119 suggested that Munc119-RIBEYE interaction is not dependent upon homo-dimerization of RIBEYE(B).

We identified that the binding of Munc119 to RIBEYE is independent of RIBEYE(B) dimerization and also the interaction site is away from the dimerization loop but close to the catalytic site. From these observations, we also suggested that Munc119 interaction with RIBEYE does not hamper the RIBEYE(B) dimerization process. We have shown that the multiple RIBEYE-RIBEYE interaction creates a scaffold for the assembly of synaptic ribbon (Magupalli *et al*., 2008). If we assume that the $NADH/NAD^+$ binding and dimerization are essential for the function of RIBEYE in ribbon synapse, Munc119 binding to the RIBEYE is an independent or related parallel event in photoreceptor synaptic transmission.

4.5. Munc119, a peripheral component of synaptic ribbons

Munc119 associate with RIBEYE *in vivo* in bovine retina and R28 retinal progenitor cells. R28 cells endogenously express Munc119 and RIBEYE in a TritonX-100 soluble fraction. In addition, even though the synaptic ribbon was purified after stringent treatment (high salt and alkaline pH) it contains very little amount of Munc119. This finding suggested that Munc119 can be specifically recruited to synaptic ribbon up to certain amount. During TritonX-100 treatment most of the Munc119 comes out in soluble fraction from the bovine retina, Munc119 transfected COS-7 cells and R28 cells. Due to its TritonX-100 soluble nature, most of the Munc119 could be present in the cytosolic and also in peripheral membrane compartment (Higashide *et al*., 1998). Most of the Munc119 present in cytosolic distribution and also in close vicinity to synaptic ribbon in OPL layer of retina. From these data, we can judge that Munc119 is most likely to be a peripheral component of synaptic ribbon which can be detached from synaptic ribbon during purification. These Munc119 depleted synaptic ribbons could specifically rebind Munc119 in synaptic ribbon pull-down assay. In support this suggestion, a large portion of Munc119 is soluble in nature (Higashide *et al*., 1998; our own unpublished data). The factors that regulate the association and dissociation of Munc119 with synaptic ribbon *in situ,* to be elucidated by further analyses.

4.6. The perspective of Munc119-RIBEYE interaction in photoreceptor ribbon synapses

The RIBEYE(B)-domain is highly homologous to CtBP1, a protein suggested functioning in membrane traffic under the name of "BARS" (brefeldin A-ADP ribosylated substrate) (Schmitz *et al*,2000). The identification of molecular interaction partners is the prime importance to analyse the function of a protein. RIBEYE is suggested to be involved in synaptic ribbon assembly through "A" domain and has enzymatic function in vesicle trafficking through "B" domain (Schmitz *et al*, 2000). We have shown that the multiple RIBEYE-RIBEYE interaction creates a scaffold for the assembly of synaptic ribbon (Magupalli *et al.*, 2008). A key in the understanding of the function of Munc119 is through its homology to PrBP/δ. PrBP/δ binds and dissociates the prenylated proteins from membrane. This enzymatic activity of PrBP/δ has been shown to be important for intracellular membrane and protein trafficking in inner and outer segments of photoreceptors (Zhang *et al*., 2004 & 2007). The tonically active ribbon synapse requires a fast protein and membrane trafficking machinery to keep the pace constant for a prolonged period. We propose that Munc119 could be fulfilling a similar type of function like PrBP/δ in photoreceptor synaptic terminals.

Another supporting evidence of Munc119 function like PrBP/δ is, both proteins shares the common interaction partners like ARL2 and ARL3 but at different sub cellular localization (Hanzal-Bayer *et al*., 2002; Kobayashi *et al*., 2003; Van Valkenburgh *et al*.,2001) These ARL (ADP ribosylation like) proteins are implicated in protein trafficking machinery (Catherine *et al*., 2003). We have shown that NADH-binding domain of RIBEYE(B) interacts with PrBP/δ homology domain. From these findings, we suggested that NADH and Munc119 binding to RIBEYE are the parallel events in protein and membrane trafficking in photoreceptor synaptic transmission. Thus Munc119 could be fulfilling similar type of function in the ribbon synapse as PrBP/δ function in the inner and outer segments. We also propose that Munc119 and RIBEYE interaction is an important part of protein and membrane trafficking machinery involved in synaptic vesicle trafficking in photoreceptor ribbon synapse. Additionally Munc119 activate the SRC type kinases in T cell receptor signalling in lymphocytes (Cen *et al.*, 2003; Gorska *et al.*, 2004). It could be possible to think that Munc119 may be activating similar type of mechanism in synaptic transmission at photoreceptor ribbon synapse.

Recently Haeseleer, 2008 identified that CaBP4 interacts with Munc119 and CaBP4 knock out mice shows the strong decrease of unc119 expression as compared to other synaptic proteins (e.g., PSD 95, SV2, syntaxin 3). CaBP4 was previously shown to modulate neurotransmitter release via regulation of presynaptic Cav1 L-type Ca2+ channels (Haeseleer *et al*., 2004). Additionally, RIBEYE co-localised with CaV1.4 alpha sub unit(Haeseleer *et al*., 2004). From these findings, we can assume that RIBEYE-Munc119-CaBP4-Cav1.4 may be form a functional network in synaptic transmission in photoreceptor ribbon synapse.

Munc119 is one of the disease genes for cone-rod dystrophy. The importance of Munc119 in synaptic neurotransmission and its capacity for pathogenicity been amply supported by the presence of an HRG4 mutation in a patient with cone–rod dystrophy and by the phenotype produced in our transgenic model expressing the identical mutation (Kobayashi *et al*.,2000). A patient with late-onset cone-rod dystrophy had the heterozygous premature termination mutation in HRG4 (human UNC119). The fundus photograph of this patient with cone–rod dystrophy showing macular atrophy (Kobayashi *et al*., 2000). The ERG recordings of this patient shows subnormal rod and cone responses with prolonged cone b-wave demonstrated the reduced photoreceptor synaptic transmission. The transgenic mouse that expresses a mutant HRG4 (identical with that found in a patient with late-onset cone–rod dystrophy) in the photoreceptor synapse shows a progressive decrease in the ERG b-wave (independent of the photoreceptor's ability to generate a c-wave), leading to retinal degeneration with prominent degeneration of the synapses (Kobayashi *et al*., 2000). This

mutation in Munc119 expresses truncated protein which contains only Proline Rich Domain (PRD). The functional part of Munc119 protein, PrBP/δ is deleted in cone-rod dystrophy patients is responsible for the interaction with RIBEYE. From these findings, we suggested that Munc119-RIBEYE interaction could play a major role in protein and membrane trafficking machinery in synaptic transmission at photoreceptor ribbon synapse.

CHAPTER 5

BIBLIOGRAPHY

Bai, C and Elledge, S.J (1996) Gene identification using the yeast two-hybrid system. Methods Enzymol. **273**, 331-347.

Cen, O., Gorska, M.M., Stafford, S.J., Sur, S and Alam, R (2003) Identification of UNC119 as a novel activator of SRC-type tyrosine kinases. J. Biol. Chem. **278**, 8837-8845.

Chinnadurai, G (2003) CtBP family proteins: more than transcriptional corepressors. Bioessays **25**, 9-12.

Chinnadurai, G (2005) CtBP Family Proteins: Unique Transcriptional Regulators in the Nucleus with Diverse Cytosolic Functions. Landes Bioscience.
http://www.ncbi.nlm.nih.gov/books/bv.fcgi?rid=eurekah.chapter.74628

Dowling, J.E (1987) The Retina: An Approachable Part of the Brain. Harvard University Press, Cambridge, MA, USA.

Fjeld, C.C., Birdsong, W.T and Goodman, R.H (2003) Differential binding of NAD+ and NADH allows the transcriptional co repressor carboxyl-terminal binding protein to serve as a metabolic sensor. Proc. Natl. Acad. Sci. USA. **100**, 9202-9207.

Florio, S.K., Prusti, R.K and Beavo,J.A (1996) Solubilization of membrane-bound rod phosphodiesterase by the rod phosphodiesterase recombinant δ subunit. J. Biol. Chem. **271**, 24036–24047.

Gluzman, Y (1981) SV40-transformed simian cells support the replication of early SV40 mutants. Cell **23**, 175-182.

Gorska, M.M., Stafford, S.J., Cen, O., Sur, S and Alam, R (2004) Unc119, a novel activator of Lck/Fyn, is essential for T cell activation. J. Exp. Med. **199**, 369-379.

Grant, S.G., Jessee, J., Bloom, F.R and Hanahan, D (1990). Differential plasmid rescue from transgenic mouse DNAs into *Escherichia coli* methylation-restriction mutants. Proc. Natl. Acad. Sci. USA. **87***,* 4645-4649.

Grodberg, J and Dunn, J.J (1988) ompT encodes the *Escherichia coli* outer membrane protease that cleaves T7 RNA polymerase during purification. J. Bacteriol. **170**, 1245-1253.

Hanzal-Bayer,M., Renault, R., Roversi, P., Wittinghofer, A and Hillig, R.C (2002)The complex of Arl2-GTP and PDE delta: from structure to function. EMBO J. **21**, 2095-2106.

Harper, J.W., Adami, G.R., Wie, N., Keyomarski, K and Elledge, S.J (1993) The p21 cdk-interacting protein Cip1 is a potent inhibitor of G1 cyclin-dependent kinases. Cell **75**, 805-816.

Heidelberger, R., Thoreson, W.B and Witkovsky, P (2005) Synaptic transmission at retinal ribbon synapses. Prog. Ret. Eye Res. **24**, 682-720.

Helmuth, M., Altrock, W., Böckers, T.M., Gundelfinger, E.D and Kreutz, M.R (2001) A transfection protocol for yeast two-hybrid library screening. Anal. Biochem. **293**, 149-152.

Higashide, T., Murakami, A., McLaren, M.J and Inana, G (1996) Cloning of the cDNA for a novel photoreceptor protein. J Biol Chem. **271**, 1797-1804.

Higashide, T., McLaren, M.J and Inana, G (1998) Localization of HRG4, a photoreceptor protein homologous to Unc-119, in ribbon synapse. Invest.Ophthalmol. Vis. Sci. **39**, 690-698.

James, P., Halladay, J and Craig, E.A (1996) Genomic libraries and host strain designed for highly efficient two hybrid selection in yeast. Genetics **144**, 1425-1436.

Katsanis, N and Fisher, E.M (1998) A novel C-terminal binding protein (CTBP2) is closely related to CTBP1, and adenovirus E1A-binding protein, and maps to human chromosome 21q21.2. Genomics **47**, 294–299.

Kobayashi, A., Higashide, T., Hamasaki, D., Kubota, S., Sakuma, H., An, W., Fujimaki, T., McLaren, M.J., Weleber, R.G and Inana, G (2000) HRG4 (UNC119) mutation found in cone-rod dystrophy causes retinal degeneration in a transgenic model. Invest. Ophthalmol. Vis. Sci. **11**, 3268-3277.

Kobayashi, A., Kubota, S., Mori, N., McLaren, M.J and Inana, G (2003) Photoreceptor synaptic protein HRG4 (UNC119) interacts with ARL2 via a putative conserved domain. FEBS Lett. **534**, 26-32.

Kubota, S., Kobayashi, A., Mori, N., Higashide, T., McLaren, M.J and Inana, G (2002) Changes in retinal synaptic proteins in the transgenic model expressing a mutant HRG4 (UNC119) Invest. Ophthalmol. Vis. Sci. **43**, 308-313.

Kumar, V., Carlson, J.E., Ohgi, K.A., Edwards, T.A., Rose, D.W., Escalante, C.R., Rosenfeld, M.G and Aggarwal, A.K (2002) Transcription corepressor CtBP is an NAD^+-regulated dehydrogenase. Mol. Cell **10**, 857-869.

Li, L., Florio, S.K., Pettenati, M.J., Rao, N., Beavo, J.A and Baehr, W (1998) Characterization of human and mouse rod cGMP phosphodiesterase delta (PDE6D) and chromosomal localization of the gene. Genomics **49**, 76-82.

Li, N and Baehr, W (1998) Expression and characterization of human PDEδ and its *Caenorhabditis elegans* ortholog Ceδ. FEBS Lett. **440**, 454–457.

Linari, M., Ueffing, M., Manson, F., Wright, A., Meitinger, T and Becker, J (1999) The Retinitis GTPase Regulator, RPGR, interacts with the delta subunit of rod cyclic GMP phosphodiesterase. Proc. Natl. Acad. Sci. USA. **96**, 1315-1320.

Maduro, M and Pilgrim, D (1995) Identification and cloning of unc-119, a gene expressed in the *Caenorhabditis elegans* nervous system Genetics **141**,977–988.

Magupalli, V.G., Schwarz, K., Alpadi, K., Natarajan, S., Seigel, G.M and Frank Schmitz (2008) Multiple Ribeye-Ribeye interactions create a dynamic scaffold for the formation of synaptic ribbon. J. Neurosci. **28**, 7954-7967.

Manning ,A.G., Crawford B.D., Waskiewicz, A.J and Pilgrim, D.B (2004) Unc-119 homolog required for normal development of the zebrafish nervous system. Genesis **40**,223-230.

Marzesco,A.M., Galli,T., Louvard,D and Zahraoui,A (1998) The Rod cGMP Phosphodiesterase delta Subunit Dissociates the Small GTPase Rab13 from Membranes J. Biol. Chem. **273** , 22340–22345.

Nardini, M., Spano, S., Cericola, C., Pesce, A., Massaro, A., Millo, E., Luini, A., Corda, D and Bolognesi, M (2003) CtBP/BARS: a dual function protein involved in transcription co-repression and Golgi membrane fission. EMBO J. **22**, 3122-3130.

Paillart, C., Li J, Matthews, G and Sterling, P (2003) Endocytosis and vesicle recycling at a ribbon synapse. J Neurosci. **23**,4092-4099.

Parsons, T.D and Sterling, P (2003) Synaptic Ribbon: Conveyor Belt or Safety Belt? Neuron **37**, 379-382.

Perin, MS., Johnston, PA., Ozcelik, T., Jahn, R., Francke, U and Südhof, T.C (1990) Structural and functional conservation of synaptotagmin (p65) in Drosophila and humans J. Biol. Chem. **266**, 615-622.

Purves, D., Augustine, G.J., Fitzpatrick, D., Katz, L.C., La Mantia, A.S., McNamara, J.O and Williams, SM (2001). Neuroscience. Second edition.

Rea, R., Li ,J., Dharia, A., Levitan, ES., Sterling, P and Kramer, R.H (2004) Streamlined Synaptic Vesicle Cycle in Cone Photoreceptor Terminals. Neuron **41**, 755-766.

Schmitz, F., Bechmann, M and Drenckhahn, D (1996) Purification of synaptic ribbons, structural components of the photoreceptor active zone complex. J. Neurosci. **16**, 7109-7116.

Schmitz, F., Königstorfer, A and Südhof, T.C (2000) RIBEYE, a component of synaptic ribbons: a proteins journey through evolution provides insight into synaptic ribbon function. Neuron **28**, 857-872.

Schmitz, F., Tabares, L., Khimich, D., Strenzke, N., dela Villa-Polo, P., Castellano-Munoz, M., Bulankina, A., Moser, T., Fernandez-Chacon, R and Südhof, T.C (2006) CSP alpha-

deficiency causes massive and rapid photoreceptor degeneration. Proc. Natl. Acad. Sci. USA. **103**, 2925-2931.

Seigel, G.M (1996) Establishment of an E1A-immortalized retinal cell culture. In Vitro Cell. Dev. Biol. Animal **32**, 66-68.

Seigel, G.M., Sun, W., Wang, J., Hershberger, D.H., Campbell, L.M and Salvi, R.J (2004) Neuronal gene expression and function in the growth-stimulated R28 retinal precursor cell line. Curr. Eye Res. **28**, 257-269.

Schaeper,U., Boyd, J.M., Sulekha,V, Uhlmann,E., Subramanian,T and Chinnadurai,G (1995) Molecular cloning and characterization of a cellular phosphoprotein that interacts with a conserved C-terminal domain of adenovirus E1A involved in negative modulation of oncogenic transformation. Proc. Natl. Acad. Sci. USA. **92**, 10467–10471.

Stahl, B., Diehlmann, A and Südhof, T.C (1999) Direct interaction of Alzheimer's disease related presenilin with armadillo protein p0071. J. Biol. Chem. **14**, 9141-9148.

Sterling, P (1998) Retina. In the Synaptic Organization of the Brain, ed. Sheperd, G. M., 205—253. Oxford University Press, New York.

Sterling, P and Matthews, G (2005) Structure and function of ribbon synapses. Trends Neurosci. **28**, 20-29.

Swanson, D.A., Chang, J.T., Campochiara, P.A., Zack, D.J and Valle, D (1998) Mammalian ortholog of C. elegans unc-119 is highly expressed in photoreceptors. Invest. Ophthalmol. Vis. Sci. **39**, 2085-2094.

Tai, A.W., Chuang, J.Z., Wolfrum, U and Sung, C.H (1999) Rhodopsin's carboxy-terminal cytoplasmic tail acts as a membrane receptor for cytoplasmic dynein by binding to the dynein light chain Tctex-1. Cell **97**, 877-887.

Thiel, G and Cibelli, G (1999) Corticotropin-releasing factor and vasoactive intestinal polypeptide activate gene transcription through the cAMP signaling pathway in a catecholaminergic immortalized neuron. Neurochemistry Int. **34**, 183-191.

tom Dieck, S and Brandstätter, J.H (2006) Ribbon synapses of the retina. Cell Tiss. Res. **326**, 339-346.

Usukura, J. and Yamada, E. (1987) Ultra structure of the synaptic ribbons in photoreceptor cells of *Rana catesbeiana* revealed by freeze etching and freeze-substitution. Cell Tissue Res. **247**, 483–488.

Van Valkenburgh, H., Shern, J.F., Sharer, J.D., Zhu, X and Kahn, R.A (2001) ADP-ribosylation factors (ARFs) and ARF-like 1 (ARL1) have both specific and shared effectors: characterizing ARL1-binding proteins. J. Biol. Chem. **276**, 22826-22837.

Wan, L., Almers, W and Chen, W (2005) Two ribeye genes in teleosts: the role of ribeye in ribbon formation and bipolar cell development. J. Neurosci. **25**, 941-949.

Weigert, R., Silletta, M.G., Spano, S., Turacchio, G., Cericola, C., Colanzi, A., Senatore, S., Mancini, R., E.V. Polishchuk, E.V and Salmona,M (1999) CtBP/BARS induces fission of Golgi membranes by acylating lysophosphatidic acid. Nature **402**, 429–433.

Yu, X and Baehr, R (2000) Nuclear localization and cell-cycle specific expression of CtIP, a protein that associates with the BRCA1 tumor suppressor. J. Biol. Chem. **275**, 18541-18549.

Zenisek, D., Steyer, J.A and Almers, W (2000) Transport, capture and exocytosis of single synaptic vesicles at active zones. Nature **406**, 849–854.

Zenisek, D., Steyer, J.A., Feldman, M.E and Almers, W (2002) A membrane marker leaves synaptic vesicles in milliseconds after exocytosis in retinal bipolar cells. Neuron **35**, 1085–1097.

Zhang, Q., Piston, D.W and Goodman, R.H (2002) Regulation of corepressor function by nuclear NADH. Science **295**, 1895−1897.

Zhang, H., Liu, X.-H., Zhang, K., Chen, C.-K., Frederick, J.M., Prestwich, G.D and Baehr, W (2004) Photoreceptor cGMP phosphodiesterase δ subunit (PDEδ) functions as a prenyl-binding protein. J. Biol. Chem. **279**, 407-413.

Zhang, H., Li, A., Doan, T., Rieke, F., Detwiler, P.B., Frederick, J.M and Baehr, W (2007) Deletion of PrBP/δ impedes transport of GRK1 and PDE6 catalytic subunits to photoreceptor outer segments. Proc. Natl. Acad. Sci. USA. **104**, 8857-8862.

LIST OF FIGURES

ABBREVIATION

A	Adenine
AD	Activation domain
ADP	Adenosinediphosphate
-ALWH	drop out medium lacking Adenine, Leucine, Tryptophan and Histidine
Amp	Ampicillin
ARL	ADP ribosylation factor like
ATP	Adenosinetriphosphate
BARS	Brefeldin A-ADP ribosylated substrate
bc	Bipolar cell
BD	Binding domain
bp	Base pair
BSA	Bovine serum albumin
CaBP4	Calcium binding protein 4
cDNA	complementary DNA
Cav1.4	Voltage gated calcium channel 1.4
C. elegans	*Caenorhabditis elegans*
CtBP1	C-terminal Binding Protein 1
CtBP2	C-terminal Binding Protein 2
CtIP	CtBP interaction protein
Cy2	Carbocyanin
Cy3	Indocarbocyanin
DNA-BD	DNA binding domain
ddH_2O	double distilled water
DMEM	Dulbecco´s modified eagle's medium
DNA	Deoxyribonucleic acid
dNTP	Deoxyribonucleotides
DTT	Dithiothreitol
E. coli	*Escherichia coli*
EGFP	Enhanced green fluorescent protein)
EDTA	Ethylenediaminetetrachloroacteicacid
ERG	Electroretinogram
FRET	Fluorescence resonance energy transfer

Gal	Galactosidase
GCL	Ganglion cell layer
GFP	Green fluorescent protein
GST	Glutathione-S-transferase
H	Histidine
HRG4	Human Retinal Gene 4
hc	Horizontal cell
INL	Inner nuclear layer
IPTG	Isopropyl-β-D-thiogalactopyranoside
IPL	Inner plexiform layer
IS	Inner segments
kDa	kilo Dalton
LB	Luria-Bertani medium
-LW	Yeast selection medium lacking leucine and tryptophan
MW	Molecular weight
Munc119	Mammalian unc119
NAD^+	Nicotinamide adenine dinucleotide (oxidized)
NBD	NADH-binding subdomain
NADH	Reduced nicotinamide adenine dinucleotide
NLS	Nuclear localization signal
ONL	Outer nuclear layer
OS	Outer segments
PBS	Phosphate buffered saline
PCR	Polymerase chain reaction
PDE6	Phosphodiesterase 6
PFA	Paraformaldehyde
PND	Postnatal day
PrBP/δ	Prenyl binding protein δ
RIM	Rab3a interacting molecule
RE(B)	RIBEYE(B)-Domain
RPGR	Retinitis Pigmentosa GTPase Regulator
rpm	Revolutions per minute
SBD	Substrate-binding subdomain
SD	Synthetic Drop out medium

SDS	Sodiumdodecylsulfate
SDS-PAGE	SDS Polyacrylamide gel electrophoresis
SNAP-25	Synaptic vesicle associated protein 25
TAE	Tris Acetate EDTA
TE	Tris EDTA
Tris	Trishydroxymethylaminomethane
UNC119	Uncoordinated 119
X-Gal	5-Bromo-4-chloro-3-indolyl-β-D-galactopyranoside
YTH	Yeast two hybrid

Curriculum Vitae

KANNAN ALPADI

Department of Neuroanatomy,
Institute for Anatomy and Cell Biology,
Faculty of Medicine, University of Saarland,
Building, 61, Kirrberger Strasse,
Homburg-66421, Saarland, Germany.
Tel: 0049-68411626195
E-mail: kannanalpadi@gmail.com

Academic Education

Ph.D. Neuroscience, University of Saarland, Germany (2005-2008)
M.Sc. Genomics, Madurai Kamaraj University, India (2003-2005)
B.V.Sc (DVM), Madras Veterinary College, TANUVAS, India (1996-2002)

Research Experience

PhD thesis (2008)
"Molecular and functional characterization of RIBEYE-Munc119 interaction in photoreceptor ribbon synapse"
Advisor: Prof. Dr. Frank Schmitz.MD, Department of Neuroanatomy, Institute for Anatomy and Cell Biology, Faculty of Medicine, University of Saarland, Germany.

Master's degree thesis (2005)

"HLA class I B association with Human Immunodeficiency Virus-Type 1 in south Indian AIDS patients".
Advisor: Prof. Dr. R. M. Pitchappan.Ph.D, Department of Immunology, Centre for Excellence in Genomics, School of Biological Science, Madurai Kamaraj University, India.

Summer training program thesis (2004)

"Sub typing and phylogenetic analysis of Human Immunodeficiency Virus type-1 based on *gp* 41 and C2V3 of *env* gene"
Advisor: Dr. Srikanth Tripathy.MD, Department of Molecular Virology, National AIDS Research Institute, Pune, India.

Publications

1. RIBEYE recruits Munc119, a mammalian ortholog of the *C. elegans* protein unc119, to synaptic ribbons of photoreceptor ribbon synapses. Kannan Alpadi, Venkat Giri Magupalli, Stefanie Käppel, Louise Köblitz, Karin Schwarz, Gail M. Seigel, Ching-Hwa Sung and Frank Schmitz. Journal of Biological Chemistry. **283**, 26461-7 (2008).

2. Multiple Ribeye-Ribeye interactions create a dynamic scaffold for the formation of synaptic ribbon. Venkat Giri Magupalli, Karin Schwarz, Kannan Alpadi, Sivaraman Natarajan, Gail M. Seigel and Frank Schmitz. Journal of Neuroscience. **28**, 7954-7967 (2008).

3. The Retinitis Pigmentosa disease protein TULP1 is a component of synaptic ribbons, and interacts with RIBEYE. Venkat Giri Magupalli, Louise Köblitz, Kannan Alpadi, C.H. Sung and Frank Schmitz (*Manuscript in preparation*).

Awards & Scholarships

M.Sc Genomics degree- University 2nd rank (2005)
IIT-GATE Ph.D Entrance Examination - 86 % (2005)
All India level M.Sc Genomics Entrance examination - 5th rank (2003)
Tamilnadu state B.V.Sc (DVM) Entrance examination - 93% (1996)
Gold Medalist - Educational district level- 3rd Rank (1996)
Gold Medalist - Educational district level- 1st Rank (1994)
National Talent Search Scholarship (1992-1996)

Reference

Prof. Dr. Frank Schmitz.MD.,
Department of Neuroanatomy,
Institute for Anatomy and Cell Biology,
Faculty of Medicine, University of Saarland,
Homburg-66421, Saarland, Germany.
Tel: +49-6841162 6012
E-mail: frank.schmitz@uniklinikum-saarland.de

Prof. Dr. P. Gunasekaran.Ph.D.,
Department of Genetics,
Centre of Excellence in Genomic Sciences,
School of Biological Sciences,
Madurai Kamaraj University,
Madurai- 625021, India.
Tel: +91-452-2459873
Email: pguna@eth.net

Professor Emeritus. Dr. R. M. Pitchappan.Ph.D.,
Department of Immunology,
Centre of Excellence in Genomic Sciences,
School of Biological Sciences,
Madurai Kamaraj University,
Madurai- 625021, India.
Tel: +91-452-2458418
Email: pitchappanrm@yahoo.co.uk

THE JOURNAL OF BIOLOGICAL CHEMISTRY VOL. 283, NO. 39, pp. 26461–26467, September 26, 2008

RIBEYE Recruits Munc119, a Mammalian Ortholog of the *Caenorhabditis elegans* Protein unc119, to Synaptic Ribbons of Photoreceptor Synapses*[S]

Received for publication, February 28, 2008, and in revised form, July 7, 2008 Published, JBC Papers in Press, July 29, 2008, DOI 10.1074/jbc.M801625200

Kannan Alpadi[‡], Venkat Giri Magupalli[‡], Stefanie Käppel[‡], Louise Köblitz[‡], Karin Schwarz[‡], Gail M. Seigel[§1], Ching-Hwa Sung[¶], and Frank Schmitz[‡2]

From the [‡]Department of Neuroanatomy, Institute for Anatomy and Cell Biology, Saarland University, Medical School Homburg/Saar, 66421 Homburg/Saar, Germany, the [§]Department of Ophthalmology, Physiology, and Biophysics, SUNY University at Buffalo, Buffalo, New York 14214, and the [¶]Margaret M. Dyson Vision Research Institute, Department of Ophthalmology, Cell and Developmental Biology, Weill Medical College of Cornell University, New York, New York 10021

Munc119 (also denoted as RG4) is a mammalian ortholog of the *Caenorhabditis elegans* protein unc119 and is essential for vision and synaptic transmission at photoreceptor ribbon synapses by unknown molecular mechanisms. Munc119/RG4 is related to the prenyl-binding protein PrBP/δ and expressed at high levels in photoreceptor ribbon synapses. Synaptic ribbons are presynaptic specializations in the active zone of these tonically active synapses and contain RIBEYE as a unique and major component. In the present study, we identified Munc119 as a RIBEYE-interacting protein at photoreceptor ribbon synapses using five independent approaches. The PrBP/δ homology domain of Munc119 is essential for the interaction with the NADH binding region of RIBEYE(B) domain. But RIBEYE-Munc119 interaction does not depend on NADH binding. A RIBEYE point mutant (RE(B)E844Q) that no longer interacted with Munc119 still bound NADH, arguing that binding of Munc119 and NADH to RIBEYE are independent from each other. Our data indicate that Munc119 is a synaptic ribbon-associated component. We show that Munc119 can be recruited to synaptic ribbons via its interaction with RIBEYE. Our data suggest that the RIBEYE-Munc119 interaction is essential for synaptic transmission at the photoreceptor ribbon synapse.

Munc119 (also denoted as RG4, Ref. 1) is a mammalian ortholog of the *Caenorhabditis elegans* protein unc119 and essential for normal vision and synaptic transmission at photoreceptor synapses (1–3). Munc119/RG4 was initially identified by a differential display screen and shown to be expressed at high levels in photoreceptor synapses (1–3). Munc119 consists of an N-terminal, 77-amino acid long proline-rich region, and a 163-amino acid long C-terminal domain that shares significant sequence homology to the prenyl-binding protein PrBP/δ[3] (previously also denoted as the δ-subunit of photoreceptor cGMP-dependent phosphodiesterase (PDE6D) (4–6). The C-terminal PrBP/δ homology domain of Munc119 is highly conserved between species and is essential for Munc119 function (1–3). The essential function of Munc119 for synaptic transmission at photoreceptor synapses and for vision has been demonstrated in a cone rod dystrophy patient with a premature termination codon mutation (5). This termination codon mutation resulted in a Munc119 protein that lacked the PrBP/δ domain. Consistently, a transgenic mouse model that reproduced this premature termination codon mutation of Munc119 displayed similarly strong disturbances of synaptic transmission at photoreceptor synapses and defects in vision (5, 7, 8). The mechanism of how Munc119 works in photoreceptor synapses is not clear.

Photoreceptor synapses are mainly ribbon-type synapses (for review, see Refs. 9–11). Ribbon synapses are specialized, tonically active chemical synapses. To maintain tonic exocytosis, ribbon synapses are equipped with specialized presynaptic structures, the synaptic ribbons (for review, see Refs. 9–11). Synaptic ribbons are presynaptic structures in the active zone complex of these synapses and are associated with large amounts of synaptic vesicles (for review, see Refs. 9–11). The protein RIBEYE is a major component of synaptic ribbons and exclusively localized to these structures (12–14). RIBEYE consists of a unique A-domain and a B-domain, which is largely identical to CtBP2 (12). RIBEYE(B) domain belongs to a family of D-isomer-specific 2-hydroxy acid dehydrogenases and binds NAD(H) with high affinity (12). Structural analyses of the CtBP protein family that also includes RIBEYE (for review, see Ref. 15) revealed the presence of two distinct subdomains: a central NADH binding domain (NBD) and a substrate binding domain (SBD) (16, 17). The RIBEYE-specific substrate that binds to the

* This work was supported by the Sonderforschungsbereich 530 (SFB530) (TPC11) and by HOMFOR (to F. S.). The costs of publication of this article were defrayed in part by the payment of page charges. This article must therefore be hereby marked "*advertisement*" in accordance with 18 U.S.C. Section 1734 solely to indicate this fact.

The nucleotide sequence(s) reported in this paper has been submitted to the GenBank™/EBI Data Bank with accession number(s) BC103449.1.

[S] The on-line version of this article (available at http://www.jbc.org) contains supplemental materials and Figs. S1–S6.

[1] Supported by the Sybil Harrington Scholar Award from Research to Prevent Blindness and 5R24EY016662.

[2] To whom correspondence should be addressed: Dept. of Neuroanatomy, Institute for Anatomy and Cell Biology, Bldg. 61, Saarland University, Medical School Homburg/Saar, 66421 Homburg/Saar. Tel.: 49-6841-1626012; Fax: 49-6841-1626121; E-mail: frank.schmitz@uniklinikum-saarland.de.

[3] The abbreviations used are: PrBP/δ, prenyl-binding protein δ; RE, RIBEYE; RE(B), RIBEYE(B) domain; NBD, NAD(H) binding domain; SBD, substrate binding domain; RE(AB), full-length RIBEYE(AB); PRD, proline-rich domain of Munc119; YTH, yeast-two-hybrid; GST, glutathione *S*-transferase; MBP, maltose-binding protein.

SBD is not yet known as well as the precise physiological function of RIBEYE in the synapse.

To better understand the physiological role and molecular composition of synaptic ribbons, we performed a YTH screen using the RIBEYE (B) domain as a bait. In this screen, we identified Munc119 as a potential RIBEYE-interacting protein.

EXPERIMENTAL PROCEDURES

Plasmids—Details on all plasmids are deposited as supplemental materials.

Yeast Two-hybrid Methods—For YTH analyses, the Gal4-based Matchmaker yeast two-hybrid system (Clontech) was used according to the manufacturer's instructions. For the YTH screening, we used a bovine retinal YTH cDNA library from the retina (18). The cDNA of the respective bait proteins were cloned in-frame with the Gal4-DNA binding domain of pGBKT7. The cDNA of the indicated prey proteins were cloned in-frame with the Gal4 activation domain of pACT2 or pGADT7. The bait and prey plasmids confer tryptophan and leucine prototrophy to the respective auxotrophic yeast strains. Yeast strains Y187 and AH109 were used that contain distinct auxotrophic marker genes: AH109 [MATa, trp1-901, leu2-3, 112, ura3-52, his3-200, Gal4Δ, gal80Δ, LYS2::$GAL1_{UAS}$-$GAL1_{TATA}$-HIS3, $GAL2_{UAS}$-$GAL2_{TATA}$-ADE2, URA3::$MEL1_{UAS}$-$MEL1_{TATA}$-lacZ] (19); Y187 [MATα, ura3-52, his3-200, ade2-101, trp1-901, leu2-3,112, gal4Δ,. met, gal80Δ, URA3::$GAL1_{UAS}$-$GAL1_{TATA}$-lacZ] (20). Bait plasmids were electroporated into AH109 yeast, prey plasmids into Y187 yeast. Preparation of electrocompetent yeasts and electroporation of yeasts were done as described (21). For identifying transformants, yeasts were plated on the respective selective plates to identify the resulting convertants to the respective prototrophy (drop out media Clontech/QBiogene). For interaction analyses, AH109 yeasts containing the respective bait plasmid were mated with Y187 yeasts containing the respective prey plasmid. Mating was performed for 5 h at 30 °C in 1 ml of YPD medium with heavy vortexing. For assessing mating efficiency, half of the mated sample was streaked on −LW plates, the other half was plated on −ALWH selective plate with 10 mM aminotriazole (3-amino 1,2,4-triazole, ATZ) added. For the matings, pSE1111 and pSE1112 that encode irrelevant proteins (22) as well as the empty bait and prey vectors were used as negative controls. Expression of β-galactosidase (β-gal) marker gene activity was qualitatively analyzed by filter assays and quantitatively with liquid assays as described (23, 24).

Cell Culture—COS- and R28 retinal progenitor cells were cultured as previously described (12, 25, 26). COS cells were transiently transfected with the DEAE-dextran method (12) or with lipofection using the perfectin reagent (PEQLAB) according to the manufacturer's instructions.

GST Pull-down Assays from Transfected COS Cells—COS cells were transfected with the indicated eukaryotic expression constructs (empty GSTpEBG, Munc119(1–240)-GSTpEBG and RE(B)-EGFP, see supplemental materials). For the experimental assays, Munc119(1–240)-GSTpEBG was co-transfected with RE(B)-EGFP. Empty GSTpEBG co-transfected with RE(B)-EGFP served as control assays. 48 h after transfection, the cells were collected from the plates and pelleted at 6,000 rpm for 5 min at 4 °C. All subsequent steps were performed at 4 °C if not denoted otherwise. The cell pellets were washed with ice-cold phosphate-buffered saline and lysed with 500 μl of ice-cold lysis buffer (100 mM Tris-HCl, pH 7.9, 150 mM NaCl, 1 mM EDTA containing 1% Triton X-100) for 30 min. Subsequently, the samples were centrifuged at 13,000 rpm for 15 min. The lysate from experiment and control assay were incubated overnight with 10 μl of washed glutathione-Sepharose beads each (Amersham Biosciences). After incubation, the samples were centrifuged at 13,000 rpm for 1 min, and the supernatants removed. The pellets were washed with ice-cold phosphate-buffered saline three times. The final pellets were boiled in 25 μl of SDS sample buffer and subjected to 10% SDS-PAGE followed by Western blot analyses with the indicated antibodies.

Immunoprecipitation from R28 Retinal Progenitor Cells—All steps were performed at 4 °C if not denoted otherwise. Washed R28 cell pellets were lysed with lysis buffer (100 mM Tris-HCl, pH 7.9, 150 mM NaCl, 1 mM EDTA, 1% Triton X-100) for 45 min on ice. The lysate was centrifuged twice at 13,000 rpm (15 min, Eppendorf centrifuge (Biofuge Fresco, rotor 3329), and supernatants were subsequently precleared by the addition of 20 μl of washed protein A-Sepharose beads (Sigma) and 10 μl of RIBEYE preimmune serum for 1 h. Following centrifugation (13,000 rpm, 1 min), the precleared lysate was divided into two equal aliquots and incubated either with 10 μl of control IgG (U2656 preimmune serum) or with 10 μl of anti-RIBEYE (U2656 immune serum) for overnight at 4 °C. After overnight incubation, 20 μl of washed protein A-Sepharose beads were added to the samples, and incubation was continued for another 1 h. Subsequently, samples were centrifuged and washed five times with incubation buffer. The washed protein A-Sepharose pellets were boiled in 30 μl of SDS sample buffer and analyzed by Western blot analyses as described below.

Immunoprecipitation from the Bovine Retina—All steps were performed at 4 °C if not denoted otherwise. For each immunoprecipitation, a freshly isolated bovine retina was incubated with 2 ml of lysis buffer (100 mM Tris-HCl, pH 7.9, 150 mM NaCl, 1 mM EDTA) containing 1% Triton X-100 for 30 min at 4 °C. Then the sample was centrifuged at 13,000 rpm for 15 min. Samples were transferred to 2-ml syringes and forcefully ejected through 23-gauge needles to mechanically disrupt the retinal tissue. Mechanical crushing through 23-gauge needles was repeated 40–50 times. The mechanical disruption is essential to fractionate synaptic ribbons and to make them accessible for immunoprecipitation. Without mechanical treatment, no RIBEYE was observed in the respective tissue lysate. After mechanical disruption, lysis was allowed to proceed for further 30 min on ice. Samples were centrifuged twice at 13,000 rpm for 30 min. The supernatant was incubated with 10 μl of Munc119 preimmune serum and 20 μl of washed protein A-Sepharose beads for 1 h at 4 °C. Afterward, the sample was centrifuged at 13,000 rpm for 15 min, and the precleared lysate was divided into two aliquots and incubated either with 10 μl of Munc119 immune serum (Munc119 V2T2.120) or with Munc119 preimmune serum (control IgG) together with 20 μl of washed protein A-Sepharose beads (overnight). After overnight incubation, samples were centrifuged at

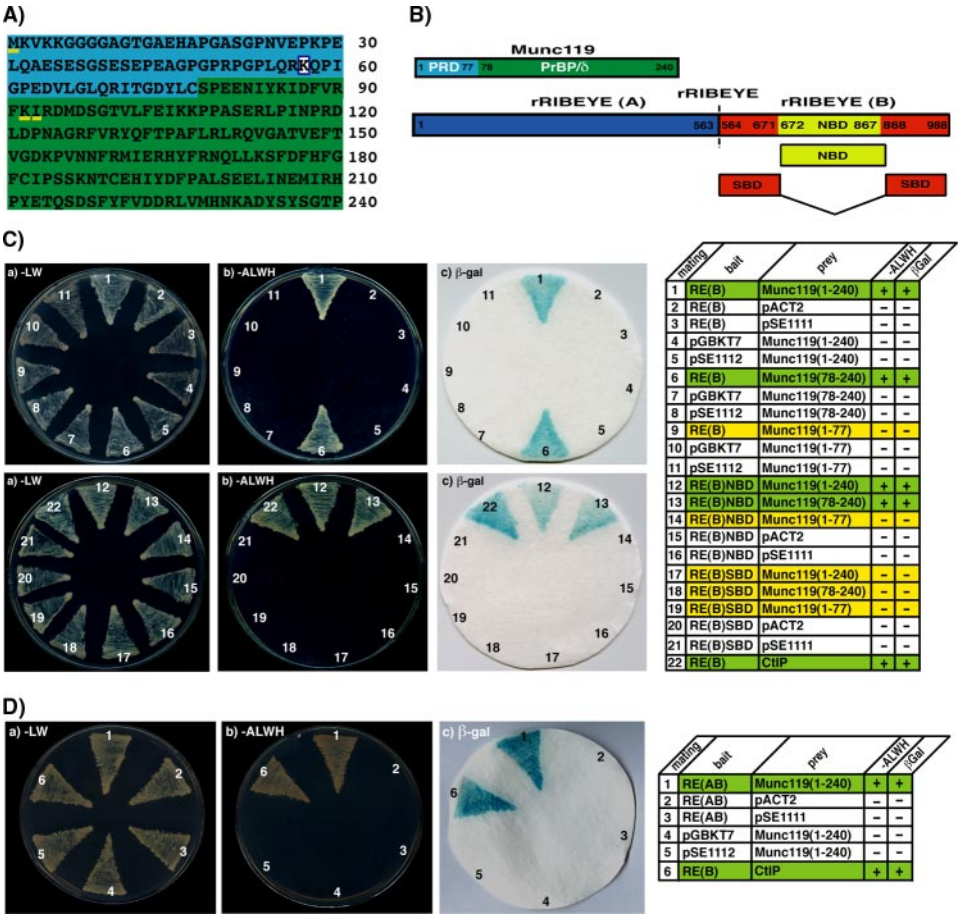

mating	bait	prey	-ALWH	βGal
1	RE(B)	Munc119(1-240)	+	+
2	RE(B)	pACT2	–	–
3	RE(B)	pSE1111	–	–
4	pGBKT7	Munc119(1-240)	–	–
5	pSE1112	Munc119(1-240)	–	–
6	RE(B)	Munc119(78-240)	+	+
7	pGBKT7	Munc119(78-240)	–	–
8	pSE1112	Munc119(78-240)	–	–
9	RE(B)	Munc119(1-77)	–	–
10	pGBKT7	Munc119(1-77)	–	–
11	pSE1112	Munc119(1-77)	–	–
12	RE(B)NBD	Munc119(1-240)	+	+
13	RE(B)NBD	Munc119(78-240)	+	+
14	RE(B)NBD	Munc119(1-77)	–	–
15	RE(B)NBD	pACT2	–	–
16	RE(B)NBD	pSE1111	–	–
17	RE(B)SBD	Munc119(1-240)	–	–
18	RE(B)SBD	Munc119(78-240)	–	–
19	RE(B)SBD	Munc119(1-77)	–	–
20	RE(B)SBD	pACT2	–	–
21	RE(B)SBD	pSE1111	–	–
22	RE(B)	CtIP	+	+

mating	bait	prey	-ALWH	βGal
1	RE(AB)	Munc119(1-240)	+	+
2	RE(AB)	pACT2	–	–
3	RE(AB)	pSE1111	–	–
4	pGBKT7	Munc119(1-240)	–	–
5	pSE1112	Munc119(1-240)	–	–
6	RE(B)	CtIP	+	+

FIGURE 1. **Interaction of RIBEYE(B) and RIBEYE(AB) with Munc119 in the YTH system.** *A*, amino acid sequence of bovine Munc119. The proline-rich domain (*PRD*, aa1–77) is colored in *blue*, the PrBP/δ-homology domain of Munc119 (aa78–240) colored in *green*. The *boxed lysine* indicates the site of a premature stop mutation that causes cone rod dystrophy in a human patient (5). The amino acids methionine 1 (*M1*), lysine 92 (*K92*), and isoleucine 93 (*I93*), which are underlined in *yellow* indicate the beginning of the reading frames of three independently obtained Munc119 YTH prey clones. The amino acid sequence of Munc119 obtained in our YTH screen is identical to the Munc119 sequence deposited at GenBank™ (accession BC103449.1). *B*, schematic domain structures of RIBEYE and Munc119. RIBEYE contains of a large N-terminal A-domain and a C-terminal B-domain. The B-domain of RIBEYE contains the NAD(H) binding subdomain (NBD, depicted in *yellow*) and the substrate binding subdomain (SBD, depicted in *red*). *C*, RIBEYE(B) interacts with the PrBP/δ-homology domain of Munc119 in YTH. Summary plates of YTH analyses obtained with the indicated bait and prey plasmids. For convenience, experimental bait-prey pairs are underlayered in color (*green* in the case of interacting bait-prey pairs; *yellow* in the case of non-interacting bait-prey-pairs; control matings are *non-colored*). *D*, RIBEYE(B) and also full-length RIBEYE (RIBEYE(AB) interact with Munc119. The interaction is mediated via the NBD of RIBEYE and the PrBP/δ homology domain of Munc119, Munc119(78–240) (*C*; matings 6,12–13). Mating 22 in *C* and mating 6 in *D* denote an unrelated positive control mating (CtIP). pSE1111 is an irrelevant prey vector, and pSE1112 an irrelevant bait vector (22).

3,000 rpm (2 min) to pellet the protein A-Sepharose beads. The pellet was washed three times with 1 ml of lysis buffer. The final pellet was boiled with SDS loading buffer and subjected to SDS-PAGE followed by Western blotting with the indicated antibodies.

Antibodies—The following antibodies were used in the present study: mouse monoclonal anti-GST (Sigma), mouse monoclonal anti-MBP (New England Biolabs), anti-RIBEYE(B) domain (U2656, 12), mouse monoclonal anti-CtBP2 (BD Biosciences), and polyclonal anti-EGFP (T3743; gift of Dr. Thomas C. Südhof, Dallas, TX). Full-length bovine Munc119-GST was used as an antigen to generate the immune serum Munc119 V2T2. For the experiments, immune serum at the 120th day after immunization was used. The antibody specifically detects Munc119 (supplemental Fig. S6). In extracts of R28 cells and bovine retina the Munc119 immune serum V2T2.120 specifically detected Munc119 at the expected running position at 35 kDa (Figs. 4 and 5 and supplemental Fig. S6).

Miscellaneous Methods—SDS-PAGE and Western blotting was performed as previously described (12). The fusion protein was expressed in BL21(DE3) as previously described (12, see also supplemental materials). Synaptic ribbons were purified as previously described (12, 27). Immunofluorescence microscopy was performed as previously described (28) using a Zeiss Axiovert 200M equipped with the respective filter sets.

RESULTS

Identification of Munc119 as a RIBEYE-interacting Protein—Using RIBEYE(B) as bait, we obtained three independent clones of Munc119 from the retinal YTH cDNA library as potential interaction partners of RIBEYE. One clone encoded full-length Munc119, the two other clones encoded truncated Munc119 proteins that started at lysine 92 (Lys-92) and isoleucine 93 (Ile-93), shortly after the beginning of the PrBP/δ-homology domain of Munc119 (Fig. 1*A*), suggesting that the PrBP/δ domain of Munc119 is probably responsible for the interaction. Using bait constructs that encoded for the PRD-(aa1–77)- or PrBP/δ-(aa78–240) domain of Munc119 we verified that the PrBP/δ-homology domain of Munc119 is indeed responsible for the interaction with RIBEYE (Fig. 1*C*). The PRD of Munc119 did not interact with RIBEYE in the YTH system. In the case of RIBEYE, the NADH binding subdomain of RIBEYE(B) domain (NBD) is mediating the interaction with Munc119. Munc119 also interacted with full-length RIBEYE indicating that the A-domain of RIBEYE is not inhibiting the interaction of the RIBEYE(B) domain with Munc119 (Fig. 1*D*). The interactions in the YTH were assayed by the growth of the respective mated yeast on −ALWH selective plates, indicating protein-protein interaction, as well as by qualitative and quantitative assessment of the β-galactosidase marker gene expression (Fig. 1, *C* and *D* and supplemental Fig. S1).

Munc119 Interacts with RIBEYE in GST Pull-down Assays—We used various independent approaches to verify the

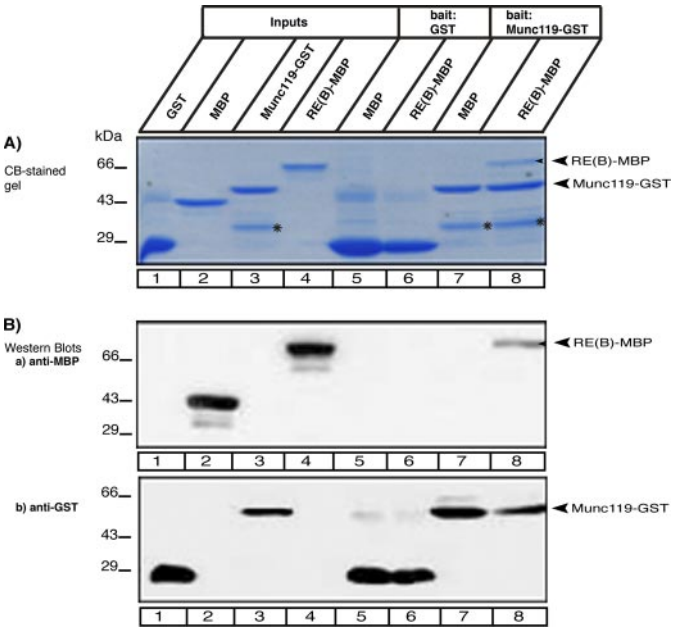

FIGURE 2. **RIBEYE(B) specifically interacts with Munc119 in fusion protein pull-down assays.** Pull-down analyses of RIBEYE(B)/Munc119 complexes using bacterially expressed fusion proteins. In *A*, pull-down experiments were analyzed by Coomassie Blue-stained polyacrylamide gel after SDS-PAGE. In *B*, by Western blot analyses with the indicated antibodies. *A* and *B*, *lanes 1–4* show the indicated purified fusion proteins (input fractions). All input lanes, except for *lane 4*, represent 50% of the input fraction. *Lane 4* represents 25% of the input fraction. In *lanes 5–8*, 100% was loaded. GST-tagged fusion proteins were used as immobilized bait proteins and MBP-tagged proteins as soluble prey proteins. Only Munc119-GST pulled-down RE(B)-MBP (*lane 8*) but not GST alone (*lane 6*). Neither GST alone nor Munc119-GST pulled-down MBP alone (*lanes 5* and *7*). The *asterisks* in *lanes 3*, *7*, and *8* of *A* label a break-down product of Munc119-GST. SDS-PAGE clearly demonstrated that Munc119-GST does not pull-down MBP alone (*A*). To further exclude that any MBP is nonspecifically pulled-down by Munc119-GST, we also analyzed the results of the pull-down assays by Western blotting with anti-MBP antibodies. *B*, Western blot analyses with anti-MBP antibodies (*B*) clearly show that only RE(B)-MBP (*lane 8*) but not MBP alone (*lane 7*) is pulled-down by Munc119-GST. GST alone does not pull-down RE(B)-MBP as well as MBP alone as shown by Western blotting with antibodies against MBP (*Ba*) demonstrating the specificity of the interaction and completely confirming the results in *A*. In *Bb*, the same blot as analyzed in *Ba* was reprobed (after stripping) with antibodies against GST to show equal loading of the bait proteins. Abbreviations: *CB*, Coomassie Blue.

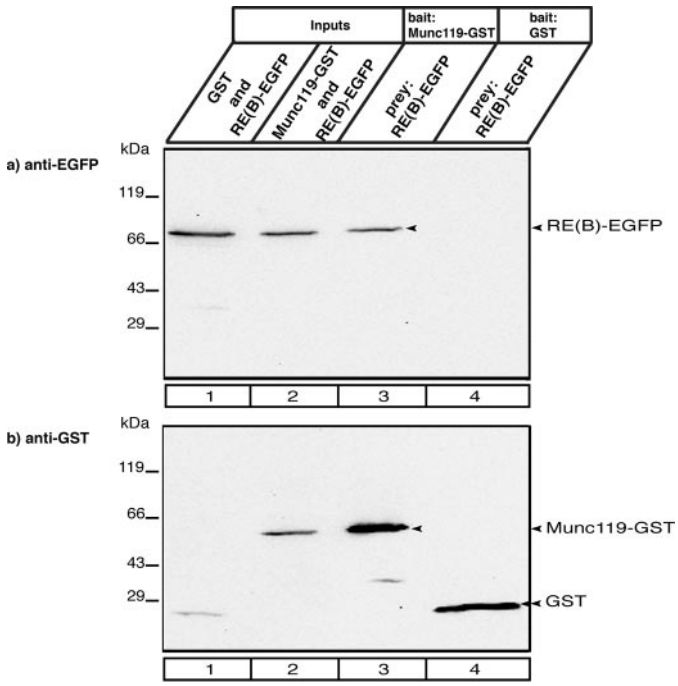

FIGURE 3. **RIBEYE interacts with Munc119 in transfected COS cells.** COS cells were co-transfected either with Munc119-GSTpEBG and RE(B)-EGFP (experimental assays) or with empty GSTpEBG and RE(B)-EGFP (control assays) using lipofection. Glutathione beads were added to the respective cell lysates. Proteins bound to the glutathione beads (*lanes 3* and *4*) were analyzed via Western blotting with antibodies against GST and EGFP. Munc119-GST pulled-down RIBEYE(B)-EGFP (*lane 3*) but not GST alone (*lane 4*) demonstrating the specific interaction between Munc119 and RIBEYE(B). *Lanes 1–2* show the respective input fractions (10% of total input); *Lanes 3* and *4* show 100% of the pulled-down proteins. In *b*, the same blot as shown in *a* was reprobed (after stripping) with antibodies against GST to show equal loading of the samples.

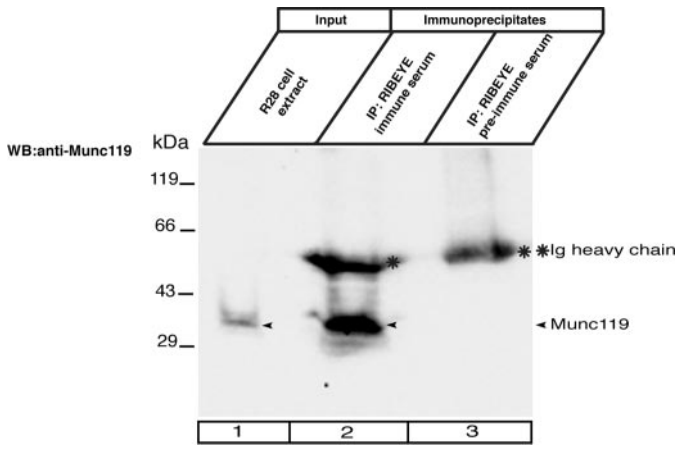

FIGURE 4. **Co-immunoprecipitation of RIBEYE and Munc119 from R28 retinal precursor cells.** R28 retinal progenitor cells endogenously express soluble Munc119 and RIBEYE, which can be readily solubilized from R28 cells by Triton X-100 lysis as described under "Experimental Procedures." Munc119 was co-immunoprecipitated by antibodies against RIBEYE from extracts of R28 retinal progenitor cells (*lane 2*). Immunoprecipitated Munc119 is indicated by an *arrowhead* in *lane 2*. The RIBEYE preimmune serum did not co-immunoprecipitate Munc119 (*lane 3*) demonstrating the specificity of the co-immunoprecipitation. *Lane 1* shows the input fraction (5% of total input); all of the protein A-beads with the immunoprecipitated proteins (100%) were loaded on the gel (*lanes 2* and *3*). *Asterisks* indicate the immunoglobulin heavy chains.

Munc119-RIBEYE(B) interaction. First, we performed pull-down experiments using bacterially expressed and purified fusion protein (Fig. 2). We used GST-tagged proteins (Munc119-GST and GST) as immobilized bait proteins and MBP-tagged proteins (RIBEYE(B)-MBP and MBP) as soluble prey proteins. Munc119-GST (but not GST alone) interacted with RIBEYE(B)-MBP (but not MBP alone) as judged by protein pull-down analyses (Fig. 2). Specificity of interaction in these fusion protein pull-downs was consistently shown by SDS-PAGE and Western blot analyses (Fig. 2, *A* and *B*). Next, we analyzed whether RIBEYE(B) interacts with Munc119 in transfected COS cells. For this purpose, COS cells were co-transfected with eukaryotic expression plasmids that encoded for RIBEYE(B)-EGFP and GST-tagged Munc119 or GST alone (as control protein). Munc119-GST (but not GST alone) pulled-down RIBEYE(B)-EGFP from a crude cell extract of transfected COS cells (Fig. 3), further demonstrating a specific interaction between the RIBEYE(B) domain and Munc119.

Immunoprecipitation of Endogenous Munc119 and RIBEYE from R28 Retinal Progenitor Cells and Bovine Retina—R28 is an E1A-immortalized retinal precursor cells line (25). These cells are

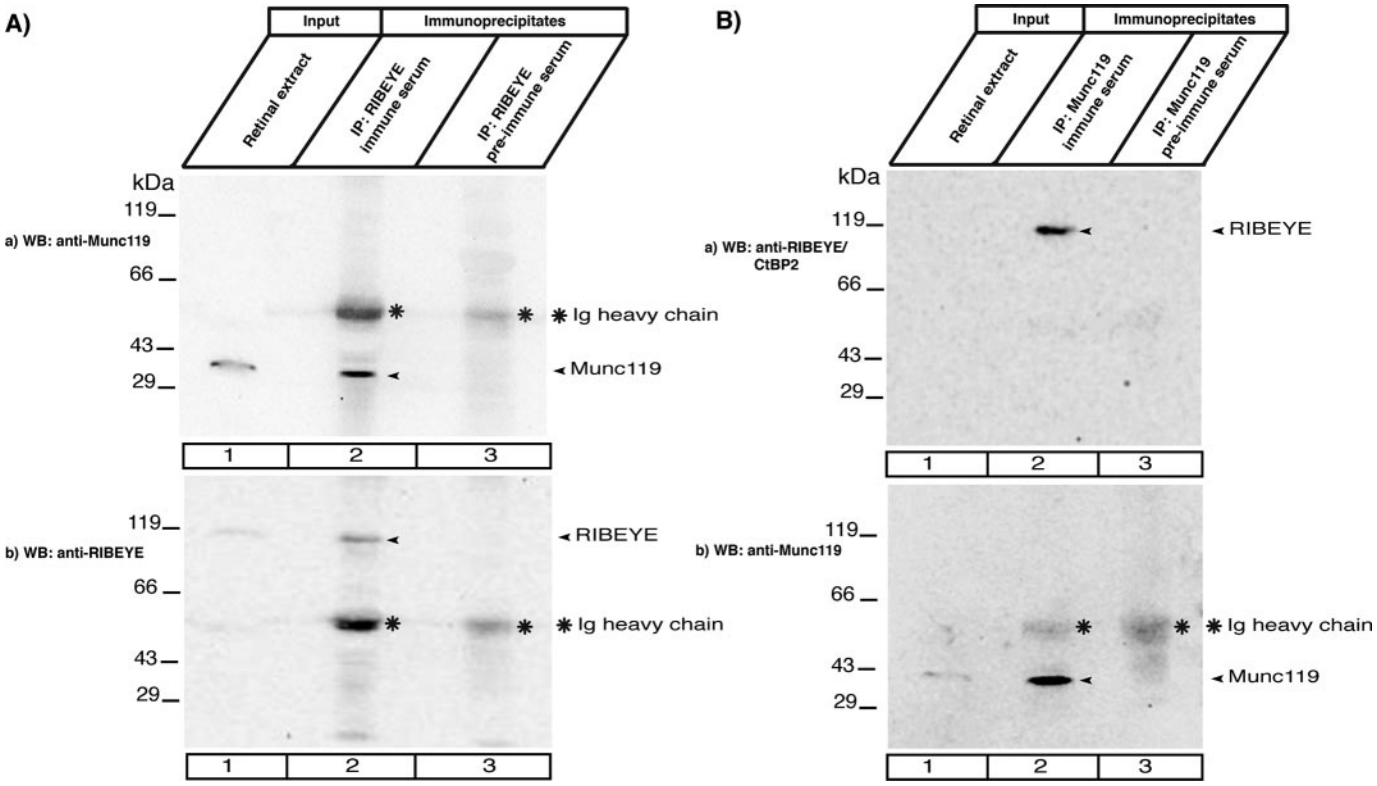

FIGURE 5. **Co-immunoprecipitation of RIBEYE and Munc119 from the bovine retina.** Co-immunoprecipitation of RIBEYE and Munc119 from bovine retina. In *A*, RIBEYE immune serum and RIBEYE preimmune serum were tested for their capability to co-immunoprecipitate Munc119. Munc119 is co-immunoprecipitated by RIBEYE immune serum (*lane 2*, *Aa*) but not by RIBEYE preimmune serum (*lane 3*, *A*). *Ab*, shows the same blot as in *Aa* but reprobed with anti-RIBEYE antibodies. This blot shows the presence of RIBEYE precipitated by the immune serum (*lane 2*) but not by the preimmune serum (*lane 3*). *Asterisks* indicate the immunoglobulin heavy chains. *Lane 1* shows the input fraction (2% of total input). The loaded 2% input fraction corresponds roughly to 200 μg of total proteins (in a volume of $\approx$20 μl). Considerably more input fraction could not be loaded on the gel for volume reasons and also not to overload the gel. Furthermore, synaptic ribbons are mechanically stable, Triton X-100-insoluble structures, which can only be extracted to a certain extent from the bovine retina by the combination of mechanical and chemical lysis. Therefore, the RIBEYE immunosignal is weak in the input fractions. RIBEYE is highly enriched in the experimental immunoprecipitates (*lane 2*) but absent in the control immunoprecipitates (*lane 3*). *Asterisks* indicate the immunoglobulin heavy chains. 100% of the protein A-beads containing the immunoprecipitated proteins were loaded on the gel for experimental and control immunoprecipitations (*lanes 2* and *3*). In *B*, Munc119 immune serum and Munc119 preimmune serum were tested for their capability to co-immunoprecipitate RIBEYE. RIBEYE is co-immunoprecipitated by Munc119 immune serum (*lane 2*, *Ba*) but not by Munc119 preimmune serum (*lane 3*, *Ba*). *Bb* shows the same blot as in *Ba* but reprobed with anti-Munc119. This blot shows the presence of Munc119 immunoprecipitated by the immune serum but not by the preimmune serume. *Asterisks* indicate the immunoglobulin heavy chains.

immature, non-fully differentiated cells that express both neuronal and glial cell markers (26). R28 cells endogenously express Munc119 (Ref. 26, Fig. 4, and supplemental Fig. S6) and RIBEYE in a Triton X-100 soluble fraction (supplemental Fig. S6 and data not shown). Therefore, we used R28 cells for immunoprecipitation experiments and tested whether RIBEYE immune serum could co-immunoprecipitate Munc119 from R28 cell extracts. RIBEYE preimmune serum served as control serum. Indeed, RIBEYE immune serum co-immunoprecipitated endogenous Munc119 whereas RIBEYE preimmune serum did not (Fig. 4).

Next, we prepared extracts from bovine retina as described under "Experimental Procedures" and tested whether antibodies against RIBEYE could co-immunoprecipitate Munc119. RIBEYE immune serum (but not RIBEYE preimmune serum) co-immunoprecipitated Munc119 together with RIBEYE showing a specific interaction of these proteins also in the retina. Similarly, Munc119 immune serum (but not Munc119 preimmune serum) co-immunoprecipitated RIBEYE together with Munc119 (Fig. 5). Because RIBEYE is exclusively present at synaptic ribbons in the mature retina (12) the co-immunoprecipitation experiments suggest that Munc119 may be a component of synaptic ribbons.

Binding of Munc119 to RIBEYE(B) Is Independent of NADH Binding to RIBEYE—Previous YTH analyses demonstrated that the NAD(H) binding subdomain (NBD) of RIBEYE(B) is mediating the interaction with Munc119. Therefore, we generated point mutants of the NBD and analyzed these point mutants of the NBD for their capability to interact with Munc119 in the YTH system to further map the interaction site of Munc119 on RIBEYE(B) domain. RIBEYE(B)G730 is an essential component of the NAD(H) binding motif, and the RIBEYE(B) point mutant RIBEYE(B)G730A does not bind significant levels of NAD(H) (12).[4] In contrast to the NAD(H) binding deficiency, RIBEYE(B)G730A still interacted with Munc119 in YTH analyses indicating that NAD(H) binding is not important for binding of Munc119 to RIBEYE(B) domain (Fig. 6). Similarly, the binding of Munc119 to RIBEYE(B) analyzed by biochemical pull-down analyses was not changed by the addition of either NAD^+ or NADH. Increasing concentrations of both NAD^+ or NADH did not significantly influence the binding of Munc119 to RIBEYE(B) (supplemental Fig. S2).

[4] K. Schwarz and F. Schmitz, unpublished data.

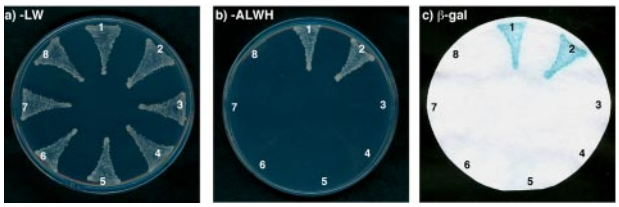

mating	bait	prey	-ALWH	βGal
1	RE(B)	Munc119(1-240)	+	+
2	RE(B)G730A	Munc119(1-240)	+	+
3	pGBKT7	Munc119(1-240)	–	–
4	pSE1112	Munc119(1-240)	–	–
5	RE(B)	pACT2	–	–
6	RE(B)	pSE1111	–	–
7	RE(B)G730A	pACT2	–	–
8	RE(B)G730A	pSE1111	–	–

FIGURE 6. **Binding of Munc119 to RIBEYE(B) is independent of NADH binding.** Summary plates of YTH analyses obtained with the indicated bait and prey plasmids. For convenience, experimental bait-prey pairs are underlayered in color (*green* in the case of interacting bait-prey pairs; control matings are *non-colored*). The NADH binding deficient RIBEYE point mutant RE(B)G730A (mating 2) interacts with Munc119 in YTH indicating that NADH binding to RIBEYE is not essential for the binding of Munc119.

We generated further point mutants located on the NAD(H) binding domain of RIBEYE, namely RE(B)D758N, RE(B)E844Q, RE(B)F848W, RE(B)K854Q, RE(B)I796A, RE(B)D820N, and RE(B)E790Q, to further map the docking site of Munc119 on the NBD of RIBEYE(B). All of these latter point mutants still interact with Munc119 except for RE(B)E844Q pointing that this amino acid is crucial for the interaction with Munc119 (supplemental Fig. S3). Glutamate E844 is located close to the NADH binding cleft of RIBEYE (12, 16, 17). As judged by NADH-dependent FRET experiments performed as described (29), this mutant still binds NADH (supplemental Fig. S4). Based on these data, the Munc119 binding region of RIBEYE appears to be topographically close to the NADH binding cleft of RIBEYE(B).

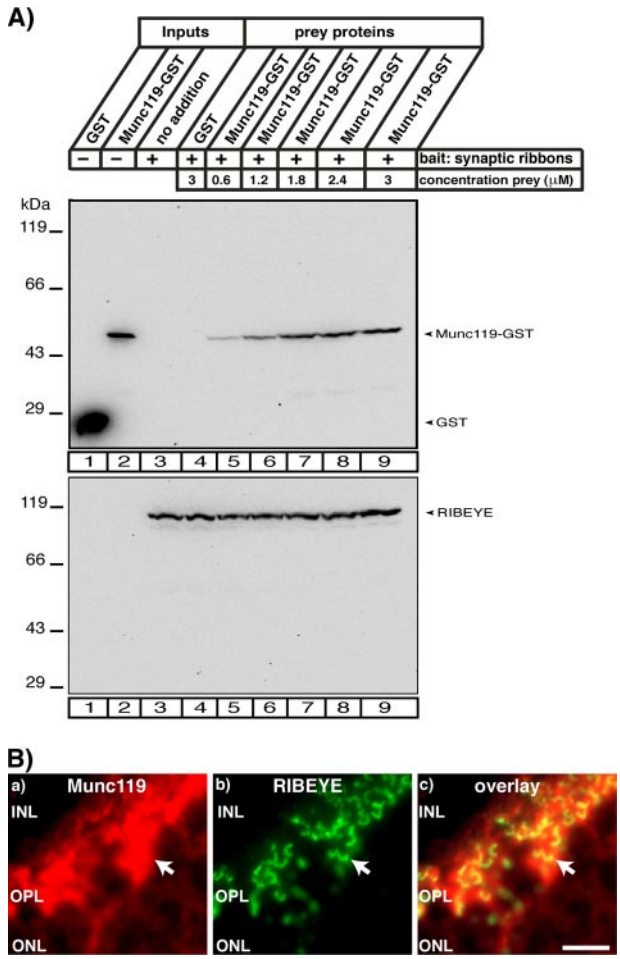

FIGURE 7. **Purified synaptic ribbons specifically recruit Munc119.** *A*, binding of Munc119 fusion protein to synaptic ribbons. 20 μg of purified synaptic ribbons were tested for their capability to bind soluble Munc119 fusion protein at the indicated concentrations. GST alone was used as control protein. Purified ribbons specifically bound Munc119-GST but not GST (*A*). For GST (*lane 1*) and Munc119-GST (*lane 2*) 10% were loaded as input; for the synaptic ribbon (*lane 3*) 100% were loaded as input. The two depicted blots show representative examples of four different experiments, which all showed the same result. The lower blot is stripped and reprobed with antibodies against RIBEYE to show equal loading of ribbons. A quantitative analysis of binding of Munc119 to synaptic ribbons is given in supplemental Fig. S5. *B*, Munc119 co-localizes with synaptic ribbons. Immunolabeling of the outer plexiform layer of the bovine retina that contain photoreceptor ribbon synapses with polyclonal antibodies against Munc119 and monoclonal antibodies against RIBEYE(B)/CtBP2. Strong immunosignals of Munc119 were found at synaptic ribbons and in close vicinity to synaptic ribbons. Abbreviations: *ONL*, outer nuclear layer; *OPL*, outer plexiform layer; *INL*, inner nuclear layer. *Scale bar*: 10 μm.

Munc119 Is Specifically Recruited to Purified Synaptic Ribbons—The co-immunoprecipitation experiments from bovine retina suggested the presence of Munc119 on synaptic ribbons (Fig. 5). Immunolabeling data clearly showed the presence of Munc119 in the presynaptic terminals at ribbon sites and also at sites close to the synaptic ribbon (Fig. 7*B*). Interestingly, purified synaptic ribbons isolated from bovine retina specifically recruited externally added soluble Munc119-GST fusion protein to synaptic ribbons (Fig. 7*A*). The binding of Munc119 to synaptic ribbons was specific because the control protein GST alone did not bind to synaptic ribbons. Because Munc119 is virtually absent from purified synaptic ribbons (Fig. 7*A*, *lane 3*), Munc119 appears to be a synaptic ribbon-associated component that can relatively easily dissociate from synaptic ribbons (see "Discussion").

The sequence of bovine Munc119 obtained in the present study by YTH screening with RIBEYE(B) as bait protein is identical to the bovine Munc119 sequence previously deposited at GenBank™ (Accession Number BC103449.1).

DISCUSSION

Munc119, a mammalian ortholog of the *C. elegans* protein unc119, is essential for synaptic transmission at the ribbon synapse and for vision (2). In the present study, we demonstrated that Munc119 interacts with the synaptic ribbon protein RIBEYE. The interaction between RIBEYE and Munc119 was consistently shown by five different independent methods, including YTH analyses, fusion protein pull-downs, interaction analyses in transfected COS cells, and immunoprecipitations from R28 retinal precursor cells and from bovine retina. The NADH binding subdomain of RIBEYE was shown to be responsible for the interaction with Munc119. Based on the analyses of RIBEYE(B) point mutants, the binding site of Munc119 appears to be close to the NADH binding site of RIBEYE; but the binding of Munc119 is independent upon NADH binding. In support of this view, RIBEYE(B)G730A that does not bind NADH still interacted with Munc119. Conversely, RIBEYE(B)E844Q that did not interact with Munc119 still bound NADH. Interestingly, the PrBP/δ-homology domain of Munc119 whose

deletion caused the dramatic defects in vision and synaptic transmission in the respective patients and transgenic mouse model (5) was shown to be responsible for binding to RIBEYE. Therefore, the interaction with RIBEYE could mediate the essential physiological function of Munc119 in synaptic transmission at the photoreceptor ribbon synapse.

Although the physiological importance of Munc119 for synaptic transmission at the photoreceptor ribbon synapse has been well documented it is not yet clear how Munc119 works at the molecular level in the synapse. A key in the understanding of the function of Munc119 is probably its high homology to PrBP/δ. PrBP/δ binds and dissociates prenylated proteins from membranes (6, 30). This enzymatic activity is important for intracellular membrane and protein trafficking (6, 30). In photoreceptors, the trafficking role of PrBP/δ predominantly occurs in the inner and outer segments. We propose that Munc119 fulfills similar functions in the photoreceptor ribbon terminals. Such a trafficking role would be particularly important for the tonically active ribbon synapses, which are characterized by intensive membrane and protein trafficking. The idea that Munc119 supports similar processes as PrBP/δ but at different subcellular locations is further supported by the finding that PrBP/δ and Munc119 share common interaction partners (Arl2/3; 31, 32, 33). Additionally, Munc119 could activate Src-type signaling kinases in the photoreceptor synapse as recently observed for Munc119 in certain cells of the immune system (34, 35). A recent study demonstrated that Munc119 binds to CaBP4 (36) and thus, RIBEYE-Munc119 complexes might also be involved in the regulation of intracellular Ca^{2+} levels in the presynaptic ribbon terminal.

We have shown that purified ribbons could specifically recruit Munc119. Purified synaptic ribbons, which go through stringent washing steps (12, 27), contain little if any Munc119. In conclusion, Munc119 is most likely a peripherally associated component of synaptic ribbons that can relatively easy dissociate from them. In support of this suggestion, a large portion of Munc119 is soluble (Ref. 2 and data not shown). Large amounts of Munc119 are present in the presynaptic terminals in close vicinity to synaptic ribbons as judged by immunolabeling. Munc119 in presynaptic photoreceptor terminals could be recruited to synaptic ribbons. The factors that regulate the association/dissociation of Munc119 with synaptic ribbons *in vivo* remain to be elucidated by future analyses.

The synaptic defects observed in Munc119 transgenic mice and Munc119-deficient patients stress the role of Munc119 for vision and synaptic processing in the visual system. The fact that the PrBP/δ homology domain is crucial for Munc119 function particularly emphasizes the physiological importance of the RIBEYE-Munc119 interaction for synaptic transmission at the photoreceptor ribbon synapse.

Acknowledgment—We thank Conny Franke for excellent technical assistance.

REFERENCES

1. Higashide, T., Murakami, A., McLaren, M. J., and Inana, G. (1996) *J. Biol. Chem.* **271,** 1797–1804
2. Higashide, T., McLaren, M. J., and Inana, G. (1998) *Invest. Ophthalmol. Vis. Sci.* **39,** 690–698
3. Swanson, D. A., Chang, J. T., Campochiara, P. A., Zack, D. J., and Valle, D. (1998) *Investig. Ophthalmol. Vis. Sci.* **39,** 2085–2094
4. Li, L., Florio, S. K., Pettenati, M. J., Rao, N., Beavo, J. A., and Baehr, W. (1998) *Genomics* **49,** 76–82
5. Kobayashi, A., Higashide, T., Hamasaki, D., Kubota, S., Sakuma, H., An, W., Fujimaki, T., McLaren, M. J., Weleber, R. G., and Inana, G. (2000) *Investig. Ophthalmol. Vis. Sci.* **11,** 3268–3277
6. Zhang, H., Liu, X.-H., Zhang, K., Chen, C.-K., Frederick, J. M., Prestwich, G. D., and Baehr, W. (2004) *J. Biol. Chem.* **279,** 407–413
7. Kubota, S., Kobayashi, A., Mori, N., Higashide, T., McLaren, M. J., and Inana, G. (2002) *Investig. Ophthalmol. Vis. Sci.* **43,** 308–313
8. Mori, N., Ishiba, Y., Kubota, S., Kobayashi, A., Higashide, T., McLaren, M. J., and Inana, G. (2006) *Investig. Ophthalmol. Vis. Sci.* **47,** 1281–1292
9. Sterling, P., and Matthews, G. (2005) *Trends Neurosci.* **28,** 20–29
10. Heidelberger, R., Thoreson, W. B., and Witkovsky, P. (2005) *Prog. Ret. Eye Res.* **24,** 682–720
11. tom Dieck, S., and Brandstätter, J. H. (2006) *Cell Tiss. Res.* **326,** 339–346
12. Schmitz, F., Königstorfer, A., and Südhof, T. C. (2000) *Neuron* **28,** 857–872
13. Zenisek, D., Horst, N. K., Merrifield, C., Sterling, P., and Matthews, G. (2004) *J. Neurosci.* **24,** 9752–9759
14. Wan, L., Almers, W., and Chen, W. (2005) *J. Neurosci.* **25,** 941–949
15. Chinnadurai, G. (2002) *Mol. Cell* **9,** 213–224
16. Kumar, V., Carlson, J. E., Ohgi, K. A., Edwards, T. A., Rose, D. W., Escalante, C. R., Rosenfeld, M. G., and Aggarwal, A. K. (2002) *Mol. Cell* **10,** 857–869
17. Nardini, M., Spano, S., Cericola, C., Pesce, A., Massaro, A., Millo, E., Luini, A., Corda, D., and Bolognesi, M. (2003) *EMBO J.* **22,** 3122–3130
18. Tai, A. W., Chuang, J. Z., Wolfrum, U., and Sung C. H. (1999) *Cell* **97,** 877–887
19. James, P., Halladay, J., and Craig, E. A. (1996) *Genetics* **144,** 1425–1436
20. Harper, J. W., Adami, G. R., Wei, N., Keyomarsi, K., and Elledge, S. J. (1993) *Cell* **75,** 805–816
21. Helmuth, M., Altrock, W., Böckers, T. M., Gundelfinger, E. D., and Kreutz, M. R. (2001) *Anal. Biochem.* **293,** 149–152
22. Bai, C., and Elledge, S. J. (1996) *Methods Enzymol.* **273,** 331–347
23. Wang, Y., Okamoto, M., Schmitz, F., Hofmann, K., and Südhof, T. C. (1997) *Nature* **388,** 593–598
24. Stahl, B., Diehlmann, A., and Südhof, T. C. (1999) *J. Biol. Chem.* **14,** 9141–9148
25. Seigel, G. M. (1996) *Dev. Biol. Anim.* **32,** 66–68
26. Seigel, G. M., Sun, W., Wang, J., Hershberger, D. H., Campbell, L. M., and Salvi, R. J. (2004) *Curr. Eye Res.* **28,** 257–269
27. Schmitz, F., Bechmann, M., and Drenckhahn, D. (1996) *J. Neurosci.* **16,** 7109–7116
28. Schmitz, F., Tabares, L., Khimich, D., Strenzke, N., DeLa Villa-Polo, P., Castellano-Munoz, M., Bulankina, A., Moser, T., Fernandez-Chacon, R., and Südhof, T. C. (2006) *Proc. Natl. Acad. Sci. U. S. A.* **103,** 2925–2931
29. Fjeld, C. C., Birdsong, W. T., and Goodman, R. H. (2003) *Proc. Natl. Acad. Sci. U. S. A.* **100,** 9202–9207
30. Zhang, H., Li, A., Doan, T., Rieke, F., Detwiler, P. B., Frederick, J. M., and Baehr, W. (2007) *Proc. Natl. Acad. Sci. U. S. A.* **104,** 8857–8862
31. van Valkenburgh, H., Shern, J. F., Sharer, J. D., Zhu, X., and Kahn, R. A. (2001) *J. Biol. Chem.* **276,** 22826–22837
32. Hanzal-Bayer, M., Renault, R., Roversi, P., Wittinghofer, A., and Hillig, R. C. (2002) *EMBO J.* **21,** 2095–2106
33. Kobayashi, A., Kubota, S., Mori, N., McLaren, M. J., and Inana, G. (2003) *FEBS Lett.* **534,** 26–32
34. Cen, O., Gorska, M. M., Stafford, S. J., Sur, S., and Alam, R. (2003) *J. Biol. Chem.* **278,** 8837–8845
35. Gorska, M. M., Stafford, S. J., Cen, O., Sur, S., and Alam, R. (2004) *J. Exp. Med.* **199,** 369–379
36. Haeseleer, F. (2008) *Investig. Ophthalmol. Vis. Sci.* **49,** 2366–2375

Cellular/Molecular

Multiple RIBEYE–RIBEYE Interactions Create a Dynamic Scaffold for the Formation of Synaptic Ribbons

Venkat Giri Magupalli,[1] Karin Schwarz,[1] Kannan Alpadi,[1] Sivaraman Natarajan,[1] Gail M. Seigel,[2] and Frank Schmitz[1]

[1]Department of Neuroanatomy, Institute for Anatomy and Cell Biology, Saarland University, Medical School Homburg/Saar, 66421 Homburg/Saar, Germany, and [2]Department of Ophthalmology, Physiology and Biophysics, State University of New York at Buffalo, Buffalo, New York 14214

Synaptic ribbons are large, dynamic structures in the active zone complex of ribbon synapses and important for the physiological properties of these tonically active synapses. RIBEYE is a unique and major protein component of synaptic ribbons. The aim of the present study was to understand how the synaptic ribbon is built and how the construction of the ribbon could contribute to its ultrastructural plasticity. In the present study, we demonstrate that RIBEYE self-associates using different independent approaches (yeast two-hybrid analyses, protein pull downs, synaptic ribbon–RIBEYE interaction assays, coaggregation experiments, transmission electron microscopy and immunogold electron microscopy). The A-domain [RIBEYE(A)] and B-domain [RIBEYE(B)] of RIBEYE contain five distinct sites for RIBEYE–RIBEYE interactions. Three interaction sites are present in the A-domain of RIBEYE and mediate RIBEYE(A)–RIBEYE(A) homodimerization and heterodimerization with the B-domain. The docking site for RIBEYE(A) on RIBEYE(B) is topographically and functionally different from the RIBEYE(B) homodimerization interface and is negatively regulated by nicotinamide adenine dinucleotide. The identified multiple RIBEYE–RIBEYE interactions have the potential to build the synaptic ribbon: heterologously expressed RIBEYE forms large electron-dense aggregates that are in part physically associated with surrounding vesicles and membrane compartments. These structures resemble spherical synaptic ribbons. These ribbon-like structures coassemble with the active zone protein bassoon, an interaction partner of RIBEYE at the active zone of ribbon synapses, emphasizing the physiological relevance of these RIBEYE-containing aggregates. Based on the identified multiple RIBEYE–RIBEYE interactions, we provide a molecular mechanism for the dynamic assembly of synaptic ribbons from individual RIBEYE subunits.

Key words: **synaptic ribbon; ribbon synapse; RIBEYE; retina; active zones; exocytosis**

Introduction

Ribbon synapses are specialized chemical synapses, e.g., in the retina and inner ear, capable to maintain rapid exocytosis of synaptic vesicles for prolonged periods of time (for review, see Fuchs, 2005; Heidelberger et al., 2005; Prescott and Zenisek, 2005; Sterling and Matthews, 2005; Nouvian et al., 2006; Singer, 2007). For this purpose, ribbon synapses are equipped with presynaptic specializations, the synaptic ribbons, which are considered to speed vesicle trafficking (for review, see tom Dieck and Brandstätter, 2006; Nouvian et al., 2006; Sterling and Matthews, 2005). Synaptic ribbons are large presynaptic structures associated with the active zone complex of ribbon synapses (for review, see Wagner, 1997). Synaptic ribbons of photoreceptor synapses are plate-like structures in three-dimensional representations that can be >500 nm in length and depth. In EM sections, retinal synaptic ribbons usually appear bar-shaped, and inner ear synaptic ribbons are usually spherical structures (for review, see Nouvian et al., 2006). Also in the retina, the assembly of the bar-shaped ribbon is believed to go through spherical ribbon intermediates, the so called synaptic spheres (for review, see Vollrath and Spiwoks-Becker, 1996; Spiwoks-Becker et al., 2004). The dimensions of synaptic ribbons in the retina can vary and are subject to changes, e.g., in response to different stimuli (lighting conditions/circadian rhythm), probably reflecting structural adaptations to different degrees of synaptic activity (for review, see Vollrath and Spiwoks-Becker, 1996; Wagner, 1997). Regardless of their shape, synaptic ribbons are associated with large amounts of synaptic vesicles and other membrane compartments (for review, see Sterling and Matthews, 2005).

We have previously identified a novel protein,"RIBEYE," as a unique and specific component of synaptic ribbons (Schmitz et al., 2000). RIBEYE is present in synaptic ribbons of all vertebrate ribbon synapses (Schmitz et al., 2000, 2006; Zenisek et al., 2004; Khimich et al., 2005; tom Dieck et al., 2005; Wan et al., 2005) (for review, see tom Dieck and Brandstätter, 2006). RIBEYE consists of a unique A-domain [RIBEYE(A)] and B-domain [RIBEYE(B)] that is identical to CtBP2 except for the first 20 aa (Schmitz et al., 2000). The B-domain of RIBEYE binds nicotinamide adenine dinucleotide (NAD^+ or NADH [NAD(H)]) with high affinity

Received Jan. 29, 2008; revised June 21, 2008; accepted June 21, 2008.

This work was supported by Deutsche Forschungsgemeinschaft Grant SFB530 TP C11 and HOMFOR (F.S.), and by Research to Prevent Blindness and National Institutes of Health Infrastructure Grant R24EY016662 (G.M.S.). We thank Drs. M. J. Schmitt and L. Köblitz (Saarland University) for the donation of plasmids and yeast strains; Dr. Susanne tom Dieck (Max Planck Institute for Brain Research Frankfurt) for the gift of anti-rat RIBEYE(A) antibody; Dr. H. T. McMahon (Medical Research Council, Cambridge, UK) for the donation of JC201 bacteria; and Dr. Jutta Schmitz-Kraemer for critically reading this manuscript.

Correspondence should be addressed to Dr. Frank Schmitz, Department of Neuroanatomy, Institute for Anatomy and Cell Biology, Saarland University, Medical School Homburg/Saar, Kirrbergerstrasse, Building 61, 66421 Homburg/Saar, Germany. E-mail: frank.schmitz@uniklinik-saarland.de.

DOI:10.1523/JNEUROSCI.1964-08.2008

 0270-6474/08/287954-14$15.00/0

and belongs to a family of D-isomer-specific 2-hydroxy acid dehydrogenases (Schmitz et al., 2000). The structural analysis of these proteins, e.g., of CtBP1, revealed the presence of two globular subdomains, namely an NAD(H)-binding subdomain (NBD) and the substrate-binding subdomain (SBD) (for a review, see Chinnadurai, 2002; Kumar et al., 2002; Nardini et al., 2003).

Previous data indicated that RIBEYE is the major component of synaptic ribbons (Schmitz et al., 2000; Zenisek et al., 2004; Wan et al., 2005). In the present study, we analyzed functional properties of RIBEYE and demonstrate that RIBEYE is capable to interact with itself. RIBEYE–RIBEYE interactions are mediated through three binding sites in the A-domain and two binding sites in the B-domain enabling multiple RIBEYE–RIBEYE interactions. RIBEYE–RIBEYE interactions can generate the three-dimensional scaffold of the synaptic ribbon and provide a molecular mechanism for the ultrastructural plasticity of these presynaptic structures.

Materials and Methods

Plasmids. Details on all plasmids and antibodies used in this study are posted in the supplemental Methods (available at www.jneurosci.org as supplemental material).

Yeast two-hybrid methods. We used the galactosidase-4 (Gal4)-based Matchmaker Yeast Two-Hybrid System (Clontech) according to the manufacturer's instructions. The cDNA of the respective bait proteins were cloned in frame with the Gal4-DNA-binding domain of pGBKT7. The cDNA of the indicated prey proteins were cloned in frame with the Gal4-activation domain of pACT2 or pGADT7. The bait and prey plasmids confer tryptophan and leucine prototrophy to the respective auxotrophic yeast strains. Yeast strains Y187 and AH109 were used that contain distinct auxotrophic marker genes: AH109 contained *MATa*, *trp1–901*, *leu2-3,112*, *ura3-52*, *his3-200*, *gal4*Δ, *gal80*Δ, *LYS2::GAL1*$_{UAS}$*-GAL1*$_{TATA}$*-HIS3*, *GAL2*$_{UAS}$*-GAL2*$_{TATA}$*-ADE2*, and *URA3::MEL1*$_{UAS}$*-MEL1*$_{TATA}$*-lacZ* (James et al., 1996); Y187 contained *MATα*, *ura3-52*, *his3-200*, *ade2-101*, *trp1-901*,*leu2-3,112*, *gal4*Δ, *met*, *gal80*Δ, and *URA3::GAL1*$_{UAS}$*-GAL1*$_{TATA}$*-lacZ* (Harper et al., 1993). Bait plasmids were always electroporated into AH109 yeast, whereas all prey plasmids were transformed into Y187. Preparation of electrocompetent yeasts and electroporation of yeasts were done as described previously (Helmuth et al., 2001). For identifying transformants, yeasts were plated on the respective selective plates to identify the resulting convertants to the respective prototrophy (drop out media Clontech/QBiogene). For interaction analyses, AH109 yeasts containing the respective bait plasmid were mated with Y187 yeasts containing the respective prey plasmid. Mating was performed for 5 h at 30°C in 1 ml of YPD medium (yeast extract, peptone, and dextrose) with heavy vortexing. For assessing mating efficiency, half of the mated sample was streaked on −LW plates [containing synthetic complete yeast medium without leucine (L) and without tryptophan (W)], and the other half was plated on −ALWH selective plate [containing synthetic complete yeast medium without adenine (A), L, W, and histidine (H)] with 10 mM 3-amino-1,2,4-triazole added. For the matings, pSE1111 and pSE1112 (Bai and Elledge, 1996) as well as the empty bait and prey vectors were used as negative controls. Expression of β-galactosidase (β-gal) marker gene expression were qualitatively analyzed by filter assays and quantitatively with liquid assays as described previously (Wang et al., 1997; Stahl et al., 1999).

Expression of RIBEYE(A)-domain. RIBEYE(A)-glutathione *S*-transferase (GST) is difficult to express in conventional prokaryotic expression systems because of its high contents of proline, serine, glycine, and arginine residues (Schmitz et al., 2000) (our unpublished observations). We identified two expression systems to express full-length RIBEYE(A)-GST fusion protein. One source were LPAAT (lysophosphatidic acid acyltransferase)-deficient JC201 bacteria (Coleman, 1990), which express full-length RIBEYE(A)-GST fusion protein although part of it is processed to smaller fragments (see Figs. 1*B*, 4*B*, 6*A*,*B*, 10*B*; supplemental Fig. 1*B*, available at www.jneurosci.org as supplemental material). The second source were methylotropic yeast *Pichia pastoris* (Cereghino and Cregg, 2000). Electroporation of JC201 and expression and purification of RIBEYE(A)-GST fusion protein was performed according to standard procedures (Schmitz et al., 2000). A certain degree of proteolytic processing of RIBEYE(A) is present in both of these systems. The proteolytic processing cannot be prevented even under optimized fermenting conditions using the BioFlo 110 fermenter (New Brunswick Scientific) with constant oxygenation of the medium, pH control, different induction times, and different induction temperatures (data not shown).

Intracellular expression of untagged RIBEYE(A) in Pichia pastoris. *Pichia pastoris* yeast strain GS115 (*his4*) (Invitrogen) was used for heterologous protein expression (Lin-Cereghino et al., 2005). Yeast cultures were grown at 30°C on synthetic minimal medium containing 0.67% yeast nitrogen base (without amino acids supplemented with ammonium sulfate and appropriate amino acid-base; Formedium). RE(A)pPIC3.5K was electroporated into freshly made electrocompetent yeasts GS115 (*his4*) as described (Lin-Cereghino et al., 2005). For electroporation, 10 μg of purified and *Sal*I-linearized plasmid DNA was used. Electroporation was performed at 1500 V (BTX ECM 399 electroporator; Biogentronix) with 2 mm gapped prechilled cuvette (Peqlab). Recombinant His$^+$ clones were selected on MD (minimal dextrose) plates (0.67% yeast nitrogen base without amino acids, 0.077% CSM-His, 2% dextrose, 0.00004% biotin, 1 M sorbitol, 1.5% agar–agar). Genomic integration of the electroporated construct was confirmed through genomic PCR (5′-AOX1-primer: GACTGGTTCCAATTGACAAGC; 3′-AOX1-primer: GCAAATGGCATTCTGACATCC). For induction of fusion protein, yeasts were first cultured in BMGY medium (1% yeast extract, 2% peptone, 0.67% yeast nitrogen base without amino acids, 0.00004% biotin, 1% glycerol, 0.1 M potassium-phosphate buffer, pH 6) at 30°C to an optical density at 600 nm (OD_{600}) of 2–6. Induction was achieved in BMMY medium (same as BMGY with 0.5% methanol instead of glycerol) at 30°C, starting the culture at an OD_{600} of 1. After every 24 h, methanol was replenished to the final volume of 0.5%. After 36 h of induction, the cells were pelleted (1500 rpm, 5 min, 4°C) and processed for extraction of fusion protein. Induced *Pichia pastoris* yeasts were mechanically cracked with 0.5 mm glass beads (Biospec/Roth) in breaking buffer (50 mM sodium phosphate, pH 7.4, 100 mM NaCl, 1 mM EDTA, 5% glycerol, 1 mM PMSF). For this purpose, 100 μl cell pellet were resuspended in 890 μl of ice-cold breaking buffer. To this mixture, ~500 μl of glass beads were added. The cracking was performed at +4°C using high-speed vortex (25× vortexing for 30 s; between vortexing, samples were chilled 30 s on ice). The lysate was centrifuged twice (13,000 rpm, 1 h at 4°C). Subsequently, the supernatant was precleared with 20 μl empty glutathione-agarose beads (Fluka) for 1 h at 4°C on a rotary wheel.

Protein pull-down assays using bacterial fusion protein. For pull-down experiments using pairs of GST- and maltose-binding protein (MBP)-tagged fusion proteins, the GST-tagged fusion proteins were usually kept immobilized on glutathione beads whereas MBP fusion proteins were used as solublized prey proteins if not denoted otherwise. Bait and prey proteins were used in equimolar amounts along with the respective control proteins. Protein concentrations were determined using the Bradford method (Bradford, 1976). For pull-down experiments, fusion protein eluates were precleared with 10 μl of empty glutathione Sepharose beads (per 1 ml of eluate) for 1 h at 4°C. Binding was performed in PBS that contained 0.5% Triton X-100 at 4°C for 12 h on a rotary wheel (500 μl incubation volume) if not denoted otherwise. Pellets were washed five times by adding an excess of PBS/Triton X-100 and subsequent spinning (13,000 rpm, 1 min, 4°C). Pellets were boiled in SDS-sample buffer and subsequently subjected to Western blot analyses with the indicated antibodies.

Miscellaneous methods. For the preparation of synaptic ribbons, synaptic ribbons were purified as described previously (Schmitz et al., 1996, 2000). Standard protein techniques were performed as described previously (Schmitz et al., 2000). For reprobing of Western blots, nitrocellulose sheets were treated with prewarmed (90°C) stripping buffer (1% SDS, 10 mM β-mercaptoethanol in PBS) and incubated at room temperature for 1 h. Immunofluorescence microscopy was performed as described previously (Schmitz et al., 2000, 2006) using a Zeiss Axiovert 200M microscope (Carl Zeiss) equipped for conventional epifluorescence microscopy with the respective filter sets for enhanced green fluorescent protein (EGFP) and monomeric red fluorescent protein (mRFP)

and equipped with an Apotome (Zeiss) to make optical sections. Transfection of COS cells was done as described previously with the DEAE-dextran method (Schmitz et al., 2000). R28 cells were transfected by lipofection using perfectin (Peqlab) according to the manufacturer's instructions. Transfected cells were usually analyzed by fluorescence microscopy 48 h after transfection if not denoted otherwise. Conventional transmission, immunogold electron microscopy, and quantification of radioactive NAD^+-binding to RIBEYE fusion proteins were performed as described previously (Schmitz et al., 1996, 2000). Thrombin cleavage of GST-tagged fusion protein was performed mostly as described previously (Chadli et al., 2000).

Results

Homodimerization of RIBEYE(A)

We used the yeast two-hybrid (YTH) system to determine whether the A-domain of RIBEYE can homodimerize. In YTH, we observed a strong self-interaction between the A-domains of RIBEYE as judged by growth on −ALWH-selective plates and expression of the β-galactosidase marker gene activity compared with the respective control matings (Fig. 1*A*, mating 1; supplemental Fig. 1*A*, available at www.jneurosci.org as supplemental material). RIBEYE(A) also interacted with full-length RIBEYE [RIBEYE(AB)] (Fig. 1*A*, mating 6). The RIBEYE-expressing yeasts were not autoactivating in YTH, as demonstrated by the lack of growth on −ALWH plates and analysis of β-galactosidase expression of the respective control matings (Fig. 1*A*, matings 2–5, 7, 8). Quantitative β-galactosidase activities determined in liquid assays are shown in supplemental Figure 1*A* (available at www.jneurosci.org as supplemental material). The homodimerization of RIBEYE(A) observed in the YTH system was also confirmed at the protein level using two different pull-down assays (Fig. 1*B*; supplemental Fig. 1*B*, available at www.jneurosci.org as supplemental material). Immobilized RIBEYE(A)-MBP fusion protein (but not immobilized MBP alone) bound soluble RIBEYE(A)-GST fusion protein (but not GST alone) (Fig. 1*B*). Similarly, immobilized RIBEYE(A)-GST specifically bound RIBEYE(A) from crude protein extracts of RIBEYE(A)-transgenic *Pichia pastoris* (supplemental Fig. 1*B*, available at www.jneurosci.org as supplemental material). GST control protein alone did not bind RIBEYE(A) from the *Pichia pastoris* extract. Thus, both YTH and protein pull-down data independently demonstrated that RIBEYE(A) interacts with RIBEYE(A).

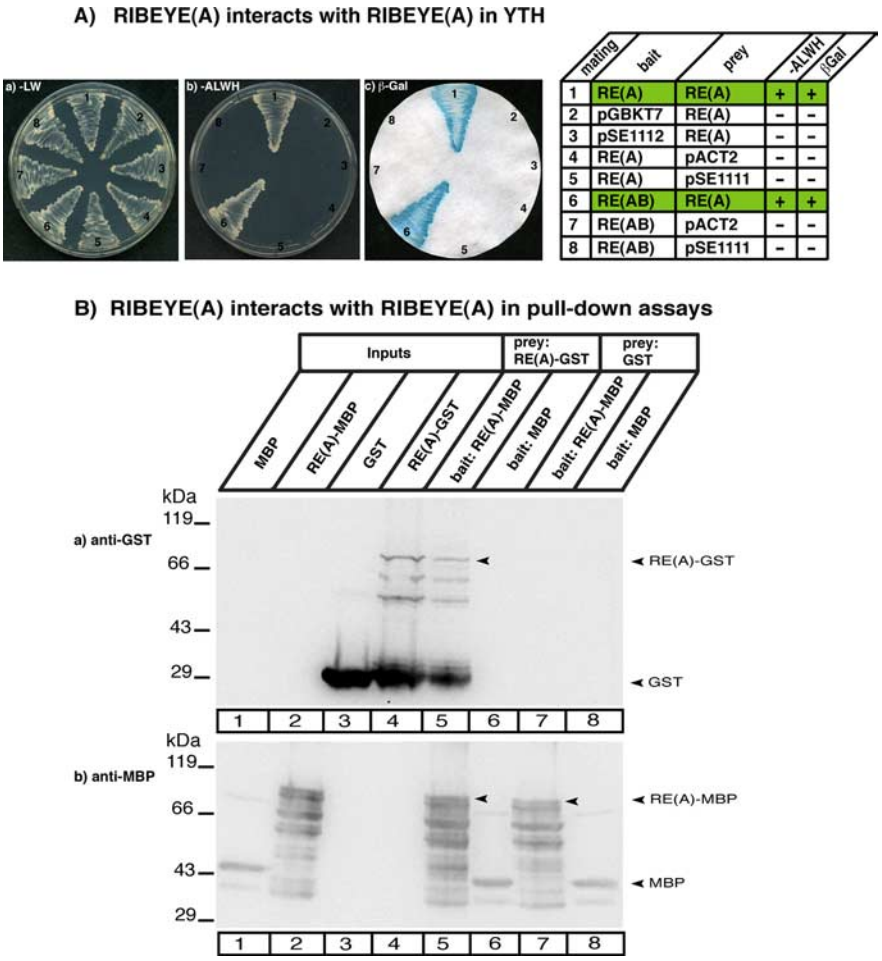

Figure 1. RIBEYE(A) interacts with RIBEYE(A). ***A***, RIBEYE(A) interacts with RIBEYE(A) in YTH. Summary plates of YTH analyses obtained with the indicated bait and prey plasmids. The indicated yeast clones growing on selective medium either for the presence of bait and prey plasmids (−LW dropout medium) or selective for protein–protein interaction (−ALWH dropout medium). For convenience, experimental bait–prey pairs are underlayered in color (green in case of interacting bait–prey pairs; control matings are not colored). RIBEYE(A) interacts with RIBEYE(A) and RIBEYE(AB) as judged by growth on selective plates (−ALWH) and expression of β-galactosidase expression (yeast matings 1, 6; ***Ab***, ***Ac***). The respective control matings (autoactivation controls; yeast matings 2–5, 7–8) did not show growth on −ALWH plates and expression of β-galactosidase activity. For quantification of the β-gal activities, see also supplemental Figure 1*A* (available at www.jneurosci.org as supplemental material). Growth on −LW plates (***Aa***) demonstrates the presence of the bait and prey plasmids in the mated yeasts. ***Ba***, ***Bb***, RIBEYE(A) interacts with RIBEYE(A) in protein pull-down experiments (Western blot analyses). RIBEYE(A)-MBP and MBP alone (control) were used as immobilized bait proteins and RIBEYE(A)-GST and GST alone (control) as soluble prey proteins. RIBEYE(A)-GST specifically binds to RIBEYE(A)-MBP (***Ba***, lane 5, arrowhead). RIBEYE(A)-GST does not bind to MBP alone (***Ba***, lane 6). GST alone also does not bind to RIBEYE(A)-MBP (***Ba***, lane 7). ***Bb*** shows the same blot as in ***Ba*** after stripping and reprobing of the nitrocellulose with anti-MBP antibodies to show equal loading of bait proteins. RIBEYE(A)-GST also specifically binds intracellularly expressed RIBEYE(A) from a crude extract of RIBEYE(A)-transgenic *Pichia pastoris* (supplemental Fig. 1*B*, available at www.jneurosci.org as supplemental material). RE(AB), full-length RIBEYE; RE(A), RIBEYE(A).

Mapping of RIBEYE(A)–RIBEYE(A) interaction

In the rat, RIBEYE(A) consists of the N-terminal 563 aa. To map the interaction sites important for RIBEYE(A)–RIBEYE(A)-interaction, we generated C- and N-terminal deletion constructs of RIBEYE(A) and tested them for their capability to interact with full-length RIBEYE(A) in YTH (Fig. 2*A*,*B*; supplemental Fig. 2, available at www.jneurosci.org as supplemental material). Most of the C-terminal region of the A-domain could be removed without abolishing the interaction with RIBEYE(A). RIBEYE(A)1–105 was the shortest N-terminal construct that could interact with full-length RIBEYE(A)-domain (Fig. 2*B*, prey 7). Therefore, the first 105 N-terminal amino acids contain a binding site for RIBEYE(A), which is subsequently denoted as the "A1" interaction site. We also analyzed N-terminal deletions of RIBEYE(A) for their interaction with full-length RIBEYE(A) (Fig. 2*B*; supplemental Fig. 2, available at www.jneurosci.org as supplemental material). Interestingly, N-terminal deletion constructs of RIBEYE that did not contain the previously identified RIBEYE(A1)-binding site also interacted with RIBEYE(A) (Fig.

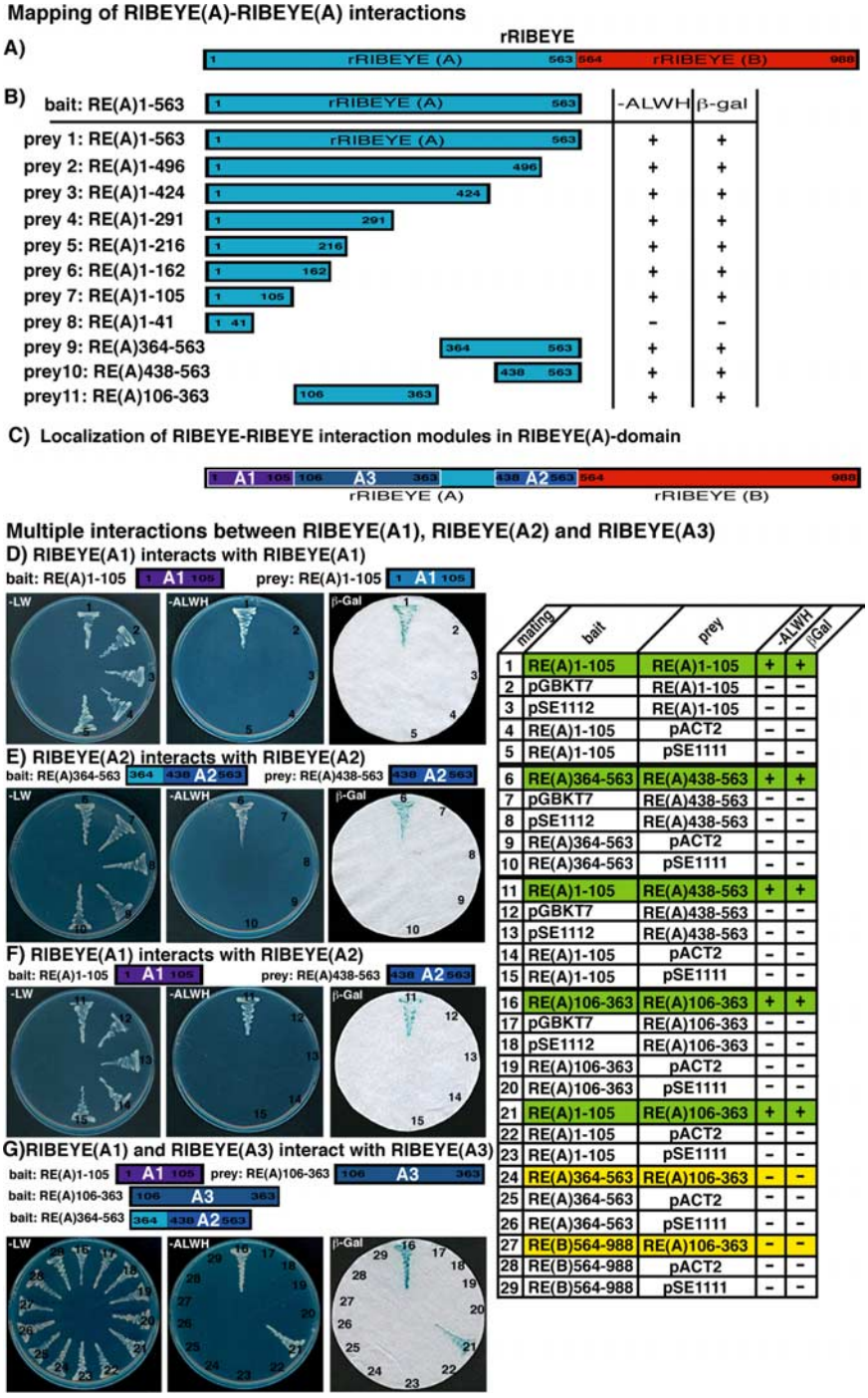

mating	bait	prey	-ALWH	βGal
1	RE(A)1-105	RE(A)1-105	+	+
2	pGBKT7	RE(A)1-105	–	–
3	pSE1112	RE(A)1-105	–	–
4	RE(A)1-105	pACT2	–	–
5	RE(A)1-105	pSE1111	–	–
6	RE(A)364-563	RE(A)438-563	+	+
7	pGBKT7	RE(A)438-563	–	–
8	pSE1112	RE(A)438-563	–	–
9	RE(A)364-563	pACT2	–	–
10	RE(A)364-563	pSE1111	–	–
11	RE(A)1-105	RE(A)438-563	+	+
12	pGBKT7	RE(A)438-563	–	–
13	pSE1112	RE(A)438-563	–	–
14	RE(A)1-105	pACT2	–	–
15	RE(A)1-105	pSE1111	–	–
16	RE(A)106-363	RE(A)106-363	+	+
17	pGBKT7	RE(A)106-363	–	–
18	pSE1112	RE(A)106-363	–	–
19	RE(A)106-363	pACT2	–	–
20	RE(A)106-363	pSE1111	–	–
21	RE(A)1-105	RE(A)106-363	+	+
22	RE(A)1-105	pACT2	–	–
23	RE(A)1-105	pSE1111	–	–
24	RE(A)364-563	RE(A)106-363	–	–
25	RE(A)364-563	pACT2	–	–
26	RE(A)364-563	pSE1111	–	–
27	RE(B)564-988	RE(A)106-363	–	–
28	RE(B)564-988	pACT2	–	–
29	RE(B)564-988	pSE1111	–	–

Figure 2. Mapping of RIBEYE(A)–RIBEYE(A) interactions. ***A***, Schematic domain structure of RIBEYE showing the N-terminal A-domain and the C-terminal B-domain. ***B***, ***C***, Summary of mapping analyses. The indicated bait and prey plasmids were used to test for the interaction of the respective proteins in the YTH system. YTH analyses of the C-terminal deletion constructs of RIBEYE(A) reveal an N-terminal site (within the first 105 aa) that interacts with RIBEYE(A). This interaction site is denoted as A1 (***C***). YTH analyses of N-terminal deletion constructs of RIBEYE(A) reveal a second interaction site in the C-terminal region of RIBEYE(A) that interacts with RIBEYE(A). This C-terminal interaction site is denoted as A2 (***C***) and covers amino acids 438–563. The A3 region (***C***) in the middle of RIBEYE(A) (amino acids 106–363) that does not contain A1 and A2 is also able to interact with full-length RIBEYE(A). ***C***, Schematic representation of the identified RIBEYE–RIBEYE interaction modules (A1, A2, A3) in the A-domain of RIBEYE. ***D–G***, The indicated minimal interaction modules (A1, A2, and A3) were tested in the YTH system for interaction with each other. For convenience, experimental bait–prey pairs are underlayered in color (green for interacting bait–prey pairs; yellow for noninteracting bait–prey pairs); control matings are not colored. ***D***, RIBEYE(A1) interacts with RIBEYE(A1) (mating 1). Matings 2–5 show the respective indicated control matings. ***E***, RIBEYE(A2) interacts with RIBEYE(A2) (mating 6). Matings 7–10 show the respective indicated control matings. ***F***, RIBEYE(A1) interacts with RIBEYE(A2) (mating 11). Matings 12–15 show the respective indicated control matings. ***G***, RIBEYE(A1) and RIBEYE(A3) interact with RIBEYE(A3) (matings 21, 16). RIBEYE(A3) does not interact with RIBEYE(B) (mating 27). Matings 22, 23, 17–20, 28, and 29 show the respective indicated control matings. No used RIBEYE constructs were autoactivating. RIBEYE(A2) does not interact with RIBEYE(A3) (mating 24). Matings 25 and 26 show the respective control matings. RE(A), RIBEYE(A); RE(B), RIBEYE(B).

2*B*, preys 9, 10; supplemental Fig. 2, available at www.jneurosci.org as supplemental material), pointing to a second homodimerization site in the C-terminal region of RIBEYE(A). We identified RIBEYE(A)438–563 as the smallest C-terminal portion of RIBEYE(A) that interacts with RIBEYE(A) (Fig. 2*B*; supplemental Fig. 2, available at www.jneurosci.org as supplemental material). This C-terminal RIBEYE(A) interaction site is denoted as "A2" in the following text. We further tested whether the midregion of RIBEYE(A), which does neither contain the N-terminal A1 interaction site nor the C-terminal A2 interaction site for its capability to interact with RIBEYE(A). This region in the midportion of RIBEYE(A), denoted as "A3," also interacted with RIBEYE(A) (Fig. 2*B*, prey 11). Thus, the A-domain of RIBEYE has three independent sites which are able to interact with full-length RIBEYE(A) (summarized in Fig. 2*C*). Supplemental Figure 2 (available at www.jneurosci.org as supplemental material) demonstrates that all of the tested RIBEYE constructs were not autoactivating as judged by the absence of growth on −ALWH and lack of expression of β-galactosidase activity.

The A1, A2, and A3 interaction modules in the A-domain of RIBEYE allow multiple RIBEYE–RIBEYE interactions

Next, we tested whether the identified RIBEYE(A1), RIBEYE(A2), and RIBEYE(A3) interaction modules in the A-domain of RIBEYE could interact with each other. We tested all possible interaction combinations between RIBEYE(A1), RIBEYE(A2) and RIBEYE(A3) in the YTH system and found that multiple interactions could take place between them. RIBEYE(A1) interacts with RIBEYE(A1), RIBEYE(A2), and RIBEYE(A3) (Fig. 2*D*,*F*,*G*). Similarly, RIBEYE(A2) interacted with RIBEYE(A2) and RIBEYE(A1) but not RIBEYE(A3) (Fig. 2*E*–*G*). RIBEYE(A3) interacted with RIBEYE(A1) and RIBEYE(A3) but not RIBEYE(A2) (Fig. 2*G*). All of these interactions between RIBEYE(A) subdomains characterized in the YTH system were confirmed by protein pull-down analyses using the respective fusion proteins (Fig. 3*A*–*D*,*F*).

Homodimerization of RIBEYE(B)

With the YTH system, we confirmed homodimerization of the B-domain of RIBEYE (supplemental Fig. 3*A*,*B*, available at www.jneurosci.org as supplemental material). The homodimerization of RIBEYE(B) is not very surprising: CtBP2,

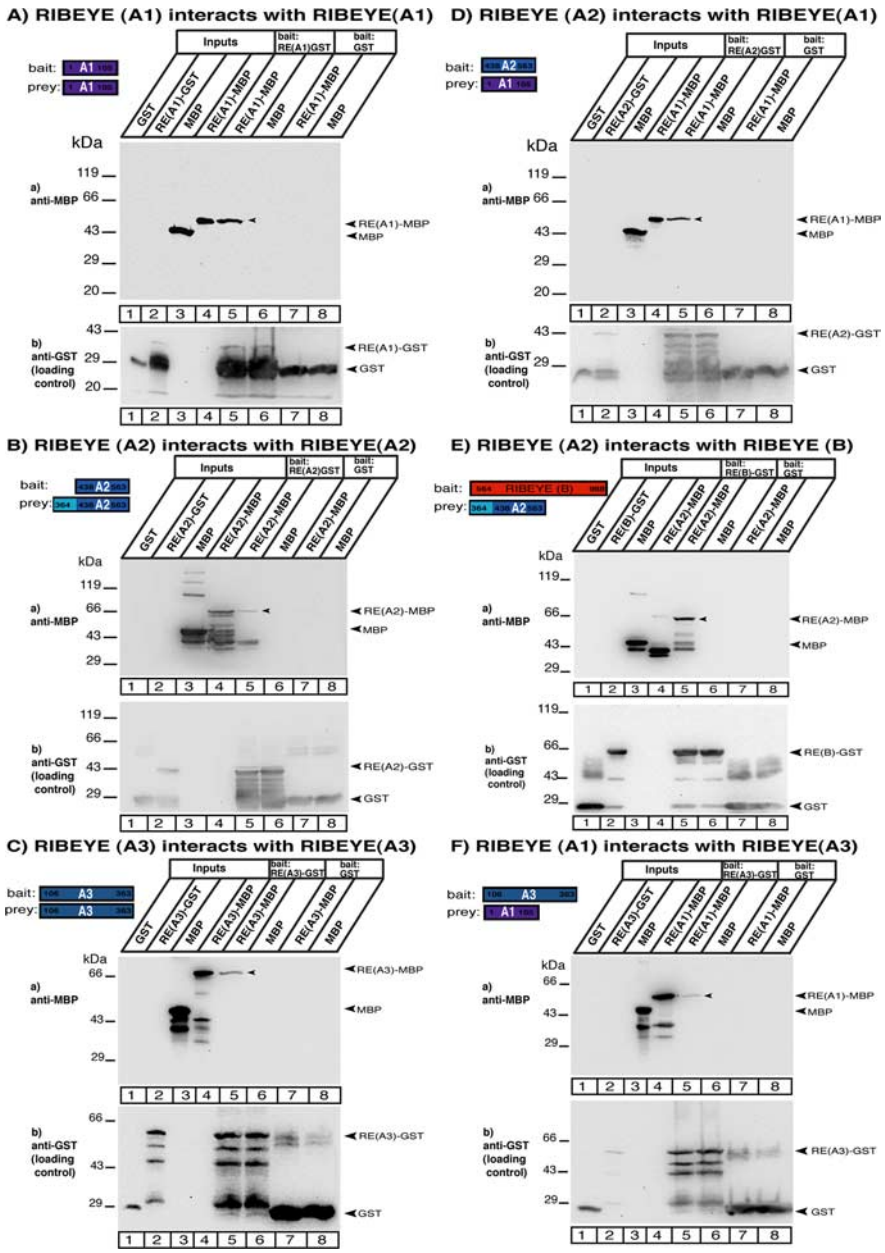

Figure 3. Multiple RIBEYE–RIBEYE interactions identified by YTH are confirmed by fusion protein pull-down experiments. Interaction analyses of the indicated RIBEYE subdomains in fusion protein pull-down analyses. GST-tagged RIBEYE proteins were used as immobilized bait proteins and eluted MBP-tagged RIBEYE proteins as soluble prey proteins. Binding of the prey proteins was analyzed by Western blotting with antibodies against MBP. Equal loading was verified by reprobing the respective blot (after stripping) with antibodies against GST. ***Aa***, ***Ab***, RIBEYE(A1) interacts with RIBEYE(A1). RIBEYE(A1)-GST (lanes 5, 6) and GST alone (lanes 7, 8; control protein) were tested for their ability to pull down RIBEYE(A1)-MBP. MBP alone served as control prey protein. Only RIBEYE(A1)-GST pulled down RIBEYE(A1)-MBP (lane 5) but not the control bait protein GST (lane 7). RIBEYE(A1)-GST does not pull down MBP alone (lane 6). ***Ab*** shows the same blot as in ***Aa*** after stripping and reprobing of the nitrocellulose with anti-GST antibodies to show equal loading of bait proteins. Lanes 1–4 show the indicated input proteins. ***Ba***, ***Bb***, RIBEYE(A2) interacts with RIBEYE(A2). RIBEYE(A2)-GST (lanes 5, 6) and GST alone (lanes 7, 8; control protein) were tested for their ability to pull down RIBEYE(A2)-MBP. MBP alone served as control prey protein. Only RIBEYE(A2)-GST pulled down RIBEYE(A2)-MBP (lane 5) but not the control bait protein GST (lane 7). RIBEYE(A2)-GST does not pull down MBP alone (lane 6). ***Bb*** shows the same blot as in ***Ba*** after stripping and reprobing of the nitrocellulose with anti-GST antibodies to show equal loading of bait proteins. Lanes 1–4 show the indicated input proteins. ***Ca***, ***Cb***, RIBEYE(A3) interacts with RIBEYE(A3). RIBEYE(A3)-GST (lanes 5, 6) and GST alone (lanes 7, 8; control protein) were tested for their ability to pull down RIBEYE(A3)-MBP. MBP alone served as control prey protein. Only RIBEYE(A3)-GST pulled down RIBEYE(A3)-MBP (lane 5) but not the control bait protein GST (lane 7). RIBEYE(A3)-GST does not pull down MBP alone (lane 6). ***Cb*** shows the same blot as in ***Ca*** after stripping and reprobing of the nitrocellulose with anti-GST antibodies to show equal loading of bait proteins. Lanes 1–4 show the indicated input proteins. ***Da***, ***Db***, RIBEYE(A2) interacts with RIBEYE(A1). RIBEYE(A2)-GST (lanes 5, 6) and GST alone (lanes 7, 8; control protein) were tested for their ability to pull down RIBEYE(A1)-MBP. MBP alone served as control prey protein. Only RIBEYE(A2)-GST pulled down RIBEYE(A1)-MBP (lane 5) but not the control bait protein GST (lane 7). RIBEYE(A2)-GST does not pull down MBP alone (lane 6). ***Db*** shows the same blot as in ***Da*** after stripping and reprobing of the nitrocellulose with anti-GST antibodies to show equal loading of bait proteins. Lanes 1–4 show the indicated input proteins. ***Ea***, ***Eb***, RIBEYE(B) interacts with RIBEYE(A2). RIBEYE(B)-GST (lanes 5, 6) and GST alone (lanes 7, 8; control protein) were tested for their ability to pull down RIBEYE(A2)-MBP. MBP alone served as control prey protein. Only RIBEYE(B)-GST pulled down RIBEYE(A2)-MBP (lane 5) but not the control bait protein GST (lane 7). RIBEYE(B)-GST does not pull down MBP alone (lane 6). ***Eb*** shows the same blot as in ***Ea*** after stripping and reprobing of the nitrocellulose with anti-GST antibodies to show equal loading of bait proteins. Lanes 1–4 show the indicated input proteins. ***Fa***, ***Fb***, RIBEYE(A3) interacts with RIBEYE(A1). RIBEYE(A3)-GST (lanes 5, 6) and GST alone (lanes 7, 8; control protein) were tested for their ability to pull down RIBEYE(A1)-MBP. MBP alone served as control prey protein. Only RIBEYE(A3)-GST pulled down RIBEYE(A1)-MBP (lane 5) but not the control bait protein GST (lane 7). RIBEYE(A3)-GST does not pull down MBP alone (lane 6). ***Fb*** shows the same blot as in ***Fa*** after stripping and reprobing of the nitrocellulose with anti-GST antibodies to show equal loading of bait proteins. Lanes 1–4 show the indicated input proteins. RE(A), RIBEYE(A); RE(B), RIBEYE(B).

which is identical to RIBEYE(B) (except for the first 20 aa) has been shown previously to homodimerize (Thio et al., 2004). CtBP1 also homodimerizes (Sewalt et al., 1999; Balasubramanian et al., 2003), and the structure of the CtBP1 dimer (tCtBP1) has been resolved (Kumar et al., 2002; Nardini et al., 2003). NAD(H) was found to stimulate the homodimerization of both CtBP1 and CtBP2 (Balasubramanian et al., 2003; Thio et al., 2004).

RIBEYE(B) also interacted with RIBEYE full-length protein indicating that the A-domain of RIBEYE does not prevent homodimerization of RIBEYE(B)-domains (supplemental Fig. 3*A*,*B*, available at www.jneurosci.org as supplemental material). The homodimerization of RIBEYE(B) is dependent on amino acids 689–716, which form the αB-loop-αC motif [homodimerization loop (HDL)] of RIBEYE(B) as judged by homology modeling (supplemental Fig. 3*D*, available at www.jneurosci.org as supplemental material). The αB-loop-αC motif in CtBP1 is important for homodimerization of CtBP1 (Nardini et al., 2003). In agreement with this prediction, homodimerization of RIBEYE(B) is completely abolished if the HDL is deleted (supplemental Fig. 3*C*, matings 1, 2, available at www.jneurosci.org as supplemental material). RIBEYE(B)ΔHDL no longer interacted with RIBEYE(B) (supplemental Fig. 3, available at www.jneurosci.org as supplemental material). The RIBEYE(B) homodimerization interface is denoted as "B1" in the following text.

Heterodimerization of RIBEYE(B) and RIBEYE(A)

We used the YTH system to test whether RIBEYE(B) can also interact with

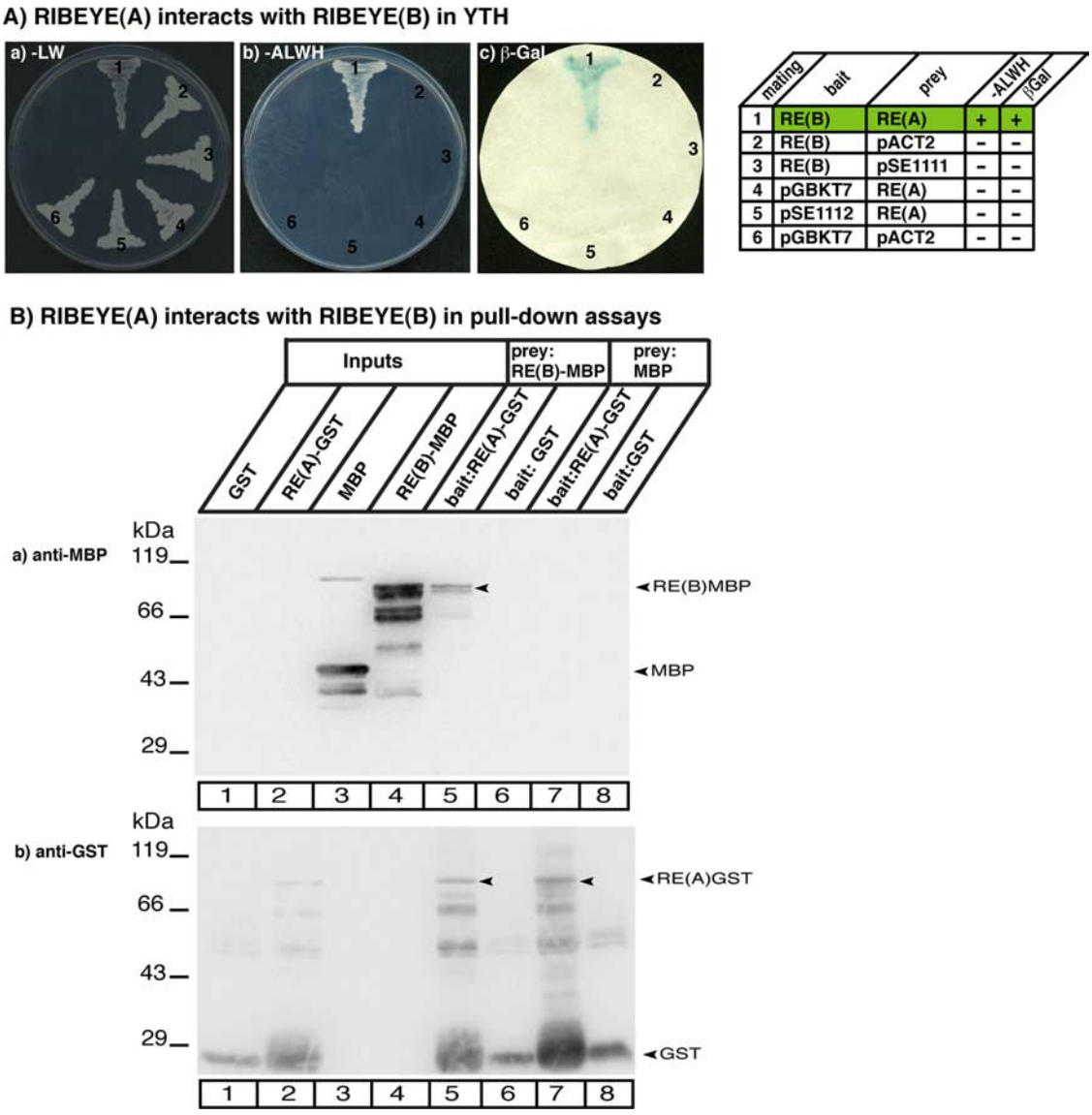

Figure 4. RIBEYE(A) interacts with RIBEYE(B). ***A***, Analyses of RIBEYE(A)–RIBEYE(B) interactions using the YTH system. Summary plates of YTH analyses obtained with the indicated bait and prey plasmids. For convenience, experimental bait–prey pairs are underlayered in color (green for interacting bait–prey pairs; control matings are not colored). RIBEYE(A) interacts with RIBEYE(B) as judged by growth on −ALWH plates and expression of β-galactosidase activity (***Ab***, ***Ac***, mating 1). ***Ba***, ***Bb***, RIBEYE(A) interacts with RIBEYE(B) in protein pull-down experiments. RIBEYE(A)-GST and GST alone (control protein) were used as immobilized bait proteins and RIBEYE(B)-MBP and MBP alone (control protein) as soluble prey proteins. After incubation, binding of the soluble prey proteins to the immobilized bait proteins was tested by Western blotting with the indicated antibodies. ***Ba***, RIBEYE(B)-MBP binds to RIBEYE(A)-GST (lane 5, arrowhead) but not to GST alone (lane 6). MBP alone binds neither to RIBEYE(A)-GST (lane 7) nor to GST alone (lane 8). ***Bb***, The same blot as in ***Ba*** after stripping and reprobing of the nitrocellulose with anti-GST antibodies to show equal loading of bait proteins. RE(A), RIBEYE(A); RE(B), RIBEYE(B).

RIBEYE(A). RIBEYE(B) showed a robust interaction with RIBEYE(A) in the YTH system as judged by growth on −ALWH selective plates and β-galactosidase marker gene expression (Fig. 4, mating 1; supplemental Figs. 4, 5, mating 1, available at www.jneurosci.org as supplemental material). This interaction between RIBEYE(A) and RIBEYE(B) was verified at the protein level using protein pull-down analyses (Fig. 4*B*). RIBEYE(A)-GST fusion protein, but not GST alone, specifically interacted with RIBEYE(B)-MBP fusion protein (but not with MBP alone) as judged by protein pull-down analyses (Fig. 4*B*). We used the YTH system to map the respective interaction sites for RIBEYE(B)–RIBEYE(A) interaction. Mapping analyses revealed that the A2 interaction site in the C-terminal portion of the RIBEYE(A) is the binding site for RIBEYE(B) (Fig. 5; supplemental Fig. 4*B*, available at www.jneurosci.org as supplemental material). On RIBEYE(B), the NBD is responsible for the interaction with RIBEYE(A) (Fig. 5*C*; supplemental Fig. 4*C*, available at www.jneurosci.org as supplemental material). These mapping data obtained by YTH analyses were confirmed by protein–protein pull-down analyses that showed interaction between RIBEYE(A2) and RIBEYE(B) (Fig. 3*E*). We used deletion and point mutants of RIBEYE(B) to further analyze the binding site of RIBEYE(A) on the NBD of RIBEYE(B) in detail. First, we tested whether the RIBEYE(B)ΔHDL deletion mutant that is no longer able to homodimerize with RIBEYE(B) (supplemental Fig. 3*C*,*D*, available at www.jneurosci.org as supplemental material) is still able to interact with RIBEYE(A). Indeed, RIBEYE(B)ΔHDL is able to interact with RIBEYE(A) as well as with full-length RIBEYE [RIBEYE(AB)] (Fig. 5*C*; supplemental Figs. 4*C*, 7, available at www.jneurosci.org as supplemental material). Next, we

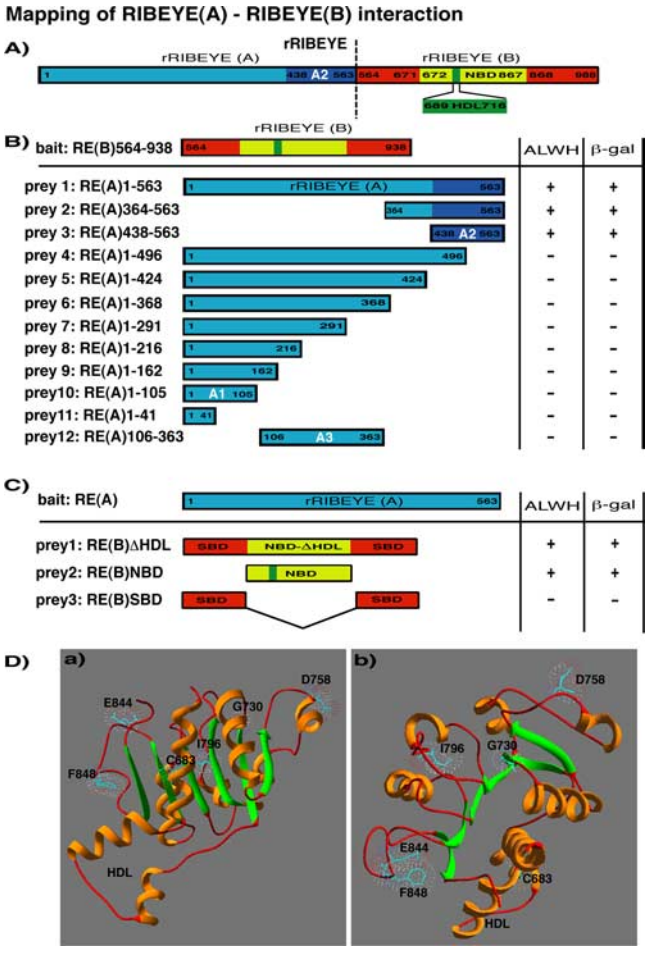

Figure 5. Mapping of RIBEYE(A)–RIBEYE(B) interaction in YTH. ***A***, Schematic domain structure of RIBEYE. The A-domain of RIBEYE is depicted in blue, the SBD of RIBEYE(B), which consists of the N- and C-terminal portions of the B-domain, is depicted in red. The HDL is depicted in green within the yellow-labeled NBD of RIBEYE(B). ***B***, ***C***, The indicated bait and prey plasmids were used to test for the interaction of the respective proteins in the YTH system. ***B***, YTH analyses of C- and N-terminal deletion constructs of RIBEYE(A) reveal that the RIBEYE(A2) site is responsible for interaction with RIBEYE(B). ***C***, YTH analyses of the indicated constructs of RIBEYE(B) reveal that the NBD (prey 2), but not the SBD (prey 3), is responsible for interaction with RIBEYE(A). The RIBEYE(B) HDL is not essential for the interaction between RIBEYE(A) and RIBEYE(B). RIBEYE(B)ΔHDL (prey 1) still interacts with RIBEYE(A). ***Da***, ***Db***, Summary of the location of distinct amino acids on the NBD that are essential for binding of RIBEYE(A). If these amino acids on the NBD of RIBEYE(B) are point mutated, RIBEYE(A) can no longer bind to RIBEYE(B) (supplemental Fig. 5, available at www.jneurosci.org as supplemental material). The lack of binding of the RIBEYE(B) point mutants to RIBEYE(A) is not caused by misfolding of the respective point mutants because all of these RIBEYE(B) point mutants homodimerized with RIBEYE(B) (supplemental Fig. 6, available at www.jneurosci.org as supplemental material). ***Da***, A lateral view of the NBD of RIBEYE(B). ***Db***, A top view on the NBD from the position of the bound NADH to the "bottom" of the molecule as seen in ***Da***. RE(A), RIBEYE(A); RE(B), RIBEYE(B).

tested different point mutants of the NBD of RIBEYE(B) for their interaction with RIBEYE(A) and RIBEYE(B). We analyzed RIBEYE(B) point mutants RIBEYE(B)G730A, D758N, I796A, E844Q, F848W, and K854Q, which are located at the outer face of the NBD (Fig. 5*D*). All of these point mutations did not prevent homodimerization with RIBEYE(B) (supplemental Figs. 5*C*, 6, available at www.jneurosci.org as supplemental material). Furthermore, RIBEYE(B)D758N, I796A, E844Q, F848W, and K854Q bound NADH as judged by NADH-dependent energy transfer from tryptophan W867 to bound NADH [performed as described by Fjeld et al. (2003)] (data not shown), demonstrating the proper folding of these point mutants. Although these point mutants did not prevent homodimerization of RIBEYE(B), all of these point mutations [except for RIBEYE(B)K854Q] completely abolished interaction with RIBEYE(A) (supplemental Fig. 5*A–C*, available at www.jneurosci.org as supplemental material). This shows that the two binding interfaces on RIBEYE(B) available for interaction with RIBEYE(A) and RIBEYE(B) are distinct from each other, albeit spatially closely related. The binding site for RIBEYE(A) covers a large portion of the NBD (Fig. 5*D*; supplemental Fig. 5, available at www.jneurosci.org as supplemental material). Interestingly, RIBEYE(B)G730, which is an essential component of the conserved NAD(H)-binding motif of RIBEYE (Schmitz et al., 2000), appears to be part of the interaction interface for RIBEYE(A): the point mutant RIBEYE(B)G730A (Fig. 5*D*) that does not bind NAD(H) (supplemental Fig. 5*D*, available at www.jneurosci.org as supplemental material) can no longer interact with RIBEYE(A) (supplemental Fig. 5*C*, available at www.jneurosci.org as supplemental material). We interpret the latter result to mean that the binding sites for NAD(H) and for RIBEYE(A) are overlapping to a certain extent (see below and Discussion). The docking site on RIBEYE(B) for RIBEYE(A) is denoted as "B2" in the following text.

NADH and NAD$^+$ inhibit RIBEYE(A)–RIBEYE(B) interaction

Because RIBEYE(A) docks to a broad interface of the NAD(H)-binding subdomain of RIBEYE(B), we analyzed whether this interaction is dependent on NAD(H). To analyze this question, we applied the pull-down assay described in Materials and Methods. We used RIBEYE(A)-GST as immobilized bait and eluted RIBEYE(B)-MBP as soluble prey protein and checked for interaction of these proteins in the presence of increasing concentrations of NADH/NAD$^+$ (Fig. 6). Increasing concentrations of NADH/NAD$^+$ strongly inhibited RIBEYE(A)–RIBEYE(B) interaction. Both NAD$^+$ as well as NADH strongly inhibited RIBEYE(A)–RIBEYE(B) interaction already at low physiological concentrations. The tested concentrations of NAD(H) are within the cellular concentration range of NAD(H) known from other studies (Zhang et al., 2002; Fjeld et al., 2003). The NAD(H) concentrations did not have any influence on the control pull downs. At all NADH/NAD$^+$ concentrations used, there was no unspecific binding of RIBEYE(B)-MBP to GST alone (supplemental Fig. 8, available at www.jneurosci.org as supplemental material). The identified interactions between the different subdomains of RIBEYE and their regulation via NAD(H) are summarized in Figure 11*B*.

RIBEYE coaggregates with other RIBEYE molecules in transfected R28 and COS cells

To determine whether the identified RIBEYE–RIBEYE interactions can also occur within the cellular context, we performed cell transfections with the indicated RIBEYE expression constructs that were differentially tagged either with EGFP or with mRFP. For transfection, we used COS7 cells and the R28 retinal progenitor cell line (Seigel, 1996; Seigel et al., 2004). R28 cells express retinal and neuronal marker proteins (e.g., opsins, β-2 arrestin, recoverin, neurotransmitter receptors, and various presynaptic and postsynaptic proteins) in addition to stem cell/precursor cell markers (e.g., nestin) (Seigel et al., 2004). If transfected alone, both RIBEYE(A) as well as RIBEYE(AB) displayed a discrete, spot-like distribution, whereas RIBEYE(B) is diffusely distributed (Fig. 7; supplemental Figs. 9–11, available at www.jneurosci.org as supplemental material), as also described previously (Schmitz et al., 2000). If RIBEYE(A)-EGFP was cotrans-

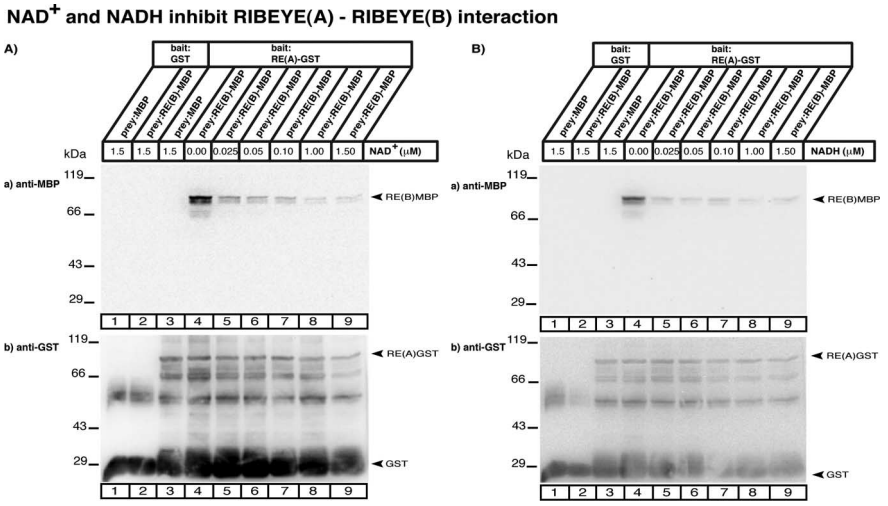

Figure 6. NADH and NAD $^+$ inhibit RIBEYE(A)–RIBEYE(B) interaction. ***Aa–Bb***, Immobilized RIBEYE(A)-GST fusion protein (0.3 μM) was incubated with 0.3 μM RIBEYE(B)-MBP in the presence of the indicated concentrations of NAD $^+$ (***Aa***, ***Ab***) or NADH (***Ba***, ***Bb***) for 3 h at 4°C in binding buffer (100 mM Tris-HCl, pH 8.0, 150 mM NaCl, 1 mM EDTA, 1% Triton X-100). After several washes with binding buffer, the pellets were boiled with SDS-sample buffer and analyzed for binding of RIBEYE(B)-MBP by Western blot analyses and probing of the Western blots with anti-MBP antibodies. Both NAD $^+$ and NADH strongly inhibited binding of RIBEYE(B) to RIBEYE(A). ***Ab***, ***Bb***, Respective loading controls in which the same blots as shown in ***Aa*** and ***Ba*** were incubated with GST antibodies after stripping of the respective blots. RE(A), RIBEYE(A); RE(B), RIBEYE(B).

fected with RIBEYE(A)-mRFP both coaggregated to the same protein clusters as judged by the large extend of colocalization of the EGFP and mRFP signals (Fig. 7*C*, arrows; supplemental Figs. 10*C*, 11*A*, available at www.jneurosci.org as supplemental material). Identical results were obtained when full-length RIBEYE(AB)-EGFP was cotransfected with RIBEYE(A)-mRFP (Fig. 7*B*, arrows). If RIBEYE(B)-EGFP was cotransfected with RIBEYE(B)-mRFP, both signals remained diffusely distributed (Fig. 7*E*). Interestingly, whenever RIBEYE(B)-mRFP was cotransfected with RIBEYE(A)-EGFP, RIBEYE(B)-mRFP redistributed from a diffuse distribution [as typical for single transfected RIBEYE(B)], to a patchy, spot-like distribution that is typical for RIBEYE(A) (Fig. 7*D*, arrow). Part of RIBEYE(B) remained diffusely distributed (Fig. 7*D*, arrowhead; supplemental Fig. 10*D*,*E*, available at www.jneurosci.org as supplemental material) probably because of the NAD(H) sensitivity of the RIBEYE(B)–RIBEYE(A) interaction (see above). NAD(H) is ubiquitously present in the cytoplasm and expected to partly dissociate RIBEYE(A)–RIBEYE(B) complexes. Interestingly, in cells double-transfected with full-length RIBEYE(AB) and RIBEYE(B), RIBEYE(B) virtually completely redistributed from the diffuse distribution to the spot-like distribution typical for RIBEYE(AB) and perfectly colocalized with RIBEYE(AB) (Fig. 7*A*, arrows; supplemental Figs. 9, 10*B*, 11*B*, available at www.jneurosci.org as supplemental material). From these latter experiments, we conclude that both homotypic domain interactions [RIBEYE(B)–RIBEYE(B) interactions] as well as heterotypic domain interactions [RIBEYE(A)–RIBEYE(B) interactions] support the interaction between RIBEYE(AB) and RIBEYE(B). As judged by the nearly complete colocalization of RIBEYE(AB) and RIBEYE(B) compared with cells double-transfected with RIBEYE(A) and RIBEYE(B), we assume that a combination of homotypic and heterotypic domain interactions is probably stronger than a single type of homotypic interactions. Qualitatively identical results were obtained for R28 cells (Fig. 7; supplemental Fig. 9, available at www.jneurosci.org as supplemental material) and COS cells (supplemental Figs. 10, 11, available at www.jneurosci.org as supplemental material). Also in COS cells, RIBEYE(A) coaggregated with RIBEYE(AB) (supplemental Fig. 10*A*, available at www.jneurosci.org as supplemental material) and RIBEYE(A) (supplemental Figs. 10*C*, 11*A*, available at www.jneurosci.org as supplemental material). Similarly, RIBEYE(B) translocated from a completely diffuse distribution to a spot-like distribution if cotransfected with RIBEYE(A) or RIBEYE(AB) [in 98 and 99%, respectively, of double-transfected cells in 100 randomly picked double-transfected cells vs 3% spot-like distribution in cells transfected with RIBEYE(B) only].

Interestingly, if RIBEYE(AB)-EGFP-transfected cells were analyzed already a few hours after transfection, the RIBEYE(AB)-containing aggregates appeared smaller and more numerous than at later time points suggesting that the smaller protein clusters could mature/coalesce to the bigger protein aggregates that are predominant at later time points (supplemental Fig. 9, available at www.jneurosci.org as supplemental material).

In conclusion, the coaggregation and colocalization data in the transfected COS and R28 cells indicate that the interaction sites between RIBEYE(A) and RIBEYE(B), either between the same type of domains (A–A, B–B) or between different domains (A–B), are also available within a cellular context.

Electron microscopy of RIBEYE-containing aggregates in transfected R28 cells

RIBEYE is the major component of synaptic ribbons and RIBEYE forms large protein aggregates in transfected cells (Fig. 7). We analyzed the ultrastructural appearance of the RIBEYE-containing aggregates by electron microscopy to find out whether these structures have similarities with synaptic ribbons (Fig. 8). Using conventional transmission electron microscopy, we observed large electron-dense aggregates in RIBEYE-EGFP-transfected R28 cells (Fig. 8*A–J*), which were absent in control cells (K). Similar, large electron-dense protein aggregates were also present in RIBEYE(AB)-EGFP-transfected COS cells but not in EGFP-transfected COS cells (data not shown). The large aggregates typically displayed a spherical shape with a diameter between of 200–500 nm. These electron-dense structures were often surrounded by vesicles which in part were physically attached to the electron-dense aggregates via thin electron-dense stalks (Fig. 8*A–J*, arrowheads). These large spherical structures were strongly positive for RIBEYE by immunogold labeling with antibodies against RIBEYE (Fig. 8*L–N*) but not reactive with antibodies against tubulin (*O*) or RIBEYE preimmune serum (*P*) (control incubations). These spherical structures have similarities to spherical synaptic ribbons of inner hair cells (for review, see Nouvian at al., 2006). Beside the large electron-dense particles we also found smaller aggregates which showed physical contacts between each other and which sometimes appeared to coalesce into larger, electron-dense structures (Fig. 8*E*,*F*). These structures were also partly physically linked to surrounding vesicles and show some resemblance to synaptic spheres, intermediate structures in the assembly and disassembly of synaptic ribbons

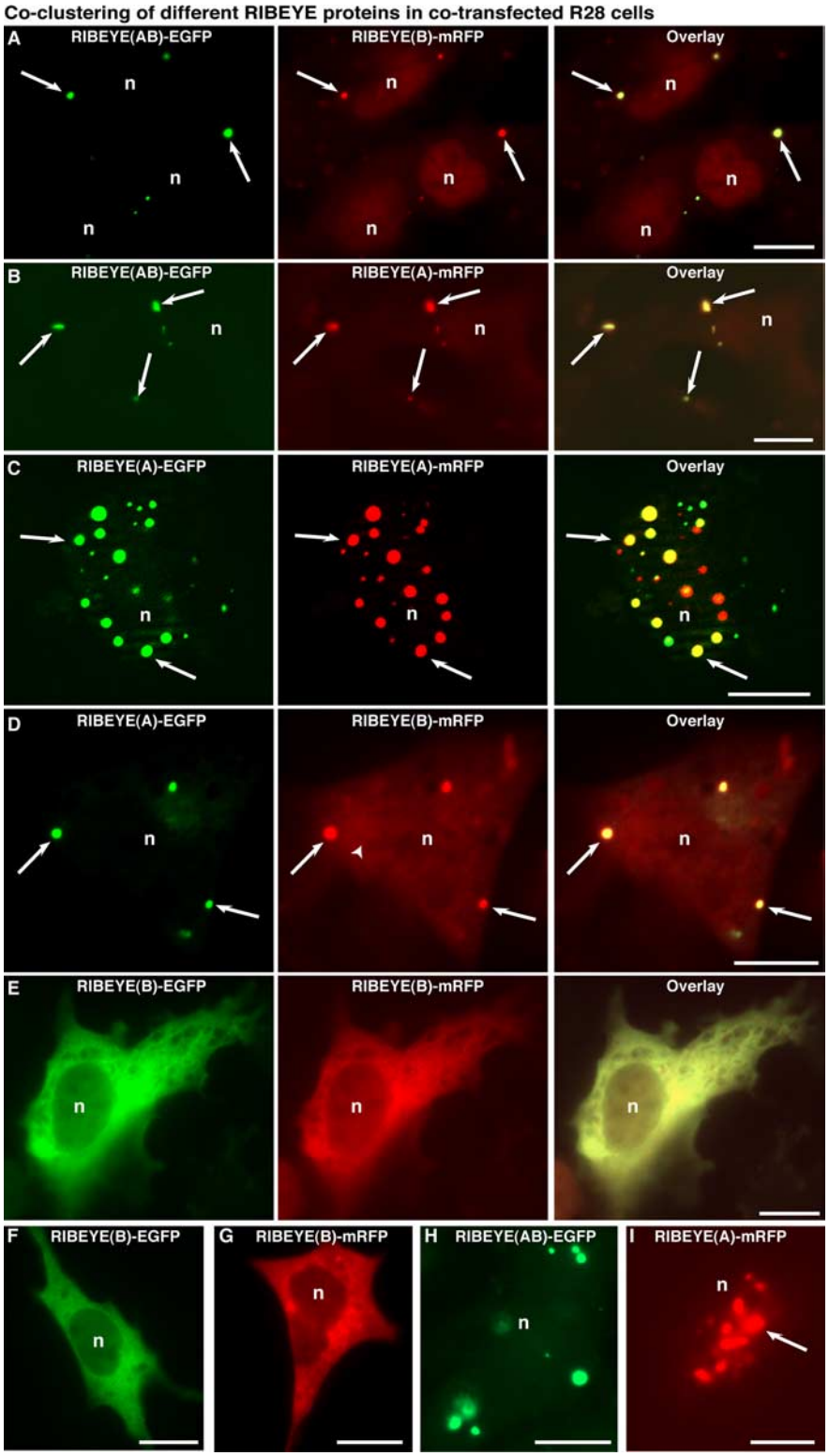

Figure 7. Coclustering of different RIBEYE-proteins in cotransfected R28 cells. ***A–H***, R28 cells were transfected with the indicated mRFP- or EGFP-tagged RIBEYE constructs. Transfected cells were analyzed for the intracellular distribution of the respective proteins via direct epifluorescence microscopy. RIBEYE(AB) (***H***) and RIBEYE(A) (***I***) show a discrete spot-like distribution, as already shown previously (Schmitz et al., 2000). In contrast, RIBEYE(B) is diffusely distributed in single-transfected cells (Schmitz et al., 2000) (***F***,***G***). ***A***, If RIBEYE(B) is cotransfected with RIBEYE(AB) (supplemental Fig. 9, available at www.jneurosci.org as supplemental material), RIBEYE(B) virtually completely redistributed from a diffuse distribution into a spot-like, RIBEYE(AB)-typical distribution and colocalized with RIBEYE(AB) (arrows) (supplemental Fig. 9*A*,*B*, available at www.jneurosci.org as supplemental material). ***D***, RIBEYE(B) also redistributed from a diffuse to spot-like distribution if cotransfected with RIBEYE(A) (supplemental Fig. 9*C*, available at www.jneurosci.org as supplemental material); part of RIBEYE(B) remained diffusely distributed (arrowhead). The higher degree of codistribution of RIBEYE(B) with RIBEYE(AB) compared with RIBEYE(A) probably represents the fact that more types of interactions can be formed between RIBEYE(B) and RIBEYE(AB) than between RIBEYE(B) and RIBEYE(A) alone (for a summary, see Fig. 11). RIBEYE(A) also coaggregated and colocalized with RIBEYE(A) (***C***, arrows). ***E***, If RIBEYE(B)-EGFP was cotransfected with RIBEYE(B)-mRFP, both proteins remained diffusely distributed and did not generate a spot-like distribution. For additional examples of transfected R28 cells, see supplemental Figure 9 (available at www.jneurosci.org as supplemental material). The arrows in ***A–D*** point to intracellular RIBEYE aggregates that contain both types of the indicated differentially tagged RIBEYE proteins. The arrow in ***I*** points to an intracellular RIBEYE(A)-containing aggregate. COS cells transfected with the respective plasmids produced qualitatively identical results (supplemental Figs. 10, 11, available at www.jneurosci.org as supplemental material). n, Nucleus. Scale bars, 10 μm.

(for review, see Vollrath and Spiwoks-Becker, 1996) (see Discussion).

RIBEYE coaggregates at bassoon-containing sites in retinal R28 progenitor cells

To further address the physiological relevance of the RIBEYE aggregates, we tested whether these structures are related to bassoon, a physiological interaction partner of RIBEYE at the active zone of ribbon synapses (tom Dieck et al., 2005). Bassoon is endogenously expressed in R28 retinal precursor cells as judged by immunocytochemistry (Fig. 9), Western blotting (supplemental Fig. 9*D*, available at www.jneurosci.org as supplemental material) and reverse transcription-PCR (data not shown). Bassoon is distributed in R28 in a spot-like manner (Fig. 9*D*, arrowheads). The RIBEYE clusters in RIBEYE(AB)-EGFP-transfected R28 cells primarily formed around this bassoon-containing clusters and colocalized with bassoon (Fig. 9*A–C*, arrows). The preferential colocalization between RIBEYE and its physiological interaction partner bassoon emphasizes the physiological relevance and ribbon-like partial function of the RIBEYE-containing protein aggregates.

Purified synaptic ribbons recruit externally added RIBEYE(A) and RIBEYE(B)

Next, we tested whether isolated, purified synaptic ribbons can recruit externally added RIBEYE(B)-GST and RIBEYE(A)-GST fusion proteins (Fig. 10). GST alone was used as control protein. Purified synaptic ribbons bound soluble RIBEYE(A)-GST and RIBEYE(B)-GST fusion proteins (Fig. 10*A*,*B*). GST control protein did not bind to synaptic ribbons (Fig. 10*Aa*, lane 6, *Ba*, lane 6) demonstrating the specificity of binding. Thus, the RIBEYE–RIBEYE in-

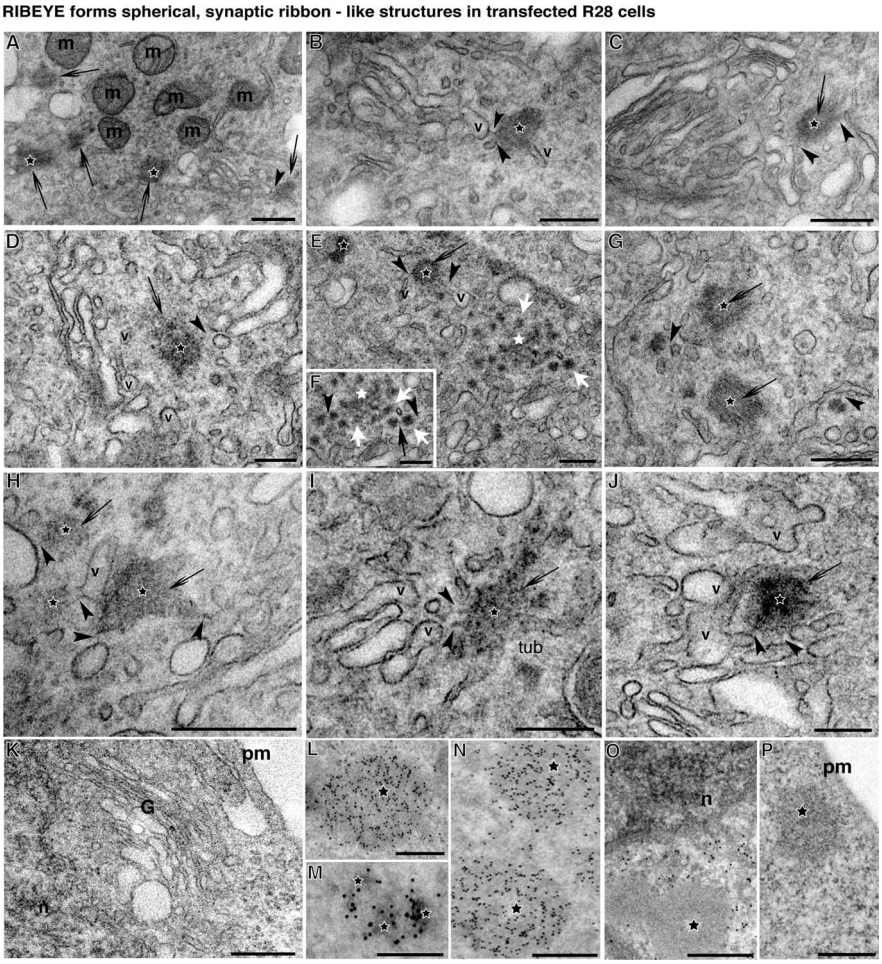

Figure 8. Electron microscopy of RIBEYE-containing aggregates in transfected R28 cells. ***A–K***, Conventional transmission microscopy of RE(AB)-EGFP- (***A–J***) and EGFP-transfected cells (***K***). ***L–P***, Immunogold electron microscopy of RE(AB)-EGFP-transfected cells immunolabeled with antibodies against RIBEYE (***L–N***), tubulin (***O***), and control immunoglobulins (RIBEYE preimmune; ***P***). ***A***, Low magnification of RE(AB)-EGFP-transfected cells. Note the presence of large electron-dense material (200–500 nm in diameter) in RIBEYE-transfected cells (***A–J***, asterisks and black arrows). These electron-dense structures are mostly spherical in shape (***A–G***, ***J***, asterisks), although more irregular profiles are also present (***H***, ***I***, asterisks). These electron-dense structures (***A–J***) were often surrounded by vesicles, which in part were physically attached to the electron-dense aggregates via thin electron-dense stalks (***A–J***, arrowheads). In addition to the large electron-dense spheres, smaller electron-dense structures could be observed (***E***, ***F***, white arrows). Neighboring small electron-dense aggregates (***E***, ***F***, white arrows) appear at least partly physically connected to each other (***F***, black arrow) and sometimes appeared to coalesce into larger, electron-dense structures (***E***, ***F***, white asterisk). ***K***, Ultrastructure of a control-transfected cell. ***L–N***, Both the large (***L***, ***N***) as well as the small (***M***) electron-dense aggregates were strongly immunolabeled by RIBEYE antibodies. The aggregates were densely decorated by immunogold particles. ***O***, ***P***, RE(AB)-EGFP-transfected cell immunolabeled with antibodies against tubulin (***O***) and RIBEYE-preimmune serum (***P***). In no case was a specific labeling of the electron-dense aggregates (asterisks) observed. n, Nucleus; m, mitochondria; G, Golgi apparatus; v, vesicles; tub, membrane tubule; pm, plasma membrane. Scale bars: ***A***, 500 nm; ***B***, 250 nm; ***C***, 400 nm; ***D–F***, 250 nm; ***G–I***, 300 nm; ***J***, 250 nm; ***K***, 400 nm; ***L–P***, 200 nm.

teraction sites are accessible on synaptic ribbons and available to recruit externally added, additional RIBEYE proteins. We verified that the binding of RIBEYE(A) to purified synaptic ribbons is independent of the attached GST tag by removing the GST tag by thrombin cleavage (Fig. 10*C*). Untagged RIBEYE(A) cosedimented with purified synaptic ribbons but not without synaptic ribbons, further confirming the specific binding of RIBEYE(A) to purified synaptic ribbons. To further evaluate the binding of RIBEYE(A) to synaptic ribbons, we also tested whether RIBEYE(A1), RIBEYE(A2), and RIBEYE(A3) (used as purified MBP-tagged fusion proteins) were able to bind to purified synaptic ribbons. RIBEYE(A1)-MBP and RIBEYE(A3)-MBP bound to synaptic ribbons whereas MBP alone did not demonstrating the specificity of the interaction. Interestingly, RIBEYE(A2)-MBP did not bind to purified synaptic ribbons although it efficiently interacted with RIBEYE(A) subunits [RIBEYE(A1), RIBEYE(A2)] in protein pull-down assays (Fig. 3). We interpret these findings that the RIBEYE(A2)-binding sites/options are probably unavailable or blocked by other proteins on purified synaptic ribbons (see Discussion). The recruitment of additional RIBEYE subunits to preexisting ribbons could explain the known dynamic growth and ultrastructural plasticity of synaptic ribbons (see Discussion). Figure 11 depicts a simplified model that schematically shows how synaptic ribbons could be built from individual RIBEYE subunits via the identified RIBEYE–RIBEYE interactions.

Discussion

Synaptic ribbons are large and dynamic macromolecular constructions in the active zone of ribbon synapses. At present, it is not clearly understood how the synaptic ribbon is made and how it functions in the synapse. In the present study, we demonstrated that RIBEYE is a scaffold protein that contains multiple interaction sites for other RIBEYE molecules. Noteworthy, the RIBEYE–RIBEYE interactions involve sites in the A-domain as well as in the B-domain of RIBEYE, i.e., three distinct interaction sites in the A-domain (A1, A2, A3) and two in the B-domain (B1, B2). We have shown that these five interaction sites allow either homotypic domain interactions [interactions between same type of domains: RIBEYE(A)–RIBEYE(A), RIBEYE(B)–RIBEYE(B)] or heterotypic domain interactions [RIBEYE(A)–RIBEYE(B)]. Homotypic domain interactions can be either homotypic or heterotypic concerning the subdomain involved. A homotypic domain interaction, e.g., RIBEYE(A)–RIBEYE(A), can be mediated either by homotypic subdomain interactions, e.g., RIBEYE(A1)–RIBEYE(A1), or by heterotypic subdomain interactions, e.g., RIBEYE(A1)–RIBEYE(A2). The cotransfection experiments demonstrated that RIBEYE proteins interact with each other and coaggregate into the same protein clusters. Given the fact that RIBEYE is the major component of synaptic ribbons (Schmitz et al., 2000; Zenisek et al., 2004; Wan et al., 2005), the multiple protein interactions of RIBEYE provide a molecular mechanism how the scaffold of the synaptic ribbon can be created. RIBEYE–RIBEYE interactions could directly link the individual RIBEYE units to each other. Because RIBEYE is present throughout the entire synaptic ribbon, RIBEYE–RIBEYE interactions could thus generate and stabilize the macromolecular structure of the synaptic ribbon. The proposed modular model of synaptic ribbons could explain how the scaffold of the

synaptic ribbon is formed mostly from a single protein component (RIBEYE). In agreement with this hypothesis, the RIBEYE aggregates in transfected R28 cells possess structural and functional similarities with synaptic ribbons. RIBEYE(AB)-transfected R28 cells formed electron-dense large protein aggregates that were partly associated with surrounding vesicles and membrane compartments. The electron-dense aggregates were usually round in shape and resembled spherical synaptic ribbons of inner hair cells (Nouvian et al., 2006). Bar-shaped/plate-shaped ribbons were not observed in the RIBEYE-transfected cells. Thus, the spherical synaptic ribbon appears to be the "basal" type of synaptic ribbon structure that is built from RIBEYE and most likely additional factors are needed to build plate-shaped ribbons from spherical ribbons. The colocalization of RIBEYE with its physiological interaction partner bassoon in R28 cells emphasizes the physiological relevance of the RIBEYE-containing protein aggregates and suggest that the RIBEYE-containing aggregates fulfill partial ribbon-like functions. Because RIBEYE is not the only component of synaptic ribbons (Schmitz et al., 2000; Wan et al., 2005), it cannot be expected that RIBEYE alone makes fully mature ribbons, e.g., with a dense and regular association of synaptic vesicles. Very likely, additional ribbon components are necessary to provide full-ribbon function and structure.

In principle, the multiple interaction sites present on RIBEYE can be important for both intramolecular and intermolecular RIBEYE–RIBEYE interactions. Intermolecular RIBEYE–RIBEYE interactions could provide the three-dimensional scaffold of the synaptic ribbon as discussed above. Intramolecular RIBEYE–RIBEYE interactions could shield the interaction sites from unwanted intermolecular interactions to keep the protein soluble. Such a shielding of binding sites could be particularly important during development and to prevent the assembly of synaptic ribbons at unwanted, unphysiological subcellular sites (e.g., outside of the presynaptic terminal).

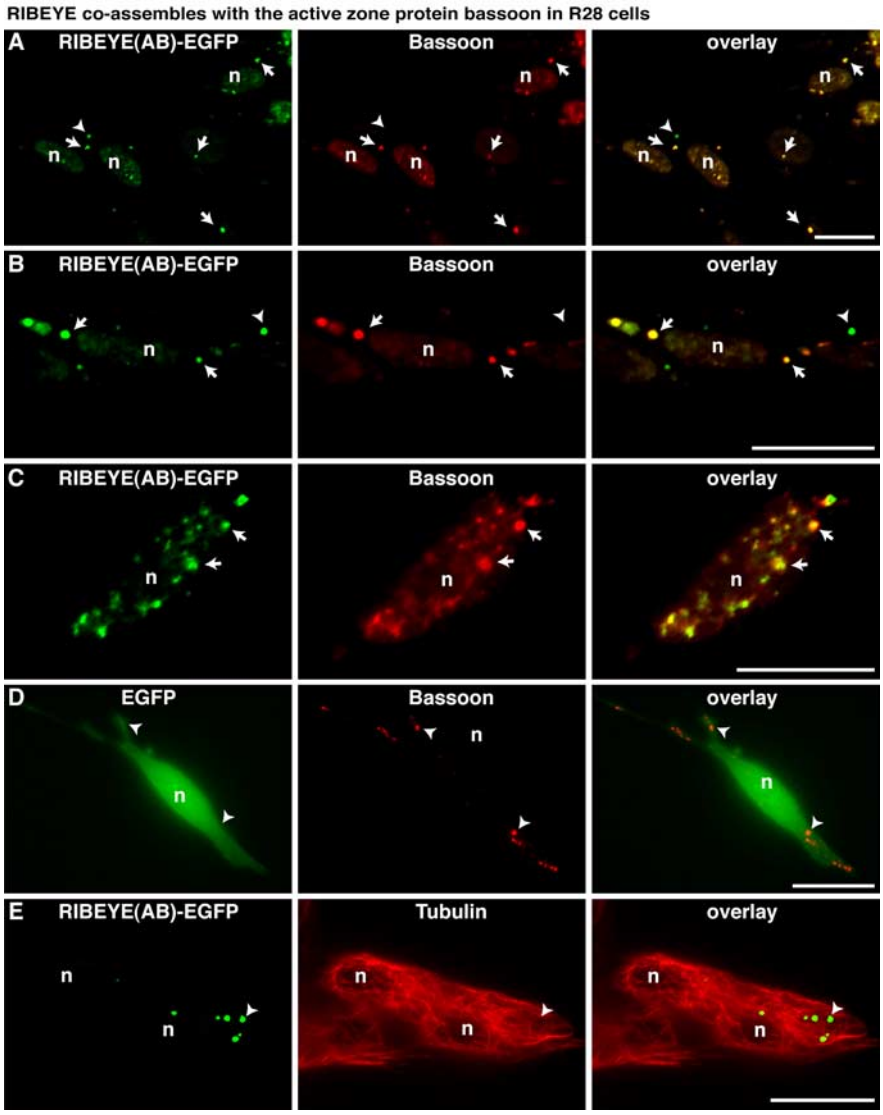

Figure 9. The RIBEYE-induced protein aggregates recruit endogenous bassoon. R28 retinal precursor cells were transfected with plasmids encoding for the indicated EGFP-tagged proteins. ***A–E***, The distribution of the endogenously present active-zone protein bassoon (***A–D***) or tubulin (***E***) was visualized by indirect immunofluorescence microscopy. In R28 cells, bassoon is endogenously present as discrete protein clusters (***A–C***, middle, arrows). Heterologously expressed RIBEYE-EGFP coaggregates with these preexisting bassoon clusters (***A–C***, arrows) but not EGFP alone (***D***). ***D***, Endogenous bassoon (arrowheads) did not recruit EGFP alone. The arrowheads in ***A*** and ***B*** show RIBEYE clusters that aggregated independent of the endogenous bassoon. ***E***, The RIBEYE(AB)-EGFP clusters (arrowhead) do not colocalize with microtubules, which were visualized by immunostaining with antibodies against tubulin. n, Nucleus. Scale bars, 10 μm.

It is likely that the interaction between different RIBEYE domains and RIBEYE molecules is regulated. In the present study, we found that NAD(H) is an important regulator of RIBEYE interactions. RIBEYE(A)–RIBEYE(B) interactions are efficiently inhibited by low, physiological concentrations of NAD(H). Both NADH and NAD^+ are very efficient in disrupting RIBEYE(A)–RIBEYE(B) complexes. Thus, NAD(H) appears to act as a molecular switch that distinguishes between two different types of RIBEYE–RIBEYE interactions: in the presence of NAD(H), RIBEYE(A)–RIBEYE(B) interactions are disassembled (this study), whereas RIBEYE(B)–RIBEYE(B) interactions are favored as judged by the NAD(H)-induced dimerization of CtBP2 (Thio et al., 2004). The binding interface on RIBEYE(B) for RIBEYE(B) interaction is spatially closely related but distinct from the binding interface on RIBEYE(B) for RIBEYE(A). This was shown by the analyses of point and deletion mutants of RIBEYE(B) that affect one type of interaction [RIBEYE(A)–RIBEYE(B) interaction] but not the other [RIBEYE(B)–RIBEYE(B) interaction] (Fig. 5*C*,*D*; supplemental Figs. 5, 6, available at www.jneurosci.org as supplemental material). The binding of NAD(H) could induce a conformation of RIBEYE(B) that favors homodimerization of RIBEYE(B) and that is incompatible with the formation of RIBEYE(B)–RIBEYE(A) heterodimers. RIBEYE(B)G730 is an essential part of the NADH-binding motif and the RIBEYE(B)G730A point mutant no longer interacts with RIBEYE(A). Therefore, one possible mechanism for the NADH-induced dissociation of the RIBEYE(A2)–RIBEYE(B) interaction

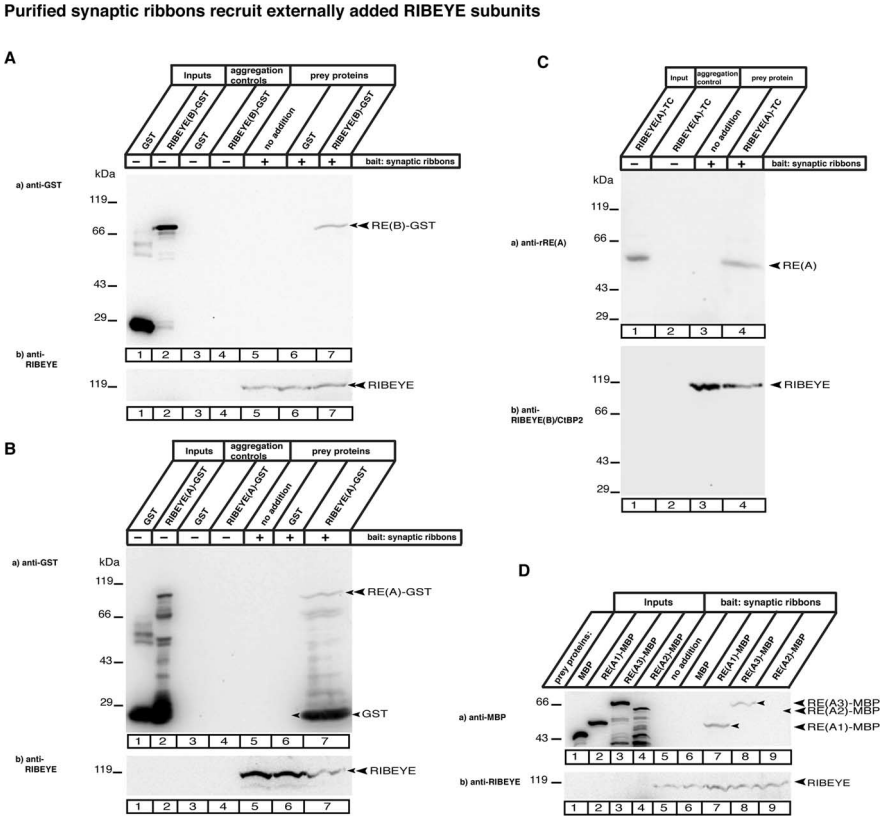

Figure 10. Synaptic ribbons recruit externally added RIBEYE subunits. Purified synaptic ribbons (180 μg) were incubated with the indicated RIBEYE fusion proteins ($\sim$3.5 μM) and then sedimented by a 1 min spin at 3.500 rpm. Fusion proteins that cosedimented with synaptic ribbons were detected by Western blotting with the indicated antibodies. ***Aa–Bb***, Lanes 1 and 2 show the respective input fractions, and lanes 3 and 4 the respective autoaggregation controls of the soluble fusion proteins to test whether ribbon-independent sedimentation of fusion proteins occurs. The autoaggregation controls show that in the absence of synaptic ribbons, no fusion proteins are found in the pellet. In contrast, if synaptic ribbons were incubated with the fusion proteins, both RIBEYE(A)-GST (***B***) as well as RIBEYE(B)-GST (***A***) sedimented with purified synaptic ribbons indicating binding to synaptic ribbons. In contrast, GST alone did not cosediment with synaptic ribbons (lane 6), demonstrating the specificity of the binding of RIBEYE fusion proteins to synaptic ribbons. As outlined in Materials and Methods, RIBEYE(A)-GST cannot be expressed exclusively as an unprocessed protein even under fermenter conditions, probably because of its high contents of proline residues and the extended shape of the molecule. In addition to full-length RIBEYE(A), degradation bands of RIBEYE(A)-GST are also visible. But full-length RIBEYE(A) is clearly expressed and binds to purified synaptic ribbons (***Ba***, lane 7), whereas GST alone does not (***Ba***, lane 6). The indicated lower band in lane 7 at $\sim$25 kDa is probably GST split-off from RE(A)-GST that piggybacks on RE(A)-GST bound to synaptic ribbons because GST is known to dimerize (Connell et al., 2008). In ***Ab*** and ***Bb***, the same blot as in ***Aa*** and ***Ba*** was stripped and reprobed with antibodies against RIBEYE (U2656) to show that equal amounts of purified synaptic ribbons were used as bait for the protein pull downs. RIBEYE signals of isolated bait synaptic ribbons are denoted by arrowheads (***Aa–Bb***, lanes 5–7). Recruitment of RIBEYE fusion protein is independent of the tag. ***Ca***, A further control to show that the recruitment of RE(A) to purified ribbons is mediated by RIBEYE(A) and not the GST-tag. Purified synaptic ribbons recruited RIBEYE(A), from which the GST-tag was removed by thrombin cleavage [RIBEYE(A)-TC, lane 4]. The autoaggregation control (lane 2) demonstrates that the coaggregation is dependent on the presence of synaptic ribbons and does not occur without ribbons. Binding of thrombin-cleaved rat RE(A) was detected by an antibody against RIBEYE(A) from the rat [anti-RE(A)] (tom Dieck et al., 2005). ***Cb***, Equal loadings of purified ribbons in lanes 3 and 4 was verified by Western blotting with a monoclonal antibody against RIBEYE(B)/CtBP2 (BD Transduction Laboratories). Lane 1 shows the input protein, RIBEYE(A) without GST-tag. ***Da***, RIBEYE(A) subdomains expressed as MBP fusion proteins are recruited to synaptic ribbons in the same manner as GST fusion proteins. RIBEYE(A1)-MBP and RIBEYE(A3)-MBP bound to synaptic ribbons (lanes 7, 8), whereas MBP alone did not (lane 6), demonstrating the specificity of the interaction. Interestingly, RIBEYE(A2)-MBP did not bind to purified synaptic ribbons (lane 9) although it efficiently interacted with RIBEYE(A) subunits [i.e., RIBEYE(A1), RIBEYE(A2)] in protein pull-down assays (Fig. 3). ***Db***, The same blot as in ***Da*** was stripped and reprobed with antibodies against RIBEYE (U2656) to show that equal amounts of purified synaptic ribbons were used as bait for the protein pull downs. RIBEYE signals of isolated bait synaptic ribbons are denoted by arrowheads (lanes 3–4 in ***Ca***, ***Cb***; lanes 5–9 in ***Da***, ***Db***). Lane 1–4 shows the input proteins (***Da***, ***Db***). RE, RIBEYE; RIBEYE(A)-TC, RIBEYE(A) generated from RIBEYE(A)-GST by a thrombin-mediated cleavage of the GST tag.

could be that the NAD(H)-binding region of RIBEYE(B) is also part of the binding interface with RIBEYE(A). If NADH binds to RIBEYE it could displace RIBEYE(A) from RIBEYE(B) and stimulate homodimerization of RIBEYE(B). By this way of thinking, NAD(H) would favor RIBEYE complexes that contain a homodimerized B-domain, which is likely important for RIBEYE function. Additionally, RIBEYE(B) displaced from RIBEYE(A2) would make the A2-binding module available for RIBEYE(A)–RIBEYE(A) interactions. By this mechanism, binding of NAD(H) could potentially initiate the assembly of synaptic ribbons. The NADH concentrations used in the present study are well in the range of the known cellular concentrations of NADH (Zhang et al., 2002; Fjeld et al., 2003) and thus very likely capable in regulating RIBEYE–RIBEYE interactions *in situ*.

The suggested modular assembly of the synaptic ribbon from individual RIBEYE units also provides a molecular explanation for the ultrastructural dynamics of synaptic ribbons by the addition or removal of RIBEYE subunits or rearrangements of RIBEYE–RIBEYE complexes. The ribbon recruitment experiments showed that binding sites for additional RIBEYE subunits are accessible and available on synaptic ribbons at a molecular level. Isolated synaptic ribbons (Schmitz et al., 1996, 2000) are able to bind externally added RIBEYE(B) and also RIBEYE(A). The multiple RIBEYE–RIBEYE interaction sites in the A-domain suggest a predominantly structural role of the A-domain as previously suggested (Schmitz et al., 2000). Probably large portions of RIBEYE(A) are likely "buried" in the core of the synaptic ribbons. Still, part of the A-domain is accessible in isolated synaptic ribbons and therefore partly exposed. In ribbon pull-down experiments (Fig. 10), RIBEYE(A1) and RIBEYE(A3) but not RIBEYE(A2) did bind to purified synaptic ribbons. Because RIBEYE(A2) can bind to both A1 and A2 interaction sites but not to the A3 interaction site, we suggest that A1 and A2 are located in the core of the ribbon, where these sites are not available for interaction with RIBEYE(A2). In contrast, the A3 region appears at least partly exposed on purified synaptic ribbons where it is free to interact with other protein, i.e., externally added RIBEYE(A1) and RIBEYE(A3) (Fig. 10*D*). Binding of RIBEYE(B) probably occurs via homodimerization of RIBEYE(B)-domains based on homologous findings with CtBP2 (Balasubramanian et al., 2003; Thio et al., 2004). This homodimerization is favored by the presence of NADH. Interestingly, RIBEYE(B) of synaptic ribbons does not bind RIBEYE(A2), although the respective fusion proteins can interact in an NAD(H)-dependent manner. Therefore, the RIBEYE(B)-binding site for RIBEYE(A2) might be blocked or the binding disfavored, e.g., by

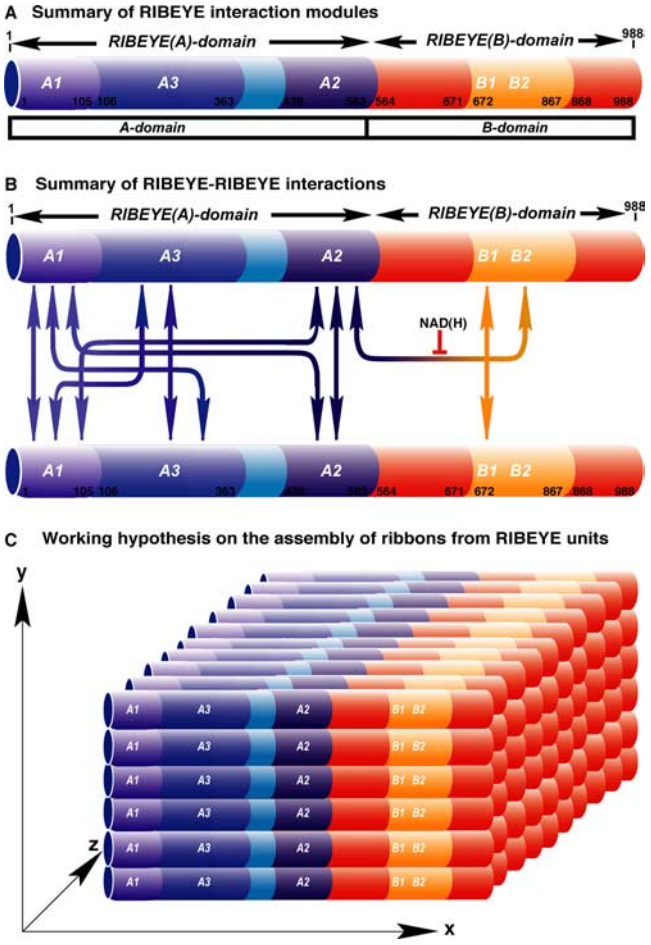

Figure 11. Schematic RIBEYE–RIBEYE interaction model. ***A***, Summary of the identified RIBEYE–RIBEYE interaction modules. In the A-domain of RIBEYE, three interaction modules are present, which are denoted as A1, A2, A3. In the B-domain of RIBEYE, two interaction modules, denoted as B1 and B2, are present. ***B***, Interaction combinations between the identified interaction modules are summarized. Only for the top RIBEYE molecule are all possible intermolecular homotypic domain interactions shown. Homotypic domain interactions, e.g., RIBEYE(A)–RIBEYE(A) interactions, can be mediated by homotypic subdomain interactions, e.g., RIBEYE(A1)–RIBEYE(A1), or by heterotypic subdomain interactions, e.g., RIBEYE(A1)–RIBEYE(A2). ***C***, A simplified, schematic working model shows how RIBEYE–RIBEYE interactions could build the scaffold of the synaptic ribbon from individual RIBEYE subunits. In this model, RIBEYE is depicted as a "linear" protein. For simplicity, a nonstaggered association of RIBEYE units is depicted based on homotypic RIBEYE–RIBEYE interactions. A possible, staggered interaction based on heterotypic RIBEYE–RIBEYE interactions is not included. *x*, *y*, and *z* represent the three-dimensional axis.

RIBEYE(B) homodimerization, or inhibited by NAD(H) bound at synaptic ribbons via the NBD of RIBEYE. Clearly, these working hypotheses have to be analyzed by future investigations and testing these assumptions will shed further light on the understanding of the construction and assembly of synaptic ribbons and how they work in the synapse.

In conclusion, our data show that RIBEYE is a scaffold protein with ideal properties to explain the assembly of synaptic ribbons as well as its ultrastructural dynamics via the modular assembly mechanism. The capability to interact with other RIBEYE proteins in multiple ways could explain how a single protein, RIBEYE, builds the scaffold for the entire ribbon (Fig. 11). Our transfection experiments actually show that RIBEYE can form aggregates that resemble spherical synaptic ribbons. The proposed modular assembly of the synaptic ribbon from individual RIBEYE subunits provides a molecular basis for the ultrastructural plasticity of synaptic ribbons (e.g., changes in size and shape of the ribbon). The binding of externally added RIBEYE to purified synaptic ribbons mimics the growth of synaptic ribbons that occurs *in situ*, e.g., under darkness in the mouse retina (Balkema et al., 2001; Spiwoks-Becker et al., 2004; Hull et al., 2006). Similarly, RIBEYE-aggregates increased in size over time in light microscopy (supplemental Fig. 9, available at www.jneurosci.org as supplemental material) and RIBEYE aggregates appeared to be able to coalesce into larger structures at the ultrastructural level. The regulation of RIBEYE–RIBEYE interactions, e.g., by NAD(H), could contribute to the regulation of structural plasticity of synaptic ribbons.

References

Bai C, Elledge SJ (1996) Gene identification using the yeast two-hybrid system. Methods Enzymol 273:331–347.

Balasubramanian P, Zhao LJ, Chinnadurai G (2003) Nicotinamide adenine dinucleotide stimulates oligomerization, interaction with adenovirus E1A and an intrinsic dehydrogenase activity of CtBP. FEBS Lett 537:157–160.

Balkema GW, Cusick K, Nguyen TH (2001) Diurnal variation in synaptic ribbon length and visual threshold. Vis Neurosci 18:789–797.

Bradford M (1976) A rapid and sensitive method for the quantitation of microgram quantities of protein utilizing the principle of protein-dye binding. Anal Biochem 72:248–254.

Cereghino JL, Cregg JM (2000) Heterologous protein expression in the methylotrophic yeast Pichia pastoris. FEMS Microbiol Rev 24:45–66.

Chadli A, Bouhouche I, Sullivan W, Stensgard B, McMahon N, Catelli MG, Toft DO (2000) Dimerization and N-terminal domain proximity underlie the function of the molecular chaperone heat shock protein 90. Proc Natl Acad Sci U S A 97:12524–12529.

Chinnadurai G (2002) CtBP, an unconventional transcriptional corepressor in development and oncogenesis. Mol Cell 9:213–224.

Coleman J (1990) Characterization of Escherichia coli cells deficient in 1-acyl-sn-glycerol-3- phosphate acyltransferase activity. J Biol Chem 265:17215–17221.

Connell E, Scott P, Davletov B (2008) Real time assay for monitoring membrane association of lipid-binding domains. Anal Biochem 377:83–88.

Fjeld CC, Birdsong WT, Goodman RH (2003) Differential binding of NAD^+ and NADH allows the transcriptional corepressor carboxyl-terminal binding protein to serve as a metabolic sensor. Proc Natl Acad Sci U S A 100:9202–9207.

Fuchs PA (2005) Time and intensity coding at the hair cell's ribbon synapse. J Physiol 566:7–12.

Harper JW, Adami GR, Wei N, Keyomarsi K, Elledge SJ (1993) The p21 Cdk-interacting protein Cip1 is a potent inhibitor of G1 cyclin-dependent kinases. Cell 75:805–816.

Heidelberger R, Thoreson WB, Witkovsky P (2005) Synaptic transmission at retinal ribbon synapses. Prog Retin Eye Res 24:682–720.

Helmuth M, Altrock W, Böckers TM, Gundelfinger ED, Kreutz MR (2001) An electrotransfection protocol for yeast two-hybrid library screening. Anal Biochem 293:149–152.

Hull C, Studholme K, Yazulla S, von Gersdorff H (2006) Diurnal changes in exocytosis and the number of synaptic ribbons at active zones of an ON-type bipolar cell terminal. J Neurophysiol 96:2025–2033.

James P, Halladay J, Craig EA (1996) Genomic libraries and a host strain designed for highly efficient two hybrid selection in yeast. Genetics 144:1425–1436.

Khimich D, Nouvian R, Pujol R, Tom Dieck S, Egner A, Gundelfinger ED, Moser T (2005) Hair cell synaptic ribbons are essential for synchronous auditory signalling. Nature 434:889–894.

Kumar V, Carlson JE, Ohgi KA, Edwards TA, Rose DW, Escalante CR, Rosenfeld MG, Aggarwal AK (2002) Transcription corepressor CtBP is an NAD(+)-regulated dehydrogenase. Mol Cell 10:857–869.

Lin-Cereghino J, Wong WW, Xiong S, Giang W, Luong LT, Vu J, Johnson SD, Lin-Cereghino GP (2005) Condensed protocol for competent cell preparation and transformation of the methylotrophic yeast Pichia pastoris. Biotechniques 38:44–48.

Nardini M, Spanò S, Cericola C, Pesce A, Massaro A, Millo E, Luini A, Corda D, Bolognesi M (2003) CtBP/BARS: a dual-function protein involved in

transcription co-repression and Golgi membrane fission. EMBO J 22:3122–3130.
Nouvian R, Beutner D, Parsons TD, Moser T (2006) Structure and function of the hair cell ribbon synapse. J Membr Biol 209:153–165.
Prescott ED, Zenisek D (2005) Recent progress towards understanding the synaptic ribbon. Curr Opin Neurobiol 15:431–436.
Schmitz F, Bechmann M, Drenckhahn D (1996) Purification of synaptic ribbons, structural components of the photoreceptor active zone complex. J Neurosci 16:7109–7116.
Schmitz F, Königstorfer A, Südhof TC (2000) RIBEYE, a component of synaptic ribbons: a protein's journey through evolution provides insight into synaptic ribbon function. Neuron 28:857–872.
Schmitz F, Tabares L, Khimich D, Strenzke N, de la Villa-Polo P, Castellano-Muñoz M, Bulankina A, Moser T, Fernández-Chacón R, Südhof TC (2006) CSPalpha-deficiency causes massive and rapid photoreceptor degeneration. Proc Natl Acad Sci U S A 103:2926–2931.
Seigel GM (1996) Establishment of an E1A-immortalized retinal cell culture. In Vitro Cell Dev Biol Anim 32:66–68.
Seigel GM, Sun W, Wang J, Hershberger DH, Campbell LM, Salvi RJ (2004) Neuronal gene expression and function in the growth-stimulated R28 retinal precursor cell line. Curr Eye Res 28:257–269.
Sewalt RG, Gunster MJ, van der Vlag J, Satijn DP, Otte AP (1999) C-Terminal binding protein is a transcriptional repressor that interacts with a specific class of vertebrate Polycomb proteins. Mol Cell Biol 19:777–787.
Singer JH (2007) Multivesicular release and saturation of glutamatergic signalling at retinal ribbon synapses. J Physiol 580:23–29.
Spiwoks-Becker I, Glas M, Lasarzik I, Vollrath L (2004) Mouse photoreceptor synaptic ribbons lose and regain material in response to illumination changes. Eur J Neurosci 19:1559–1571.
Stahl B, Diehlmann A, Südhof TC (1999) Direct interaction of Alzheimer's disease-related presenilin 1 with armadillo protein p0071. J Biol Chem 274:9141–9148.
Sterling P, Matthews G (2005) Structure and function of ribbon synapses. Trends Neurosci 28:20–29.
Thio SS, Bonventre JV, Hsu SI (2004) The CtBP2 co-repressor is regulated by NADH-dependent dimerization and possesses a novel N-terminal repression domain. Nucleic Acids Res 32:1836–1847.
tom Dieck S, Brandstätter JH (2006) Ribbon synapses of the retina. Cell Tissue Res 326:339–346.
tom Dieck S, Altrock WD, Kessels MM, Qualmann B, Regus H, Brauner D, Fejtová A, Bracko O, Gundelfinger ED, Brandstätter JH (2005) Molecular dissection of the photoreceptor ribbon synapse: physical interaction of Bassoon and RIBEYE is essential for the assembly of the ribbon complex. J Cell Biol 168:825–836.
Vollrath L, Spiwoks-Becker I (1996) Plasticity of retinal ribbon synapses. Microsc Res Tech 35:472–487.
Wagner HJ (1997) Presynaptic bodies ("ribbons"): from ultrastructural observations to molecular perspectives. Cell Tissue Res 287:435–446.
Wan L, Almers W, Chen W (2005) Two ribeye genes in teleosts: the role of Ribeye in ribbon formation and bipolar cell development. J Neurosci 25:941–949.
Wang Y, Okamoto M, Schmitz F, Hofmann K, Südhof TC (1997) Rim is a putative Rab3 effector in regulating synaptic-vesicle fusion. Nature 388:593–598.
Zenisek D, Horst NK, Merrifield C, Sterling P, Matthews G (2004) Visualizing synaptic ribbons in the living cell. J Neurosci 24:9752–9759.
Zhang Q, Piston DW, Goodman RH (2002) Regulation of corepressor function by nuclear NADH. Science 295:1895–1897.